UNIVERSITY OF LIÈGE

ASTROPHYSICAL INSTITUTE

ATLAS OF REPRESENTATIVE COMETARY SPECTRA

BY

P. SWINGS and L. HASER

Technical Final Report under Contract AF 61 (514)-628

The research reported in this document has been sponsored in part by the Geophysics Research Directorate of Air Force Cambridge Research Center, Air Research and Development Command, United States Air Force, through the European Office, ARDC.

ATLAS OF REPRESENTATIVE COMETARY SPECTRA

UNIVERSITY OF LIÈGE

ASTROPHYSICAL INSTITUTE

ATLAS OF REPRESENTATIVE COMETARY SPECTRA

BY

P. SWINGS and L. HASER

«Technical Final Report under Contract AF 61 (514)-628»

«The research reported in this document has been sponsored in part by the Geophysics Research Directorate of Air Force Cambridge Research Center, AIR RESEARCH AND DEVELOPMENT COMMAND, UNITED STATES AIR FORCE, through the European Office, ARDC».

TABLE OF CONTENTS

TABLE OF CONTENTS

FOREWORD

The need for an Atlas of Representative Cometary Spectra has been felt for several years by workers in numerous fields. On various occasions, especially at the meetings of the International Astronomical Union in Zurich (1948) and Rome (1952) and at the Liège Symposium on Cometary Physics (1952), many astronomers expressed the wish to have such an atlas prepared. The offer of the senior author, as Chairman of the I. A. U. Commission on the Physics of Comets, to attempt to prepare and publish the Atlas was received with great interest by all his colleagues on the Commission. As a result the I. A. U. made a modest grant to encourage such work. We are grateful to the Executive Committee of the I. A. U. for this first encouragement.

The need for the Atlas was not only felt by the astrophysicists working in the field of cometary physics, but possibly even more by research people engaged in solar physics, meteor astronomy, cosmogony of the solar system, upper atmosphere physics, combustion phenomena and flame spectroscopy.

A few good reproductions of cometary spectrograms are to be found in the astronomical literature, and several elaborate discussions on cometary spectra have been published. Most such discussions however deal with the spectrograms of a specific comet and with its individual characteristics. It is well known that each comet displays its own individual behavior, together with features which are common to all comets. Moreover the appearance of a cometary spectrogram depends greatly on the telescope and on the dispersing instrument.

We have tried to illustrate as many aspects as possible of cometary spectroscopy, by combining spectra of many comets taken with different types of telescopes and dispersing systems, at various heliocentric distances. The related laboratory spectra are also reproduced. Each of the twenty three plates is accompanied by a short description of the main features, together with the corresponding observational data, such as the heliocentric distances and the instrumental conditions. In addition an introductory text provides the essential information on the observational and instrumental factors and on cometary physics, as well as the description of the observed cometary bands and their laboratory counterparts, including wavelength lists. In this introduction we consider only the topics which are required for a clear understanding of the Atlas; we do not intend it to be a general exposé on cometary physics.

Our endeavors would have failed if we had not enjoyed the privilege of the generous and wholehearted cooperation of all the colleagues whose help was requested, especially of the members of the I. A. U. Commission on the Physics of Comets. The response from practically all the cometary spectroscopists all over the world has been most gratifying, and is a clear sign that there is a real need for the Atlas. We also wish to express our indebtedness to the directors of the following observatories who have contributed copies of cometary spectrograms obtained at their institutions: Cordoba, Hamburg, Haute-Provence, Lick, Lyon, McDonald, Meudon, Michigan, Mt Wilson, Sonneberg, Stockholm, Uccle and Victoria, and to other research workers belonging to these institutions who generously responded to our call for spectrograms and for advice.

Altogether copies of 350 spectrograms obtained during this century (plus one of comet Swift, 1899 I) were received; this collection represents a high proportion of all good cometary spectrograms ever obtained anywhere. Table I gives the list of all the available spectrograms. It includes the catalogue number in the «Catalogue Général des Orbites de Comètes, de l'an — 466 à 1952» by F. Baldet and Miss G. de Obaldia ([1]) (col. 1), the definitive designation (col. 2), the provisional designation (col. 3) the discoverers' names (col. 4), the absolute magnitudes (col. 5), the *n*-coefficients (col. 6), the perihelion distance (col. 7), the period (col. 8), and the numbers of slit- and objective prism spectrograms which were available for the Atlas (col. 9 and 10). The data in col. 5 and 6 were taken mainly from the papers by the Czech astronomers ([2]). For each spectrogram r and $\frac{dr}{dt}$ were computed independently of any ephemeris, on the basis of the best orbits available. Many microphotometer tracings were made, sometimes at various distances from the center of the head. Altogether 126 tracings were made; these as well as copies of all spectrograms are at the disposal of workers in the field of cometary physics.

All the spectrograms were helpful in our systematic examination of the behavior of cometary spectra, but not all could be reproduced in the Atlas, although an attempt was made to include as many facets of the problem as possible. The spectrograms reproduced in the plates are collected in Table II which includes the numbers in Baldet's catalogue (col. 1), the designations (col. 2, 3, 4), the date of perihelion passage in universal time T (col. 5), the angle ω between the ascending node and the perihelion (col. 6), the longitude of the ascending node Ω (col. 7), the inclination i of the orbital plane to the ecliptic (col. 8), the perihelion distance q (col. 9), the semi-major axis a in case of elliptical orbits (col. 10), the eccentricity e (col. 11), the orbital period P in sidereal years (col. 12), the date of the equinox to which the orbital plane refers (col. 13), and the plate and spectrogram numbers (col. 14).

In preparing the Atlas we have tried to illustrate as completely as possible the following properties:

the relative intensities of the molecular emissions;

the profiles of the emission bands;

the spatial distribution of the emissions in the head and tail;

the relative intensities of the continuous spectrum and of the molecular emissions, and their variations with r;

the different aspect of spectrograms obtained with different instruments and photographic emulsions;

the « individuality » of comets.

For the reproduction there has been a careful retouching of scratches and other defects.

Our special thanks are due to the Air Research and Development Command, United States Air Force, which supported and sponsored the preparation and publication of the Atlas. More particularly, we express our deep gratitude to the scientists in the Geophysics Research Directorate in Cambridge, Mass., and to the A. R. D. C. Officers in the European Office in Brussels for their understanding and help during all phases of the work. We also wish to thank Dr. B. Rosen for his efficient help in relation to the descriptions of the band systems. Finally it is a pleasure to record here our appreciation of the expert work of the Ceuterick Press. In particular, our thanks go to Mr. L. Pitsi, its director, for his cooperation.

TABLE I

Spectroscopic Material at our Disposal and Essential Characteristics of the Comets

N	Def. Des.	Prov. Des.	Name	H_0	n	q	P	Number of Spectrograms	
								Slit	O.P.
462	1899 I	1899 *a*	Swift	6.68	3.17	0.327	—	1	—
478	1903 IV	1903 *c*	Borrelly	6.50	2.38	0.330	—	1	1
499	1907 IV	1907 *d*	Daniel	4.39	3.62	0.512	8 741	3	1
503	1908 III	1908 *c*	Morehouse	3.94	5.14	0.945	—	—	10
508	1910 I	1910 *a*	Big Comet	4.90	3.8	0.129	3 906 000	1	1
509	1910 II	1909 *c*	Halley	5.62	4.03	0.587	76.03	3	3
516	1911 IV	1911 *g*	Beljawsky			0.303	—	1	—
517	1911 V	1911 *c*	Brooks	5.64	3.64	0.489	2 126.2	5	23
518	1911 VI	1911 *f*	Quénisset	6.31	3.64	0.788	9 245.6	—	5
522	1912 II	1912 *a*	Gale	6.28	3.21	0.716	56 649	—	3
575	1925 I	1925 *c*	Orkisz	5.89	3.07	1.109	—	—	1
601	1927 IX	1927 *k*	Skjellerup			0.176	—	1	—
511	1930 III	1930 *c*	Wilk	8.64	4.5	0.482	486.9	—	1
614	1930 VI	1930 *d*	Schwassmann-Wachmann			1.011	5.427	—	1
626	1932 V	1932 *k*	Peltier-Whipple	7.36	11.4	1.037	281.75	—	1
645	1936 II	1936 *a*	Peltier	6.77	4.75	1.100	1 542	5	7
650	1937 II	1937 *c*	Wilk-Peltier	10.26	3.36	0.621	—	1	—
653	1937 V	1937 *f*	Finsler	6.19	0.55	0.863	160 000	2	38
654	1937 VI	1937 *k*	Encke	9.50	6.1	0.33	3.28	1	2
656	1939 I	1939 *a*	Kosik-Peltier	8.0		0.717	1 651	—	20
658	1939 III	1939 *d*	Jurlof-Achmarof-Hassel			0.528	7 489	2	8
670	1941 I	1940 *c*	Cunningham	5.81	1.99	0.368	—	29	2
673	1941 IV	1941 *c*	De Kock-Paraskevopoulos	5.79	2.0	0.790	18 111	5	6
677	1941 VIII	1941 *d*	Van Gent	6.91	3.64	0.875	—	7	—
681	1942 IV	1942 *a*	Whipple-Bernasconi-Kulin	5.9		1.445	—	5	—
687	1943 I	1942 *g*	Whipple-Fedtke	5.22	2.93	1.354	2 274	17	17
700	1945 V	1945 *b*	Kopff			1.496	6.1899	1	—
704	1946 II	1946 *d*	Pajdusakova-Rotbart-Weber	9.87	2.62	1.016	—	—	2
719	1947 XI	1947 *i*	Encke	9.9	6.32	0.341	3.30	5	—
720	1947 XII	1947 *n*	Great Southern Comet	6.0	2.0	0.11	—	17	—
722	1948 I	1947 *k*	Bester	6.31	4.4	0.748	—	22	3
725	1948 IV	1948 *g*	Honda-Bernasconi	8.0	6.0	0.208	—	5	6
				7.54	5.39				
732	1948 XI	1948 *l*	Eclipse-Comet	4.3	7.6	0.135	171 000	10	1
				5.36	3.66				
748	1951 I	1950 *b*	Minkowski	6.1	2.1	2.572	—	5	2
749	1951 II	1951 *a*	Pajdusakova			0.720	—	2	—
760	1952 III	1951 *l*	Schaumasse	6.8	2.1	1.19	8.172	—	4

TABLE II

Comets which are presented in the Atlas, and Essential Orbital Data

Comet No.	Designations	Name	T	(in U.T.)	ω	Ω	*i*	*q*	*a*	*e*	P in years	Equ.	Plate and Spectrogram No.
478	1903 IV 1903 *c*	Borrelly	Aug.	28.10410	127.3281	293.5481	84.9972	0.329660	—	1	—	1903.0	XVI, 5.
499	1907 IV 1907 *d*	Daniel	Sept.	4.46153	294.4322	143.0483	8.9681	0.512173	424.3	0.998793	8,741	1910.0	XIV*a*, 5; XIV*b*, 2; XV*a*, 6; XVI, 7, 10; XXIII*b*, 5, 6.
503	1908 III 1908 *c*	Morehouse	Dec.	26.2561	171.5770	103.1614	140.1789	0.945300	—	1.000692	—	1908.0	V, 2; VI *a*, 1-5; VI *b*, 1-4; XIX *a*, 6.
508	1910 I 1910 *a*	Big Comet	Jan.	17.58815	320.8944	88.7650	138.7822	0.128975	24,800	0.9999948	3,906,000	1910.0	XV *b*, 4; XVIII *b*, 4.
509	1910 II 1909 *c*	Halley	April	20.1998	11.7044	57.2700	162.2117	0.587326	17.9474	0.967275	76.0327	1910.0	XIV *a*, 1; XVII, 5, 6, 7, 8; XIX *b*, 4.
			April	20.1794	»	»	»	0.58716	17.9467	0.967283	76.0288	1910.0	
516	1911 IV 1911 *g*	Beljawsky	Oct.	10.76396	71.7013	88.6527	96.4656	0.303424	—	1.000167	—	1911.0	XV *a*, 7.
517	1911 V 1911 *c*	Brooks	Oct.	28.23834	153.0242	292.9492	33.8036	0.489427	163.35	0.99704	2,126.2	1911.0	IV, 7; V, 1, 4, 6, 7; VII *a*, 1-7; VII *b*, 1-7; VIII *a*, 1-6; XV *a*, 5; XVIII *a*, 3,6; XIX *a*, 4.
518	1911 VI 1911 *f*	Quénisset	Nov.	12.84928	122.0286	35.1864	108.0917	0.787635	440.5	0.998212	9,245.6	1911.0	XVIII *a*, 5; XIX *a*, 2.
522	1912 II 1912 *a*	Gale	Oct.	5.45828	25.6322	297.0031	79.8056	0.716114	1,434.8	0.999501	56,649	1912.0	XVII, 13, 14; XVIII *b*, 5.
523	1912 III 1912 *c*	Borrelly	Oct.	21.4584	99.6764	143.7828	124.6450	1.10711	—	1	—	1912.0	XIX *a*, 5.
645	1936 II 1936 *a*	Peltier	July	8.9551	148.4696	134.0482	78.5508	1.099870	133.5	0.991760	1,542	1936.0	XIX *b*, 1.
650	1937 II 1937 *c*	Wilk-Peltier	Febr.	21.84934	32.1811	56.8639	26.3333	0.621478	—	1	—	1937.0	VIII *b*, 1; XVII, 12.
653	1937 V 1937 *f*	Finsler	Aug.	15.66139	114.8262	58.5417	146.4127	0.862774	2,955	0.999708	160,610	1937.0	IV, 7; VIII *b*, 2; XIII, 1, 2; XIX *a*, 1; XXIII *b*, 2, 3, 4.
654	1937 VI 1937 *h*	Encke	Dec.	27.25	184.9478	334.6911	12.5472	0.332347	2.20918	0.849561	3.28357	1937.0	IX, 1-3; XVIII *a*, 4.
656	1939 I 1939 *a*	Kosik-Peltier	Febr.	6.85381	169.0342	288.7561	63.5252	0.716503	139.69	0.994871	1,651	1939.0	XVII, 9, 10, 11.
658	1939 III 1939 *d*	Jurlof-Achmarof-Hassel	April	10.1686	89.2473	311.4283	138.1054	0.528271	382.8	0.998620	7,489	1939.0	XV *b*, 5, 6, 7; XVI, 8, 9.
670	1941 I 1940 *c*	Cunningham	Jan.	16.23136	199.5808	295.7494	49.8725	0.368043	—	1	—	1940.0	I, 1-11; II, 1-10; IV, 1, 3; XIV *a*, 2; XIV *b*, 5, 6; XV *a*, 1-4; XVI, 1-4; XVIII *a*,7; XIX *a*, 7, 8; XX *a*, 1, 2; XXI, 1, 3.
673	1941 IV 1941 *c*	De Kock-Paraskevopoulos	Jan.	27.6535	268.6693	42.2619	168.1947	0.790003	689.7	0.998854	18,111	1941.0	XVII *b*, 2.
677	1941 VIII 1941 *d*	Van Gent	Sept.	3.19730	85.3474	256.7302	94.5005	0.874622	—	1.000968	—	1941.0	X, 6-10; XIV *a*, 3; XIX *a*, 7; XX *a*, 3, 4.
681	1942 IV 1942 *a*	Whipple-Bernasconi-Kulin	April	30.8333	223.4177	340.1241	79.4447	1.445303	—	1.000893	—	1942.0	X, 1-5; XIV *a*, 7; XX *a*, 5, 6.
687	1943 I 1942 *g*	Whipple-Fedtke	Febr.	6.7187	39.8195	100.0230	19.7140	1.353628	172.92	0.992172	2,274	1943.0	IV, 4; VIII *b*, 3, 4; XIX *a*, 3; XX *b*, 1.
704	1946 II 1946 *d*	Pajdusakova-Rotbart-Weber	May	11.43592	22.2671	301.2565	169.5581	1.018251	—	1	—	1946.0	XIX *b*, 2.
719	1947 XI 1947 *i*	Encke	Nov.	26.3268	185.1836	334.7450	12.3520	0.341054	2.21863	0.846277	3.30466	1950.0	IX, 4-6; XVI, 6; XIX *a*, 9.
720	1947 XII 1947 *n*	Great Southern Comet	Dec.	2.58734	196.2059	336.6043	138.5130	0.110071	—	1.000032	—	1950.0	IV, 6; XII *a*, 1-8; XV *b*, 1-3; XVIII *b*, 6.
722	1948 I 1947 *k*	Bester	Febr.	16.43302	350.2410	270.6914	140.5633	0.747809	—	1	—	1947.0	III,1-9; IV,5; V, 3, 5; XIII, 3-5; XI V*b*, 1, 3; XVII, 3, 4; XVIII *b*, 1; XIX *b*, 3, 6; XX *b*, 2; XXIII *a*, 1, 2.
725	1948 IV 1948 *g*	Honda-Bernasconi	May	15.90624	317.0433	203.1328	23.1617	0.207707	—	1	—	1948.0	VIII *b*, 7; XII *b*, 1-7.
732	1948 XI 1948 *l*	Eclipse Comet	Oct.	27.4288	107.2613	210.3290	23.1227	0.135383	3,080	0.999956	171,000	1950.0	IV, 2; XI, 1-8; XIV *a*, 6; XV *b*, 8; XVII, 1, 2; XVIII *b*, 3; XIX *b*, 5; XX *b*, 3, 4; XXIII *b*, 1.
748	1951 I 1950 *b*	Minkowski	Jan.	15.04490	192.4608	38.1851	144.1497	2.572318	—	1.000855	—	1950.0	VIII *b*, 5,6; XIV *a*, 4, 8; XIV *b*, 4, 7; XX *b*, 5-7.
749	1951 II 1951 *a*	Pajdusakova	Jan.	30.49223	68.7217	310.5148	87.8859	0.719848	—	1.003119	—	1951.0	XVIII *b*, 7.
760	1952 III 1951 *l*	Schaumasse	Febr.	10.6512	51.8257	86.3819	12.0320	1.194230	4.05701	0.705638	8.17164	1950.0	VIII *b*, 8; XIX *b*, 7.

INTRODUCTORY REMARKS

Definitions

A comet consists of a solid nucleus (or an assembly of solid bodies) surrounded by the head or coma, from which one or several tails often extend to considerable distances in a direction usually opposite, or nearly so, to the Sun.

The «nucleus» may be actually observed only in very exceptional cases when the comet is at a small geocentric distance. It is a body (or assembly of bodies) of reduced size, with a diameter of the order of one kilometer (*). It is the source of the gaseous molecules and of the solid particles observed in the head and tail.

The «head» is a nearly spherical diffuse nebulosity surrounding the nucleus; it has no sharp limit. The head of a bright comet may reveal structures of varied complexity, such as the «envelopes»: these do not appear on the spectrograms of the Atlas. Often either a fairly sharp or a nebulous condensation appears in the central part of the head. While this central condensation is usually responsible for the main part of the observed continuous spectrum it should not be considered as the actual solid nucleus which is so small that the contribution of its solar reflected continuum is minor compared to that of the central condensation, at least at fairly small heliocentric distances. At great distances from the nucleus the luminosity of the head is due to atoms and molecules in the gaseous state; on the other hand the central condensations contain probably solid particles giving rise to the reflected solar spectrum, although polyatomic molecules whose electronic spectra are in the unobservable ultraviolet region may also contribute by scattering of the solar radiation. When comets are at large heliocentric distances (such as in the case of Comet Schwassmann-Wachmann II) the diffuse head gives only a solar spectrum [3]. This indicates that the head consists only of solid particles and (or) polyatomic molecules surrounding a nucleus.

Comet tails have usually a delicate structure characterized by streamers and condensations. As will be seen in the Atlas these appear on the objective prism spectrograms.

The notions of nucleus, head, central region of head, tail and condensations in tail will become clearer after the discussion of the spectra and their assignment to specific molecules.

(*) The arrangement of the Atlas is independent of any hypothesis as to the nature and structure of the nucleus, head and tail. We are inclined to think of the nucleus as a single solid body of a very tenuous nature (low density, roughly 0.05 according to Whipple). Among other suggestions regarding the nature of the nucleus are a system of small solid blocks or a cloud of meteoric dust.

General aspect of a cometary spectrogram

The spectrograms of the Atlas cover the region λ3000-λ6800. A few grating spectrograms covering the region λ6500-λ9000 have been obtained at the McDonald Observatory [4], but they are too weak or of too low contrast to stand reproduction.

The main features of all spectrograms are :

a) emission bands extending to different distances in the head and the tail;

b) a solar spectrum usually restricted to the central part of the head (although it may also extend into the tail).

Neither the discrete band emissions nor the solar reflected spectrum show a sharp limit of extension in the head; they fade out gradually with increasing distance from the center. The rate of fade out («gradient») differs for the various molecular emissions, and is most rapid for the reflected solar continuum.

Different instruments have different abilities to reveal the spectroscopic features of a comet. Generally objective prism spectrographs have a low resolution, but are well adapted to the observation of extended faint objects, such as cometary tails. Normally a slit spectrograph gives only the spectrum of the head. Only in the case of a high speed slit spectrograph which can be oriented along the image of the tail can slit spectrograms of the tail be obtained; the B-grating spectrograph of the McDonald Observatory [5] with which slit spectrograms of the tail of Comet 1948 I were obtained fulfills such conditions. A slit spectrograph with quartz or glass prisms may have an excellent resolution in the ultraviolet and blue-violet region, but has a low resolution in the red. A grating spectrograph may provide good resolution at greater wave lengths.

A comet is a diffuse extended source of light. Hence a slit spectrograph will give higher resolution than an objective prism or a slitless spectrograph of equal dispersion and optical qualities. The resolution of an objective prism is not only determined by the dispersion, the guiding, the turbulence of the atmosphere and the optical qualities of the instrument, but also by the extensions of the individual band emissions into the head. In the focal plane of an objective prism each monochromatic emission is reproduced in its two dimensional extension which differs for the different molecules. It is impossible to resolve two emissions which differ in wave length (converted into mm. on the plate) to an extent smaller than the geometrical half widths of the emissions on the plate. As far as spectral resolution is concerned an objective prism for cometary spectra should thus have a high angular dispersion and a short focal length. This is the case for the Meudon and Lyons objective prisms.

Nightglow- or twilight emissions often appear on slit spectrograms of comets; they are easily recognized since they extend with fairly uniform intensity (except for vignetting effects) over the whole length of the slit (see plates n° II and III). Of course objective prism plates do not reveal background emissions, such as nightglow, twilight or moon light; these simply produce a more or less uniform background on the plate, thus fixing a lower limit to the surface brightness of the detectable objects.

Instrumental influences

When estimating the extensions of the different emissions into the head, great attention must be paid to the chromatic aberration (if a refractor is used) and to the quality of the guiding (see plate XXIII*b*). The relative intensities are similarly affected.

As previously stated all the cometary emissions of the head have an approximately spherical intensity distribution around the nucleus. They fade out gradually with increasing distance from the nucleus. The slit usually bisects the head. The intensity distribution along each spectral line—which is a monochromatic geometrical image of the slit, hence of the narrow strip of the cometary head— is thus a picture (*) of the molecular distribution within the head, as a function of the distance from the nucleus.

The intensity distribution along a spectral line—hence, the «length» of the line, and the estimated extension of the corresponding molecule in the head—may be considerably perturbed by trailing the image on the slit. A simple mathematical treatment shows that the relative intensities of two emission lines, one confined to the central part of the comet, the other having a considerable extension, may be changed by a factor of 5 or more in the central region.

Similarly the chromatic aberration of a refractor may provide an erroneous impression of the relative central intensities of two emissions.

The intensity of the solar reflected spectrum which is normally confined in a very small region near the nucleus is especially affected by trailing or by chromatic aberration. In many cases the «length» of the solar spectrum on a cometary spectrogram gives an idea of the amount of trailing; this in turn makes it possible to correct the relative intensities of different emissions.

The slit width affects the relative intensities of perfectly monochromatic lines and of the continuum (or of a blend of very close lines). Indeed a narrow slit is desirable if one wishes to increase the contrast between the discrete emissions and the solar continuum.

Finally if a comet is observed at very large zenith distance and if the slit is turned perpendicular to the horizon, the atmospheric dispersion which lies along the slit may result in an

(*) To convert the intensity distribution along the spectral line (i.e. along the narrow strip of head) into the radial molecular distribution within the head requires a simple mathematical treatment.

inclination of the cometary spectrum relative to the comparison spectra. If the slit is not perpendicular to the horizon anomalous intensity relations between bands may occur as a result of atmospheric dispersion.

Basic principles for the identification of cometary emissions

Wavelength coincidences between cometary and laboratory emissions provide only a first clue toward an identification. Great caution has to be exercised before a cometary emission may be safely assigned to a specific molecule ([6]). This is essentially due to two facts: (1) the wave lengths and profiles of the cometary emissions are not accurately known on account of the low dispersion and resolution which must necessarily be used; (2) the physical conditions within the comet and the excitation mechanism of the cometary emissions can not be duplicated in the laboratory. The molecules in cometary heads and tails are in a state of extremely low density (of the order of 10^6 molecules per cm^3 or less). They are exposed to the electromagnetic solar radiation (X-, ultraviolet-, visual-, infrared- and radio-waves) as well as to corpuscular solar emissions (electrons, protons, heavier ions, all of various velocities). The solid nucleus which liberates the molecules has a very small mass.

As a result of the low densities, collisions between molecules of the head are practically absent; the concepts of temperature and Boltzmann distribution have no meaning.

The solar radiation is responsible for the formation of the molecules which are observed spectroscopically. A cometary nucleus which is approaching the Sun from a large heliocentric distance is at a low temperature. In the neighborhood of the sun, molecules are evaporated, or sublimated, or ejected from the surface. These «parent» molecules become photodissociated by solar radiation, and give rise to the spectroscopically observed radicals. Other processes for the production of the observed radicals will be envisaged later on. The solar radiation contributes also primarily to the physical conditions of the molecules in the head. The distributions of the molecules in their vibrational and rotational states result from the absorption of solar quanta and from the subsequent emissions. These distributions may be computed if the various transition probabilities involved are known.

Since the mass of the nucleus is too small to retain the molecules, even if the latter have only their thermal velocities at low temperatures, the head of a comet is a transient atmosphere which must be continuously replenished.

As a result of these peculiar conditions one may expect the band emission to be simply a fluorescence mechanism. The cometary molecules absorb the solar radiation; from the excited levels thus reached they fall down to lower levels with emission of their spectrum. On account of the presence of Fraunhofer absorption lines in the solar spectrum the excited cometary bands may and do have a complex profile. The radial velocity of the comet relative to the sun shifts the exciting radiation by Doppler effect; as a result the profiles and even the absolute intensities of the cometary bands depend to some extent on the radial velocity of the comet, hence on the orbital data. This matter will be considered again later on.

The profiles of the cometary bands differ from those in the laboratory. The bands of all the heteronuclear molecules (CN, CH, OH, NH,...) exhibit a rotational intensity distribution corresponding roughly—but by no means exactly—to a low temperature; the rotational intensity distributions of the bands of C_2 (homonuclear molecule) are approximately of the high temperature type. The complexity of the profiles, due to the Fraunhofer lines of the exciting solar radiation has been mentioned earlier. Details on the comparison between theoretical and observed rotational intensity distributions may be found in papers by P. Swings ([7]), A. McKellar ([8]) and J. Hunaerts ([9]).

Identification work must involve consideration of these complex profiles. It may be noticed that excitation by collisions as in the polar aurora would give rise to rotational distributions of the normal laboratory type ([10]). The absence of such «auroral» types from all observed cometary spectra indicates that fluorescence is always the major excitation mechanism.

Spectrum of the head of a comet; wavelength table

Table III contains a list of the wave lengths of the emissions appearing in the spectrum of the head of a comet; the identifications are given whenever available. The list covers the spectral region λ3000-λ8200. For different spectral regions the adopted wave lengths have been taken from measurements of various cometary spectra obtained with different types of dispersive instruments: quartz-prism spectrographs for the region λ3000-3850, glass-prism spectrographs from λ3850 to λ4400, grating instruments for $\lambda > 4400$.

The following data are found in the table:
(1) the estimated relative intensities and the wave lengths;
(2) the emitting atom or molecule, whenever known;
(3) the corresponding electronic transition;
(4) the vibrational transition;
(5) the rotational line notation.

The list is divided into spectral ranges within which the estimated relative intensities have some meaning for a given comet at a specific heliocentric distance. From one group to another the relative intensities may differ considerably in different comets or in one comet at different heliocentric distances.

TABLE III

Spectrum of the Head of a Comet. — Wavelength Table

I (*a*)	I (*b*)	λ	Molecule	Band System	Vibrational Transition	Rotational Line
(2)		3078.7	OH	$A^2\Sigma^+ - X^2\Pi_i$	0 — 0	$Q_1 + {}^QP_{21}$ (1.5)
(1)	(1)	3081.7	OH	»	0 — 0	${}^QP_{21}$ (3.5) + P_1 (1.5)
(2)	(3)	3086.3	OH	»	0 — 0	P_1 (2.5)
(4)	(5*n*)	3090.2	OH	»	0 — 0	${}^QR_{12} + Q_2$ (1.5); Q_2 (2.5); ${}^QR_{12} + Q_2$ (0.5); R_1 (3.5).
(1)	(5)	3093.7	OH	»	0 — 0	${}^PQ_{12}$ (0.5)
(3)	(5)	3096.3	OH	»	0 — 0	${}^PQ_{12} + P_2$ (1.5)
(2)	(5)	3099.5	OH	»	0 — 0	${}^PQ_{12} + P_2$ (2.5); ${}^OP_{12}$ (1.5)
	(0)	3103	OH	»	0 — 0	P_2 (3.5)
	(1)	3107	OH	»	0 — 0	${}^OP_{12}$ (2.5)
	(2)	3135.0	OH	$A^2\Sigma^+ - X^2\Pi_i$	1 — 1	$Q_1 + {}^QP_{21}$ (1.5)
	(3)	3137.9	OH	»	1 — 1	$R_2 + P_1$ (1.5); ${}^QP_{21}$ (3.5).
	(0)	3140.6	OH	»	1 — 1	R_2 (0.5)
	(1)	3142.9	OH	»	1 — 1	P_1 (2.5)
	(3)	3147.5	OH	»	1 — 1	${}^QR_{12} + Q_2$ (1.5); Q_2 (2.5); ${}^QR_{12} + Q_2$ (0.5); P_1 (3.5)
	(2)	3150.5	OH	»	1 — 1	${}^PQ_{12}$ (0.5)
	(2-1)	3153.7	OH	»	1 — 1	${}^PQ_{12} + P_2$ (1.5)
	(1)	3156.8	OH	»	1 — 1	${}^OP_{12}$ (1.5); ${}^PQ_{12} + P_2$ (2.5)
	(0)	3159	OH	»	1 — 1	P_2 (3.5)
	(2)	3350.8	NH	$A^3\Pi_i - X^3\Sigma^-$	0 — 0	${}^RP_{31}$ (0)
	(4)	3354.1	NH	»	0 — 0	${}^RQ_{21}$ (0); $Q_3 + {}^QP_{32}$ (1); $Q_3 + {}^QP_{32}$ (2).
	(8)	3357.9	NH	»	0 — 0	R_1 (0); $Q_2 + {}^QR_{23} + {}^QP_{21}$ (2).
	(2)	3361.5	NH	»	0 — 0	$Q_1 + {}^QR_{12}$ (2); $Q_1 + {}^QR_{12}$ (1); P_3 (2).
	(2)	3364.7	NH	»	0 — 0	$P_2 + {}^RQ_{23}$ (2)
	(3)	3369.1	NH	»	0 — 0	$P_1 + {}^PQ_{12} + {}^PR_{13}$ (2); $P_2 + {}^PQ_{23}$ (3)
	(1)	3372.0	NH	»	0 — 0	$P_1 + {}^PQ_{12} + {}^PR_{13}$ (3); P_3 (4); $P_2 + {}^PQ_{23}$ (4).
	(1-0)	3565	OH^+	$^3\Pi - {}^3\Sigma$	0 — 0	R_3 (1) to R_3 (4)
	(2)	3572.2	CN	$B^2\Sigma^+ - X^2\Sigma^+$	1 — 0	Maximum in R — branch near R(14)
			CN	»	2 — 1	» » » R (5)
			OH^+	$^3\Pi - {}^3\Sigma$	0 — 0	Q_3 (1); Q_3 (2)
	(1-2)	3577.3	CN	$B^2\Sigma^+ - X^2\Sigma^+$	1 — 0	Maximum in R — branch near R (5)
			CN	»	2 — 1	» in P — branch near P (5)
	(2-3*n*)	3584.3	CN	»	1 — 0	P (2) to P (14); Maximum at P (9).

TABLE III (*continued*)

Spectrum of the Head of a Comet. — Wavelength Table

I	λ	Molecule	Band System	Vibrational Transition	Rotational Line
(1-0*n*)	3618.6				
(1*n*?)	3625.5				
(2)	3674.3				
(1-2)	3692.7				
(1)	3699.7				
(1-2*n*?)	3717.9				
(2-1)	3780.4				
(1-2)	3784.5				
(2)	3804.0				
(1-2*n*)	3808.9				
(1)	3829.4				
(1) from	3851.0				
to	3854.2	CN	$B^2\Sigma^+ - X^2\Sigma^+$	0 — 0	R (20) — R (27)
(0-1)	3857.69			+ 1 — 1	R (7) — R (16)
(1-0)	3858.35				
(1)	3859.40	CN	»	0 — 0	R (19)
(3*s*)	3862.41	CN	»	0 — 0	R (16)
(5)	3863.40	CN	»	0 — 0	R (15)
(4*s*)	3865.07	CN	»	0 — 0	R (13)
(4*n*)	3867.12	CN	»	0 — 0	R (11); R (10).
(6*n*)	3869.21	CN	»	0 — 0	R (9); R (8); R (7).
(3*n*)	3872.12	CN	»	0 — 0	R (4); contribution of R (3) and R (5).
(4*n*)	3873.50	CN	»	0 — 0	R (2); R (1).
(7) from	3876.5	CN	»	0 — 0	P (3) — P (6)
to	3878.4				
from	3879.6				
to	3883.0	CN	»	0 — 0	P (9) — P (22)
with maxima at					
(10*n*)	3880.46	CN	»	0 — 0	P (11)
(15*s*)	3882.02	CN	»	0 — 0	P (17)
(0)	3866.18	CN	$B^2\Sigma^+ - X^2\Sigma^+$	0 — 0	R (12)
(1*s*)	3866.89	CN	»	0 — 0	R (11)
(1*s*)	3867.68	CN	»	0 — 0	R (10)
(1*s*)	3868.44	CN	»	0 — 0	R (9)
(1*s*)	3869.23	CN	»	0 — 0	R (8)
($1^1/_2 s$)	3870.04	CN	»	0 — 0	R (7)
($1^1/_2 s$)	3870.71	CN	»	0 — 0	R (6)
(1*s*)	3872.06	CN	»	0 — 0	R (4)
($1^1/_2$)	3872.47	CN	»	0 — 0	R (4); R (3).

TABLE III (*continued*)

Spectrum of the Head of a Comet. — Wavelength Table

I	λ	Molecule	Band System	Vibrational Transition	Rotational Line
(1*s*)	3873.47	CN	$B^2\Sigma^+ - B^2\Sigma^+$	0 — 0	R (2)
($^1/_2$)	3874.25	CN	»	0 — 0	R (1)
(4*n*)	3877.30	CN	»	0 — 0	P (3) — P (5)
(8*n*) broad max. at	3880.16	CN	»	0 — 0	P (10); P (11).
Longward edge at	3881.57	CN	»	0 — 0	P (15)
(0)	3886.6	CH	$B^2\Sigma - X^2\Pi$	0 — 0	$Q_2 + {}^QR_{12}$ (0.5)
(1-2*n*)	3889.1	CH	»	0 — 0	$Q_2 + {}^QR_{12}$ (1.5) $Q_1 + {}^QP_{21}$ (1.5) and (2.5)
	3890.6	CH	»	0 — 0	${}^PQ_{12}$ (0.5); $Q_2 + {}^QR_{12}$ (2.5); $Q_1 + {}^QP_{21}$ (3.5).
(1)	3893.1	CH	»	0 — 0	$Q_2 + {}^QR_{12}$ (3.5); P_1 (1.5); $Q_1 + {}^QP_{21}$ (4.5).
(1-2)	3897.2	CH	»	0 — 0	$Q_2 + {}^QR_{12}$ (4.5); $Q_1 + {}^QP_{21}$ (5.5); P_2 (1.5); P_1 (2.5).
(1-2)	3902.6	CH	»	0 — 0	${}^OP_{12}$ (1.5); P_2 (2.5); P_1 (3.5).
(1-2)	3908.3	CH	»	0 — 0	P_2 (3.5); ${}^OP_{12}$ (2.5); P_1 (4.5)
(1)	3914.5	CH	»	0 — 0	P_2 (4.5); P_1 (5.5).
(1-0)	3921.5	CH	»	0 — 0	P_2 (5.5); P_1 (6.5)
(2*n*?)	3950.2	C_3			
(1)	3954.0	C_3 + CH^+	$^1\Pi - {}^1\Sigma$	(1 — 0)	R (1) to R (4)
(1-2)	3960.2	C_3			
(1-2)	3963.5	C_3 + CH^+	$^1\Pi - {}^1\Sigma$	(1 — 0)	Q (1); Q (2).
(2)	3972.7	C_3 + CH^+	$^1\Pi - {}^1\Sigma$	(1 — 0)	P (2)
(1-2)	3979.7	C_3			
(3)	3987.2	»			
(4*n*)	3992.6	»			
(1-0)	3997.5	»			
(2)	4002.2	»			
(1)	4007.5	»			
(4)	4013.2	»			
(4*n*)	4019.4	»			
(1-0)	4024.3	»			
(1-0)	4027.6	»			
(2)	4033.2	»			
(5)	4039.6	»			

TABLE III (*continued*)

Spectrum of the Head of a Comet. — Wavelength Table

I	λ	Molecule	Band System	Vibrational Transition	Rotational Line
(5)	4043.6	C_3			
(6)	4051.6	»			
(1-2)	4054.2	»			
(1-2)	4064.3	»			
(2-3)	4068.4	»			
(4)	4074.4	»			
(1-0)	4084.8	»			
(1-0)	4090.0	»			
(2)	4099.5	»			
(1-0)	4109.4	»			
(1-0*n*)	4124.4	»			
(0-1)	4137.8	»			
A. McKellar has obtained the C_3 — bands with higher resolution and found further maxima at	4014.37	C_3			
	4016.2	»			
	4050.43	»			
	4066.17	»			
(1-0)	4180	CN	$B^2\Sigma^+ - X^2\Sigma^+$	1 — 2	R (10)
(1-0)	4184	»	»	1 — 2	R (6)
(2)	4193	»	»	0 — 1	R (15); (16) +
				1 — 2	P — branch
(2)	4197	»	»	0 — 1	R (11), (12), (13).
(0-1)	4206	»	»	0 — 1	R (2), (3).
(1)	4210.2	»	»	0 — 1	P (2), (3).
(6*n*)	4214.7	»	»	0 — 1	P (4) to P (20)
(1)	4231	CH^+	$^1\Pi - {}^1\Sigma$	0 — 0	R (0); R (1)
(1-2)	4238.5	CH^+	»	0 — 0	Q (1); Q (2)
(1)	4254.4	CH^+	»	0 — 0	P (3)
(0-1)	4281	CH	$A^2\Delta - X^2\Pi$	0 — 0	R_2 (4.5) + R_1 (5.5) + ${}^RQ_{21}$ (5.5)
(1-0)	4285.7	»	»	0 — 0	R_2 (3.5) + ${}^RQ_{21}$ (4.5)
(1-2)	4291.7	»	»	0 — 0	R_2 (2.5) + ${}^RQ_{21}$ (4.5) + R_1 (3.5)
(3*n*)	4297.3	»	»	0 — 0	R_2 (1.5) + ${}^RQ_{21}$ (2.5) + R_1 (2.5)
(2-3*s*)	4300.2	»	»	0 — 0	R_2 (0.5) + ${}^RQ_{21}$ (1.5)
(4*s*)	4303.9	»	»	0 — 0	R_1 (1.5)
(6*n*)	4313.2	»	»	0 — 0	Q_1 (2.5) to (6.5) + Q_2 (1.5) to (5.5) + ${}^QP_{21}$ (2.5) to (6.5) + ${}^QR_{12}$ (1.5) to (5.5).
(1-2)	4392.3	»	»	0 — 0	P_1 (3.5) + P_2 (2.5) + ${}^PQ_{12}$ (2.5)
(1-2)	4334.2	»	»	0 — 0	P_1 (4.5) + P_2 (3.5) + ${}^PQ_{12}$ (3.5)

TABLE III (*continued*)

Spectrum of the Head of a Comet. — Wavelength Table

I	λ	Molecule	Band System	Vibrational Transition	Rotational Line
(1-0)	4339.0	CH	$A^2\Delta - X^2\Sigma$	0 — 0	$P_2\ (4.5) + {}^pQ_{12}\ (4.5) + P_1\ (5.5)$
(0-1)	4344	»	»	0 — 0	$P_2\ (5.5) + {}^pQ_{12}\ (5.5) + P_1\ (6.5)$
(0-1)	4348	»	»	0 — 0	$P_2\ (6.5) + {}^pQ_{12}\ (6.5) + P_1\ (7.5)$
	4364.3	C_2	$A^3\Pi_g - X^3\Pi_u$	4 — 2	
	4371.1	»	»	3 — 1	
	4380.9	»	»	2 — 0	
(2)	4462.8				
(1)	4484.5				
(1)	4504				
	4541				
(1)	4570.2	CN ?			
(1)	4585.9	CN ?			
(1)	4598				
(1)	4612.9	CN	$B^2\Sigma^+ - X^2\Sigma^+$	0 — 2	Maximum in P — branch
(2)	4628.7				
(2)	4645				
(2)	4662.2				
(8)	4669.5	C_2 ?	$A^3\Pi_g - X^3\Pi_u$	6 — 5	
(15)	4676.2	C_2	»	5 — 4	
(15)	4682.7	C_2	»	4 — 3	
(8)	4687.7				
(10)	4692.6				
(25)	4695.5	C_2	»	3 — 2	
(10)	4708.8				Possible contribution of $C^{12}C^{13}$ (3 — 2)
(30)	4713.2	C_2	»	2 — 1	
(3)	4719.0				Possible contribution of $C^{12}C^{13}$ (2 — 1)
(3)	4728.1				
(20)	4734.9	C_2	»	1 — 0	
(1)	4742.9	$C^{12}C^{13}$?	»	1 — 0	
(2)	4746.4				
(0.5)	4791				
(1)	4839.4				
(1)	4872.4				
(1)	4898.2				
(2)	4924.3				
(1)	4897				
(3)	5007.6				

TABLE III (*continued*)

Spectrum of the Head of a Comet. — Wavelength Table

I	λ	Molecule	Band System	Vibrational Transition	Rotational Line
(3)	5029.0				
(2)	5054.4				
(2)	5069				
(2)	5097.3	C_2	$A^3\Pi_g - X^3\Pi_u$	2 — 2	
(3)	5128.2	C_2	»	1 — 1	
(1)	5144.0	C_2	»	0 — 0	Structure in 0 — 0 band
(5)	5164.9	C_2	»	0 — 0	
(1)	5182.4				
(1)	5201.1				
(1)	5249.1				
(1)	5283.7				
(1)	5316.0				
(1)	5332.7				
(1)	5351.6				
(1)	5381.1				
(1.5)	5416.5				
(1)	5427.9				
(1)	5444.2				
(2)	5466.2	C_2	$A^3\Pi_g - X^3\Pi_u$	4 — 5	
(1)	5483.1	C_2	»		Structure in (3 — 4)-band
(2)	5498.9	C_2	»	3 — 4	
(1)	5518.6	C_2	»		Structure in (2 — 3)-band
(2)	5538.5	C_2	$A^3\Pi_g - X^3\Pi_u$	2 — 3	
(3)	5582.5	C_2	»	1 — 2	
(4)	5634.1	C_2	»	0 — 1	
(1)	5679.0				
(2)	5702.2				
(2)	5732.5				
(1)	5797.8				
(1)	5817.4				
(1)	5836.2				
(1)	5868.9				
(3)	5889.6	Na	D_1, D_2		
(1)	5933.4				
(1)	5959.6	C_2	$A^3\Pi_g - X^3\Pi_u$	4 — 6	
(2)	5974.9				
(1)	5990.2				
(2)	5998.0	C_2	$A^3\Pi_g - X^3\Pi_u$	3 — 5	
(1)	6017.2				
(1)	6033.8				
(1)	6054.4	C_2	$A^3\Pi_g - X^3\Pi_u$	2 — 4	

TABLE III (*continued*)

Spectrum of the Head of a Comet. — Wavelength Table

I (a)	I (b)	λ	Molecule	Band System	Vibrational Transition	Rotational Line
(2)		6094.8				
(1)		6106.6				
(2)		6118.0	C_2	$A^3\Pi_g - X^3\Pi_u$	1 — 3	
(1)		6157.1				
(1)		6186.5	C_2	$A^3\Pi_g - X^3\Pi_u$	0 — 2	
(3)		6297.3				
(2)		6329.5				
(2)		6345.2				
(1)		6360.6				
(1)		6538.6				
(1)		6557.0				
(2)		6571.9				
(2)		6580.3				
(2)		6596.5				
(3)		6615.6				
(2)		6636.9				
(2)		6670				
(2)		6722.1				
(2)		6748.7				
(2)		6762.1				
		from 7858 to 7957 strong maximum at 7906 structure in the blue wing at 7876				
		from 8046 to 8164 maximum at 8106				
		further weak emissions 7088				
		7381				
		8242				
		8783				

REMARKS TO TABLE III

(0 — 0) band of OH. — The wave lengths are the mean values from measurements of the spectra of the following comets: 1941 I, 1941 VIII, 1942 IV and 1948 I. The relative intensities are those in 1941 I (*a*) and in 1948 I (*b*). For details on the identifications and relative intensities, see J. Hunaerts [11].

(1 — 1) band of OH. — The wave lengths are from Comet 1948 I. For details, see J. Hunaerts [11]. For a discussion of the possible contribution of the $C^2\Sigma - A^2\Pi$ system of CH, see J. Hunaerts [12].

(0 — 0) band of NH. — The wave lengths are from 1941 I. Details of the identifications have been generously contributed by J. Hunaerts (unpublished).

(1 — 0) band of CN and (0 — 0) band of OH^+. — Wave lengths from 1941 I.

Region λ 3618 - λ 3830. The wave lengths are taken from P. Swings [13]. All these emissions are confined in the central part of the head.

(0 — 0) band of CN. — Two sets of wave lengths are given: one [14] from Comet 1948 XI, the other [15] from Comet 1943 I.

(0 — 0) bands of the $^2\Sigma - {}^2\Pi$ and $^2\Delta - {}^2\Pi$ transitions of CH. The wave lengths are from Comet 1941 I [16]. For details on the identifications, see J. Hunaerts [12].

C_3 emissions. — The wave lengths are from Comet 1941 I [16].

(0 — 0) and (1 — 0) bands of CH^+. See the discussions by P. Swings [17] and A. McKellar [18].

Region λ 4416 to λ 6762. The wave lengths are from grating spectrograms of Comet 1947 XII [4]. For the contributions of $C^{12}C^{13}$, see P. Swings[17], N. T. Bobrovnikoff [19] and A. McKellar [18].

Region $\lambda > 7000$. — The wave lengths are from grating spectrograms [4].

It is difficult to estimate the precision of the wave lengths; for $\lambda > 4400$ it is of the order of $\pm$ 1 Å.

The pure fluorescence excitation mechanism may be checked on the basis of the profiles of the OH-, NH-, CN- and CH-bands. For C_2 the matter is not so simple, and some doubt as to the excitation mechanism may remain since certain structures within the bands may possibly not be explained by a simple fluorescence of the C_2 molecules. Possibly these structures belong to other molecules or to isotopes. The laboratory bands of C_3 and NH_2 have not been analyzed as yet, so that a check on the excitation mechanism is impossible. In the case of C_3 one may wonder whether the bands could not be due to the impact of solar protons, since these bands are obtained in the laboratory in the presence of hydrogen. However all the cometary spectrograms show always the same structure of the λ4050 group, irrespective of the solar activity.

Description of the individual bands in the spectrum of the head of a comet

OH

The (0-0) and (1-1) transitions of the $A^2\Sigma^+ - X^2\Pi_i$ system of OH were first identified by Swings, Elvey and Babcock ([16]) in Comet 1941 I; they were later confirmed in several comets. The calculations of the theoretical profiles of the OH emissions by J. Hunaerts ([11]) were based on the assumption of a pure fluorescence excitation. Striking differences between the relative intensities in 1941 I and 1948 I were interpreted as due to the different radial velocities of these comets relative to the sun: 1941 I, $v = +$ 22.2 Km/sec.; 1948 I, $v = -$ 34.6 Km/sec.

The (0-0) and (1-1) bands lie near λ 3090 A and λ 3140 A, that is near the short wavelength limit of possible observation. At great zenith distances the band absorption of terrestrial ozone may affect the relative line intensities.

The strongest (0-0) band consists of 9 lines, the (1-1) band of 10; all involve only low rotational quantum numbers ($\leqslant 5$), in accordance with the heteronuclear character of the radical. Most observed emissions are actually blends of rotational lines belonging to various branches of the bands.

Around λ 3000 A the reflected solar spectrum of the central part of the head is very weak; as a result the OH-bands stand out clearly.

With lower resolution the (0-0) band consists of three diffuse lines, the central one at λ 3090 A. As for the (1-1) band it is then a diffuse emission near λ 3140 A, without clear maximum. The relative intensities and the extensions into the head change from one comet to an other. The difference in profile is illustrated in figure 1, showing microphotometer tracings for Comets 1941 I and 1948 I which had greatly differing radial velocities.

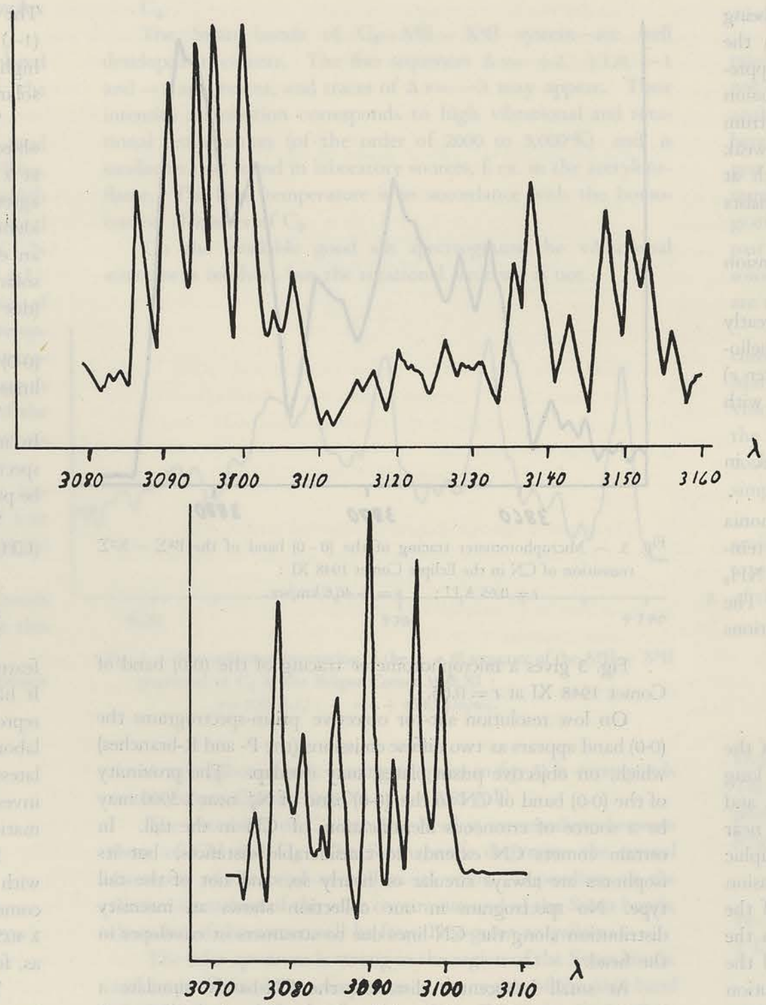

Fig. 1. — Microphotometer tracings of the $A^2\Sigma^+ - X^2\Pi_i$ transition in Comet Bester 1948 I and Comet Cunningham 1941 I.
a) (0 — 0) and (1 — 1) bands of Comet Bester 1948 I : $r = 1.05$ A.U.; $v = +$ 22,0 km/sec.
b) (0 — 0) band of Comet Cunningham : $r = 0{,}87$ A.U.; $v = -$ 34,4 km/sec.

The (0-0) band of the Fortrat system of CH coincides approximately with the (1-1) band of OH. However the CH-Fortrat band does not contribute appreciably to the cometary emissions. This was shown in Hunaerts' elaborate treatment ([11]). It is evident also from the fact that the much stronger violet system of CH was weak in Comet 1948 I in which the emission near λ 3140 was well defined; the Fortrat system of CH could not have contributed in this case.

The parent molecule of the OH-radical is usually supposed to be H_2O. Since the OH-emission is observed at large heliocentric distances ($r = 1.8$ A.U.) and since H_2O- ice has a very low vapor pressure at low temperature, some mechanism other than sublimation from pure H_2O-ice has to be found for the production of the OH-radicals. This production may result either from chemical reactions at or near the surface of the solid nucleus, or from the presence of solid hydrates, or from the liberation of trapped radicals. Emission by chemiluminescence is excluded because of the conformity of the OH-profile to the fluorescence mechanism. Moreover a chemiluminescent emission would be limited to a very small «nuclear» region, and would be too weak since each molecule would emit only one light quantum.

The OH-radicals must have a high relative abundance in comets, since the oscillator strength of the λ 3090 band is small (compared to CN), and since the solar radiation is fairly weak in the ultraviolet.

NH

The (0-0) band of the $A^3\Pi_i - X^3\Sigma^-$ system of NH was first identified in Comet 1941 I; it was later found in several other comets. The complex structure of the band renders the calculation of theoretical profiles rather difficult.

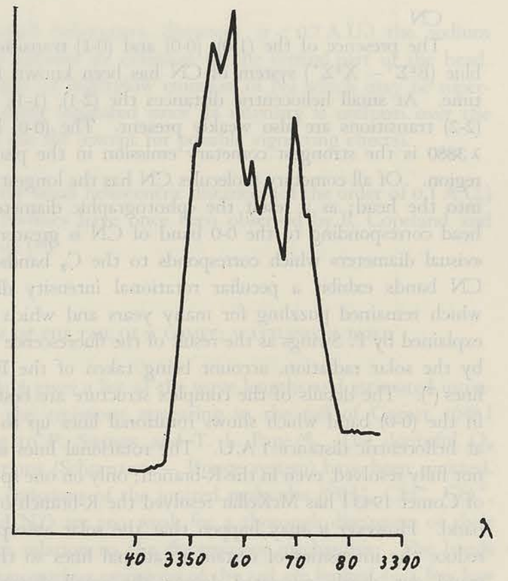

Fig. 2. — Microphotometer tracing of the (0 - 0) band of the $A^3\Pi - X^3\Sigma$ transition of NH in Comet Cunningham 1941 I : $r = 0.87$ A.U.; $v = -$ 34.7 km/sec.

The band consists of seven lines, the strongest of them being at λ 3358 A. Fig. 2 gives a microphotometric tracing in the case of Comet 1941 I at $r = 0.87$ A.U. The profile is not appreciably affected by the ozone absorption bands. The NH-emission stands out clearly on account of the weakness of the solar spectrum naer λ 3358, and of the great extension into the head. On weak exposures only one sharp line appears; it is the Q-branch at λ 3358. On low resolution spectrograms the emission consists of two diffuse features centered at λ 3358 and λ 3369.

The NH-radical shows approximately the same extension into the head as C_2.

The intensity ratio of the OH and NH bands differs greatly in different comets. In a specific comet it also varies with heliocentric distance, the OH band appearing sooner (at greater r) than NH, but strengthening much more slowly than NH with decreasing r.

Only the lowest rotational levels ($\leqslant 3$) are observed, in accordance with the heteronuclear character of NH.

The parent molecule is usually supposed to be ammonia (NH_3) which has a higher vapor pressure than water at low temperature. It seems probable that a sufficient amount of NH_3 molecules may be sublimated by heating of the icy nucleus. The NH-radical would be formed by successive photodissociations of NH_3.

CN

The presence of the (1-0), (0-0) and (0-1) transitions of the blue ($B^2\Sigma^+ - X^2\Sigma^+$) system of CN has been known for a long time. At small heliocentric distances the (2-1), (1-1), (1-2), and (2-2) transitions are also weakly present. The (0-0) band near λ 3880 is the strongest cometary emission in the photographic region. Of all cometary molecules CN has the longest extension into the head; as a result the «photographic diameter» of the head corresponding to the 0-0 band of CN is greater than the «visual diameter» which corresponds to the C_2 bands. All the CN bands exhibit a peculiar rotational intensity distribution which remained puzzling for many years and which was fully explained by P. Swings as the result of the fluorescence excitation by the solar radiation, account being taken of the Fraunhofer lines (7). The details of the complex structure are best observed in the (0-0) band which shows rotational lines up to about 20 at heliocentric distance 1 A.U. The rotational lines are usually not fully resolved, even in the R-branch; only on one spectrogram of Comet 1943 I has McKellar resolved the R-branch of the (0-0) band. However it may happen that the solar absorption lines reduce the intensities of certain rotational lines so that others stand out clearly separated despite the small dispersion: this was the case on spectrograms of 1948 XI where R (13) and R (19) appeared isolated.

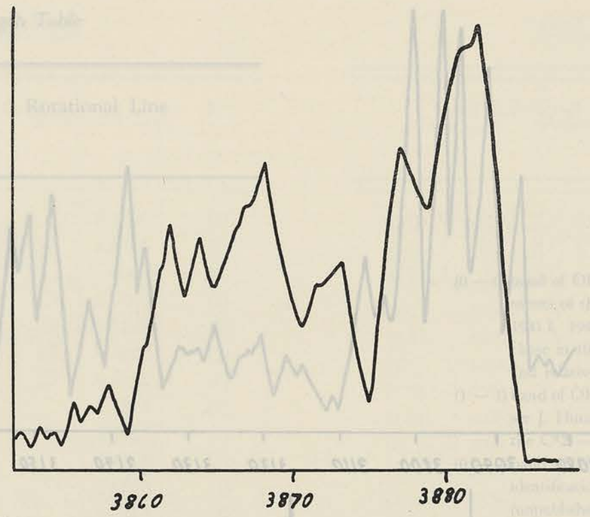

Fig. 3. — Microphotometer tracing of the (0 - 0) band of the $B^2\Sigma - X^2\Sigma$ transition of CN in the Eclipse Comet 1948 XI : $r = 0{,}65$ A.U.; $v = +46{,}6$ km/sec.

Fig. 3 gives a microphotometer tracing of the (0-0) band of Comet 1948 XI at $r = 0.65$.

On low resolution slit- or objective prism-spectrograms the (0-0) band appears as two diffuse emissions (the P- and R-branches) which, on objective prism plates, may overlap. The proximity of the (0-0) band of CN to the (0-0) band of N_2^+ near λ 3900 may be a source of erroneous identification of CN in the tail. In certain comets CN extends to considerable distances, but its isophotes are always circular or nearly so, and not of the tail type. No spectrogram in our collection shows an intensity distribution along the CN-lines due to streamers or envelopes in the head.

At small heliocentric distances the CN-bands simulate a higher rotational temperature, characterized by a displacement of the structure toward higher rotational quantum numbers.

The (0-0) band is present on all spectrograms taken at $r < 3$ A.U. It is absent—as well as any other band—on the spectrograms of Comet Schwassmann-Wachmann II (r about 6)(3).

The presence of the red system $A^2\Pi - X^2\Sigma$ of CN is still doubtful (4) (14) (20). The two strongest infrared emissions, λ 7906 and λ 8106, have provisionally been assigned to this system.

The parent molecule is usually supposed to be HCN or C^2N^2.

CH

The (0-0) transitions of the two systems $B^2\Sigma - X^2\Pi$ and $A^2\Delta - X^2\Pi$ are observed, the second being by far the strongest. The Fortrat system ($C^2\Sigma - X^2\Pi$) is absent (see description of the (1-1) band of OH), although its oscillator strength seems to be high. This absence is probably due to the fact that the exciting solar radiation is much weaker near λ 3140 than near λ 4300.

The $A^2\Delta - X^2\Pi$ band has often been observed, even on objective-prism plates; it has a conspicuous Q-branch maximum at λ 4313. Only the low rotational lines ($\leqslant 7$) are observed, in agreement with the heteronuclear character of CH. The detailed identification of the features observed on slit spectrograms requires an elaborate discussion of the fluorescence excitation, since the solar spectrum has a complex profile in the region of the G-band (due mainly to the solar CH-molecules) (12).

The $B^2\Sigma - X^2\Pi$ band extends longward of the head of the (0-0) band of CN; it consists of regularly spaced, weak rotational lines.

The CH-emission lines are the shortest observed in comets. In many cases they are hardly longer than the solar reflected spectrum of the central part of the head. They may thus easily be partly hidden by features of the solar spectrum.

The parent molecule is usually supposed to be methane (CH_4) or acetylene (C_2H_2).

C_3

The «λ 4050 group» which is one of the most prominent features of cometary spectra remained unidentified until recently. It had been observed in emission in comets long before it was reproduced in the laboratory. It has now been found in various laboratory sources, and it is also observed in absorption in the latest carbon stars (N-stars). It is of great importance in the investigation of combustion phenomena and solid carbon formation.

In several laboratory sources the λ 4050 group is associated with a broad continuum extending from λ 3400 to λ 5000. In comets there is no evidence for this continuum even when the λ 4050 bands are strong and there is no superposed solar spectrum, as, for example, in comet Encke 1947 XI.

The assignment of the λ 4050 group to C_3 was based on isotopic effects, rotational analysis and other criteria; it appears quite convincing; C_3 is probably a linear symmetrical molecule C-C-C.

In most comets the C_3 band consists of a group of about 30 fairly narrow emissions extending from λ 3950 to λ 4140, the strongest maximum being at λ 4052.

Recent strong exposures of oxy-acetylene flame spectra on high contrast plates taken by N. H. Kiess (21) and by others reveal structure extending to λ 3600: the ultraviolet features observed by N. H. Kiess explain probably the weak emissions appearing shortward of the (0-0) band of CN, in certain comets in which λ 4052 is very strong. These ultraviolet emissions which are short and vary in intensity like the λ 4050 group are not

easily measured on account of the presence of the complex reflected solar spectrum.

The rotational analysis of the C_3 bands has not been completed as yet; neither is anything known definitely regarding the vibrational analysis.

The C_3 emissions are short, although slightly longer (and sometimes differently distributed in the head) than the CH-lines. C_3 is the second emission to appear in the head of a comet which approaches the sun (near 2 A.U.), CN (0-0) being the first. Around $r = 1.7$ A.U. λ 4052 is approximately as intense as (0-1) of CN in the central region of the head. Beginning around $r = 1.5$ A.U. the available spectrograms show clearly the steady decrease of the intensity ratio C_3/CN with decreasing r. The inverse development is true after perihelion passage. Unfortunately no spectrogram of the same comet before and after perihelion passage is available; however on spectrograms of different comets of the same general type the post-perihelion behavior of C_3/CN appears to be simply the inverse of the preperihelion behavior.

On low resolution spectrograms (objective prism, or low dispersion slit spectrograms) the λ 4050 group consists of four short emissions; on strong exposures one or two additional emissions appear on either side.

Because of their small extension into the head the C_3 bands may reveal separate details on objective prism plates, while this would not be true for the CN band.

A microphotometric tracing is given in fig. 4; it corresponds to Comet 1941 I at $r = 1.00$ A.U.

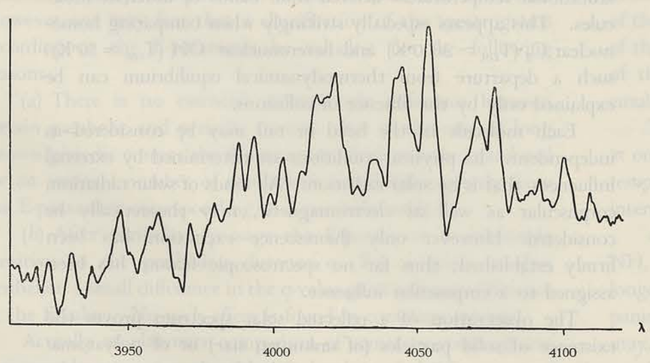

Fig. 4. — Microphotometer tracing of the λ 4050 group in Comet Cunningham 1941 I :
$r = 1{,}00$ A.U.; $v = -33{,}5$ km/sec.

C_2

The Swan bands of C_2—$A^3\Pi - X^3\Pi$ system—are well developed in comets. The five sequences $\Delta v = +2, +1, 0, -1$ and -2 are present, and traces of $\Delta v = -3$ may appear. Their intensity distribution corresponds to high vibrational and rotational temperatures (of the order of 2000 to 3,000°K) and is similar to that found in laboratory sources, f. ex. in the acetylene-flame. The high temperature is in accordance with the homonuclear character of C_2.

On the available good slit spectrograms the vibrational structure is resolved, but the rotational structure is not.

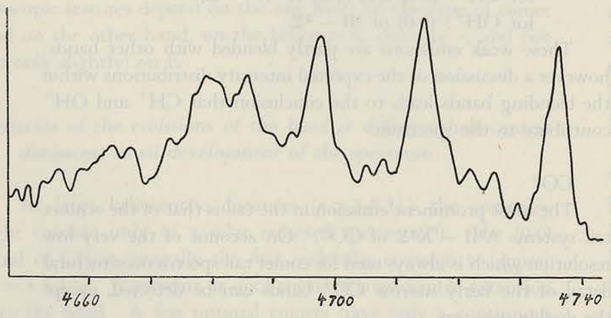

Fig. 5. — Microphotometer tracing of the (1 — 0) sequence of the $A^3\Pi - X^3\Pi$ transition of C_2 in the Eclipse Comet 1948 XI :
$r = 0{,}65$ A.U.; $v = +46{,}63$ km/sec.

A microphotometric tracing is given in fig. 5; it corresponds to the Eclipse Comet 1948 XI at $r = 0{,}65$ A.U.

The extension of C_2 into the head is intermediate between those of CN and C_3. The Swan bands determine the «visual diameter» of the head as well as its color. Depending on the relative intensities of the solar continuum and of the Swan bands, the color of the comet will be from blue-green to yellow.

The solar spectrum is strong in the region of the Swan bands, and its profile is not as complex as in the region of the (0-0) band of CN. As a result the fluorescence profile of the C_2 bands is very similar to that in a laboratory source. We shall return to this matter in the section on the laboratory data.

The C_2 emission appears around $r = 1.8$ A.U.; the (0-0) band is first visible, but the whole system develops quickly with decreasing r.

The vibrational bands of a sequence may sometimes be separated on objective prism spectrograms, but they often are not, on account of the large extension of the C_2 molecules in the head.

There is evidence for the presence of the isotopic molecule $C^{12}\,C^{13}$ in certain comets. However C^{13} is never so abundant relative to C^{12} as in the N-stars.

NH_2

The α-band of ammonia is probably due to NH_2 and is certainly present in comets. However detailed assignments can not be made safely, since the laboratory spectrum has not been analyzed as yet. There are many wavelength coincidences between cometary features and laboratory emissions. The strongest lines of the α-band are in the region λ > 5000A, where numerous cometary emissions have been found on prism- and grating spectrograms: these emissions are confined to the central part of the head. Doubtlessly a number of assignments, including some of the strongest short cometary lines in the red region are real.

Attempts have been made to assign numerous cometary emissions to the α-band in the region from λ 4400 A upward. Many of these assignments should only be considered as provisional, pending an analysis of the laboratory spectrum. Since the intensity distribution within the cometary bands may differ considerably from that in the laboratory assignments based on a simple wavelength coincidence are fraught with danger.

One strong NH_2-line at λ 6298 is blended with the nightglow emissions, λ 6300 [01]. However it may often be detected as a peak in the intensity of the nightglow line in the central part of the comet.

The parent molecule is probably NH_3.

Atomic lines

At small heliocentric distances ($r < 0.7$ A.U.) the sodium D-doublet appears in emission in the central part of the head. The twilight or nightglow emission of Na which may be superposed is easily separated since its intensity is uniform over the length of the slit (except for possible vignetting effects).

At very small heliocentric distances (of the order of 0.1 A.U.) Fe- and Ni-lines have once been observed by R. Copeland and J. G. Lohse ([22]).

Spectrum of the tail of a comet; wavelength table

Table 4 gives a list of the wave lengths and estimated intensities of the emissions appearing in the tail of Comet 1948 I according to P. Swings and T. L. Page ([4]). The doubtful O_2 identifications (Schumann — Runge system) have been omitted.

The emissions of the ionized molecules (OH^+, CH^+, CO^+, CO_2^+ and N_2^+) are too weak for a thorough discussion of their profiles in relation to the fluorescence mechanism. The bands of all heteronuclear emissions of the tail are limited to a few low rotational lines, suggesting the same fluorescence excitation as in the head.

TABLE 4

Spectrum of the Tail of a Comet; Wavelength Table

I	λ	Emitter	Band system	Vibrational Transition
(2)	3378.0	CO_2^+	$^2\Pi - {}^2\Pi$	1 — 0
(1)	3388.2	CO_2^+	»	2 — 1
(1-0)	3416	CO^+	$A^2\Pi - X^2\Sigma$	6 — 0
(1-0)	3431	CO^+	»	6 — 0
(1)	3478			
(4)	3509.1	CO_2^+	$^2\Pi - {}^2\Pi$	0 — 0
		CO^+	$B^2\Sigma - A^2\Pi$	2 — 0
(1-0)	3525			
(2)	3545.4	CO_2^+	$^2\Pi - {}^2\Pi$	2 — 2
		N_2^+	$B^2\Sigma - X^2\Sigma$	3 — 2
(4)	3580.4	CN	$B^2\Sigma^+ - X^2\Sigma^+$	1 — 0
		CO^+	$A^2\Pi - X^2\Sigma$	5 — 0
		N_2^+	$B^2\Sigma - X^2\Sigma$	1 — 0
(2)	3594	CO^+	$A^2\Pi - X^2\Sigma$	5 — 0
		OH^+	$^3\Pi - {}^3\Sigma$	0 — 0
(2*n*)	3616.3	OH^+	$^3\Pi - {}^3\Sigma$	0 — 0
(4)	3674.0	CO_2^+	$^2\Pi - {}^2\Pi$	0 — 1
(2)	3695	CO^+	$A^2\Pi - X^2\Sigma$	6 — 1
		CO_2^+	$^2\Pi - {}^2\Pi$	1 — 2
(1)	3709	CO^+	$A^2\Pi - X^2\Sigma$	6 — 1
		CO^+	$B^2\Sigma - A^2\Pi$	1 — 0
(1)	3726	CO^+	$B^2\Sigma - A^2\Pi$	1 — 0
(1)	3741			
(3)	3781.3	CO^+	$A^2\Pi - X^2\Sigma$	4 — 0
(2)	3802.5	CO^+	»	4 — 0
(1-0)	3839	CO_2^+	$^2\Pi - {}^2\Pi$	0 — 2
(4)	3913.7	N_2^+	$B^2\Sigma - X^2\Sigma$	0 — 0
(2)	3951.3	CO^+	$B^2\Sigma - A^2\Pi$	0 — 0
(1)	3983	CO^+	»	0 — 0
(7)	4001.5	CO^+	$A^2\Pi - X^2\Sigma$	3 — 0
(6)	4024	CO^+	»	3 — 0
(0-1)	4096			
(2*n*)	4124	CO^+	$A^2\Pi - X^2\Sigma$	4 — 1
(1)	4140	CO^+	»	4 — 1
(1)	4171			
(1)	4231	CO^+	$B^2\Sigma - X^2\Pi$	0 — 1
		N_2^+	$B^2\Sigma - X^2\Sigma$	1 — 2
(5)	4250.9	CO^+	$A^2\Pi - X^2\Sigma$	2 — 0
(4)	4273.8	CO^+	»	2 — 0
		N_2^+	$B^2\Sigma - X^2\Sigma$	0 — 1
(2)	4543.8	CO^+	$A^2\Pi - X^2\Sigma$	1 — 0
(1)	4568.5	CO^+	»	1 — 0
(0-1)	5048	CO^+	»	1 — 1

On the whole the evidence is rather in favor of the same fluorescence excitation mechanism for all the molecular bands of the head and tail.

Description of the individual bands of the tail of a comet

CH^+ and OH^+

The strongest bands of these two ions are found in the head; they have a small extension into the tail.

The transitions concerned are:

for CH^+: (0-0) and (1-0) of $^1\Pi - {}^1\Sigma$,

for OH^+: (0-0) of $^3\Pi - {}^3\Sigma$.

These weak emissions are partly blended with other bands; however a discussion of the expected intensity distributions within the blending bands leads to the conclusion that CH^+ and OH^+ contribute to the spectrum.

CO^+

The most prominent emission in the tail is that of the «comet tail system» $A^2\Pi - X^2\Sigma$ of CO^+. On account of the very low resolution which is always used for comet tail spectra no structural detail of the fairly narrow CO^+ bands can be detected, except the double structure.

Weaker emissions of comet tails may be assigned to the Baldet-Johnson system $B^2\Sigma - A^2\Pi$ of CO^+, whose lower level is the excited state of the comet tail system. The low intensity of this system is consistent with the weakness of solar radiation in the region around λ 2100 which is required for the excitation from the ground state $X^2\Sigma$ to the upper state $B^2\Sigma$.

N_2^+

The $B^2\Sigma - X^2\Sigma$ system is observed in comet tails ,the strongest transition being (0-0), λ 3914; the N_2^+ bands are similar to those observed in the twilight glow.

The N_2^+ bands are usually weaker than those of CO^+; the N_2^+ bands seem broader, a fact which is consistent with the homonuclear character of N_2^+.

CO_2^+

Once the C. T. and B. J. bands of CO^+, and the N_2^+ emissions have been assigned, there still remain strong emissions in the ultraviolet region of the comet tail spectra. These have been assigned by Swings and Page [4] to the CO_2^+ bands. The most characteristic CO_2^+ bands in comet tails are λ 3509 and λ 3674.

Discussion of CN^+

A rather striking coincidence has been observed between intensity maxima observed on comet tail spectrograms and the (0-1) band, $c^1\Sigma - a^1\Sigma$ system, of CN^+ near λ 3403. A careful study shows that the observed intensity maxima are actually features of the solar spectrum (moonlight) which was superimposed on the comet tail spectra. On the basis of the cometary material which is at present in existence and of the available analysis of the CN^+ spectrum, there is no evidence for CN^+ in comets. However this question should be kept in mind by future observers of cometary spectra.

Continuum in comet tails

At small heliocentric distances a comet tail may reveal a continuous spectrum in addition to the CO^+, N_2^+ and CO_2^+ bands. The molecular bands may even be absent. In this case the tail consists mainly of solid particles reflecting the solar radiation.

Distribution of the neutral and ionized molecules

Only molecular ions are found in the tail at large distances from the head; these ions may also be present in the head even on the sunward side. The neutral molecules are confined to the head. We have found no unambiguous case of a comet tail consisting of neutral molecules; erroneous identifications are easy on low resolution spectrograms.

General remarks on the cometary molecules

All the observed emissions belong to physically stable, but chemically highly reactive neutral molecules (radicals) or ions. The predominance of radicals requires a very low density in the head. The same result is evident from the very different «rotational temperatures» derived from bands of different molecules. This appears especially strikingly when comparing homonuclear C_2 ($T_{rot} \simeq 3000°K$) and heteronuclear OH ($T_{rot} \simeq 50°K$): such a departure from thermodynamical equilibrium can be explained only by the absence of collisions.

Each molecule in the head or tail may be considered as independent. Its physical conditions are determined by external influences, that is by solar radiation. All kinds of solar radiation, corpuscular as well as electromagnetic, may theoretically be considered. However only fluorescence excitation has been firmly established; thus far no spectroscopic feature has been assigned to a corpuscular influence.

The observation of a reflected solar spectrum proves the existence of solid particles (of unknown size) or of polyatomic molecules in a small central part of the head surrounding the solid nucleus.

It is difficult to draw a more detailed picture of the structure

of the solid nucleus and of the liberation of the gases than F. L. Whipple ([23]) has done in his «icy conglomerate» model. How and where do the spectroscopically observed radicals originate? There are three possibilities. The radicals may be formed in the head itself by an external influence (mainly photodissociation by solar ultraviolet radiation) from chemically stable molecules issued from the solid nucleus by sublimation, desorption or sputtering caused by electromagnetic or corpuscular radiation from the sun. In the solid nucleus the molecules would be present as pure ices, solid hydrates or adsorbed gases. The radicals may also have been trapped in the crystal structure of the chemically stable molecules at low temperatures and be liberated by the effect of solar radiation ([24]). Chemical reactions, possibly triggered by trapped radicals, may also take place in a thin layer at the surface of the nucleus.

Behavior of the molecular bands and of the continuum

Use of the heliocentric distance as a parameter

On all of the Atlas plates the cometary spectrograms have been classified according to the heliocentric distance r. This distance defines the amount of solar radiation which reaches the comet per cm² per second. There is no better parameter for the classification of cometary spectrograms and for the subsequent discussion of the behavior of the bands and continuum.

One may wonder whether the whole solar energy received by the solid nucleus in its course either on a periodic orbit or on a parabolic orbit does not affect the chemical and physical conditions of the surface of the nucleus, hence of the surrounding cometary atmosphere produced by the nucleus. The determination of the total amount of energy E received per cm² of the nucleus is easily computed in terms of the solar constant. However one may fear that a classification of the spectrograms according to the E-parameter be valueless for the following reasons:

(*a*) There is no essential spectroscopic difference between certain parabolic and periodic comets. Yet in the case of long known periodic comets the E-parameter which may be calculated for an assumed number of revolutions would differ greatly from the E-parameter corresponding to a parabolic orbit.

(*b*) After perihelion passage the E-parameter is extremely sensitive to the perihelion distance q. For a given r after perihelion a small difference in the q-value gives a drastic difference in the E-value. No such effect is found in cometary spectra.

Actually an elaborate comparison of cometary spectrograms corresponding to approximately equal values of the E-parameter has not led us to any interesting systematic result. It has clearly appeared that a classification based on the heliocentric distance r (equivalent to dE/dt) is more satisfactory than an E-classification, and that it is indeed the only possible one in the present status of our knowledge of cometary physics. The changes in the main spectroscopic features of a comet are determined by the situations prevailing at the instants of observation (or possibly in the very near past), and not by the whole history of the comet.

This does not mean that there are no individual differences among comets: the opposite is true as will be seen later in this section. But the slow changes in the crust of the nucleus due to the accumulated influence of the solar radiation affect the atmospheres of comets less than the changes in heliocentric distance in the neighborhood of the sun. Generally speaking the spectroscopic features depend on the one hand on the type of comet and on the other hand, on the heliocentric distance r, and not (or only slightly) on E.

Behavior of the emissions of the head at different heliocentric distances; usual development of the spectrum

At large heliocentric distances ($r > 3$ A.U.) the cometary light consists only of a solar reflected spectrum ([3]). The (0-0) band of CN is generally the first molecular emission to appear ($r \simeq 3$ A.U.). It presents at once the usual considerable extension into the head. A few unusual comets have only a continuous spectrum at all heliocentric distances, even at $r < 1$ A.U.

Around $r = 2$ A.U. the C_3- and NH_2-emissions appear. They are much shorter than the CN-lines; their intensities may be compared to those of CN and the continuum in the central part of the head. Around $r = 2$ the C_3 emission is stronger than the (0-1) band of CN; the intensity ratio of C_3 and CN(0-1) is still greater than 1 at $r = 1.5$, but decreases with decreasing r. The NH_2 emission appears to vary little relative to the continuum. Variations in the relative intensities of the short NH_2-lines and of the other cometary emissions are not easily detected on account of the customary strength of the solar spectrum in the red region, of the scarcity of observational material in the visual range, and of the usually peculiar sensitivity curves of the panchromatic emulsions.

The Swan bands appear around $r = 1.8$ A.U.; they exhibit at once their normal extension into the head, as well as their high temperature distribution of the rotational and vibrational line intensities.

Around $r = 1.5$ A.U. all other molecular emissions (OH, NH, CH) are present. In certain comets, the continuum is no longer predominant; in others it still appears strongly, accompanied by the molecular bands; in exceptional cases the continuum may appear with the (0-0) band of CN only.

For $r < 1.5$ A.U. the molecular bands are often strong enough to reveal their structure. A distinction must be made between the homonuclear (C_2, C_3) and heteronuclear (CN, CH, OH, NH) molecules. The profiles of the C_2 and C_3 bands do not vary appreciably with r. Weaker emissions of C_3 or some structure within the Swan bands may occasionally be observed, but they are probably a consequence of a greater intensity or of a higher resolution rather than of an important variation in the profile. On the contrary the profiles of the OH-, NH-, CH- and CN-bands vary with r and with dr/dt. The observations of profiles of OH and NH are rather scanty, yet show definite variations; the observations of CH are difficult (shortness of the lines!). The bands of CN provide the amplest evidence for the variations of the profiles. At $r = 2$, only (0-0) is present with rotational lines up to $J = 10$. At $r = 1.5$, J goes to 15. At $r < 1$, (1-0), (0-0) and (0-1) are present, with traces of (1-1), (1-2) and (2-2); J may be as high as 20 or even 25 at very small r. The changes in rotational structure do not represent changes in temperature, since the latter has no physical meaning; they may be interpreted by the fluorescence mechanism of excitation.

After perihelion passage the development proceeds in the opposite sense. The only clear difference between pre- and post-perihelion spectra appears in the profiles of CN; it is due to the considerable change in radial velocity going for example from $v \simeq -30$ Km/sec. to $v \simeq +30$ Km/sec. The shift in the exciting solar spectrum corresponding to such a variation in radial velocity appears clearly in the profile of CN.

No other systematic difference between pre- and post-perihelion spectrograms has been observed. However this conclusion is only based on spectrograms of different comets: for no comet have pre- and post-perihelion spectra been available. An effort should be made in this direction; it will require a collaboration between northern and southern observers who should endeavor to obtain spectrograms under similar instrumental conditions.

None of the spectrograms at our disposal reveals a clear structure of the lines or of the continuum that could be related to a visible structure appearing on photographs of the head. Such a correlation would require extremely good instrumental conditions.

Changes in the relative intensities of the continuum and of the molecular emissions do not appear to be related to the heliocentric distance. The only observed regularities are:

(*a*) The continuum is always predominant at large r;

(*b*) A comet which has a strong continuum between $r = 1$ and 1.5 may be expected to retain it for $r < 1$.

Behavior of the emissions of the tail

The development of the tail spectrum can best be followed on objective prism plates or on direct photographs taken with filters. Comets begin to produce a tail at heliocentric distances varying from $r = 1.5$ downward. The tail becomes more pro-

minent with decreasing r, but considerable fluctuations may occur both in its structure and its intensity.

The distributions of the CO^+- and N_2^+-molecules in the tail seem to be the same. From the scanty material on CO_2^+ in Comet 1948 I it also appears that CO_2^+ has approximately the same distribution. It seems that CH^+ and OH^+ have shorter extensions.

There has been a widespread tendency to try to explain the different classes of tails by the presence of different molecules. This view is not confirmed by a critical examination of our tail spectrograms. The emission in all the tails consists of the bands of the ionized molecules CO^+, N_2^+ and CO_2^+ (with a minor contribution of CH^+ and OH^+), with an occasional contribution or even predominance (at small r, $r < 0.2$) of a solar continuum. As far as we were able to ascertain no appreciable contribution of neutral molecules to tail spectra has been conclusively demonstrated; no CN- or C_2-tail has been found in our collection of spectrograms.

At small heliocentric distances the activity of the tail increases, and a continuous spectrum may appear together with an enormous extension of the tail.

With the available dispersions it is impossible to determine spectroscopically the cometocentric velocities of the emitting molecules or of the scattering particles.

Relative intensities of the CN, C_2, CH *and* C_3 *bands in the spectra of different comets*

We have already mentioned that the intensity ratio of the main ultraviolet bands, those of OH and NH, varies considerably from one comet to another. Differences exist also in the behavior of the four molecules which are observed in the blue-violet region, a convenient spectral region on account of the fairly uniform sensitivity of the photographic emulsions.

On all our spectrograms we compared the intensity of the (0-1) band of CN in the central region of the head with those of C_3 (λ 4052), of CH (λ 4313) and of C_2 (2-0 band at λ 4381) in the same region.

(1) *Relative intensities of the* (0-1) *band of* CN *and of the* C_3 *band in the central region of the head.*

At $r < 0.6$ CN is usually stronger than C_3. For most comets, the range from $r = 0.6$ to 1.0 is a transition region between $CN > C_3$ and $CN < C_3$. At $r > 1.0$ C_3 is usually stronger. However for certain comets the transition occurs at greater heliocentric distances, for example at $r = 1.2$. At $r = 2$ C_3 is always stronger than (0-1) of CN which begins to disappear at $r > 2$.

There is no essential difference between pre- and post-perihelion spectra.

(2) *Relative intensities of the* (0-1) *band of* CN *and of the* (0-0) *band of* CH *in the central region of the head.*

For $r > 1.2$ all comets show CN > CH. But at $r < 1.2$ two very different developments occur.

A first group of comets retains the relation CN > CH for the whole observed range of heliocentric distance.

A second group has CN > CH for $r < 0.8$ and for $r > 1.2$, but shows CN < CH for $0.8 < r < 1.2$. This is the case for Comets 1910 II, 1947 XI and 1948 I, which were all observed after perihelion passage; no observation for $r < 0.7$ is available. Comet 1941 I which was observed before perihelion displays a similar behavior, but has CN < CH for $r = 0.5$.

(3) *Relative intensities of the* (0-1) *band of* CN *and of the* (2-0) *band of* C_2 *in the central region of the head.*

We found no example of $CN < C_2$. Almost all comets show $CN > C_2$ at all heliocentric distances; however between $r = 0.4$ and 1.2 a few comets, such as 1907 IV, 1908 III, 1910 II, 1939 III, 1947 XI showed $CN \simeq C_2$ for a short time.

All such comparisons lead us to believe that most comets have their individual characters, that is individual chemical compositions. It would seem that the abundance ratio which is most sensitive and most characteristic is the ratio of carbon to hydrogen. This may possibly lead eventually to the discovery of «genetic families» of comets of different chemical composition, which may have originated either in the original solar nebula, or in proto-Jupiter, proto-Saturn, etc... However a decision on this matter is not warranted yet.

Relations between the spectroscopic and integrated observations

We already stated that the spectrograms of comet heads do not reveal structures such as halos or envelopes. We may however try to find out whether the spectra are related somehow to other integrated properties, such as the absolute magnitude (H_0), the rate of change of the brightness of the head with heliocentric distance (n-factor) and the «diameter» (d) of the head. The values of H_0 and n have been given in table 2 whenever available. They are defined by the usual formula

$$H_0 = m - 5 \log \Delta - 2.5\, n \log r,$$

where

m = observed magnitude,
Δ = geocentric distance,
r = heliocentric distance,
H_0 = magnitude for $\Delta = r = 1$,
n = rate of change (brightness formula $I = I_0 . \Delta^{-2} . r^{-n}$).

For a spherical solid body, $n = 2$. For self-luminous objects, $n > 2$. There are a number of practical reasons why the formula is of very limited meaning, in addition to its empirical character; actually the same reasons apply to other proposed formulae which appear less empirical:

(*a*) The luminosity curve of a comet rarely varies smoothly with r.

(*b*) It is difficult to obtain a good estimate of the visual or photographic magnitudes (which may moreover be quite different).

(*c*) The measured brightness integrates over as many components as there are different molecules emitting in the spectral region concerned, plus sometimes a continuum (example: visual observations integrate over the C_2 and NH_2 bands, plus the continuum; photographic observations in the violet integrate over CN, C_3, CH, C_2 and the continuum). Each molecule has a specific behavior in relation to r.

These difficulties of cometary photometry and the need for monochromatic magnitudes have been stressed recently in great detail ([25]). Yet, pending precise monochromatic magnitudes, the classical formula and the corresponding values of H_0 and n may be useful in a limited sense. In the determination of H_0 and n the short duration phenomena in the head are smoothed out; a comparison between different comets is thus made possible. Moreover the correlation between the spectroscopic phenomena and the values of H_0 and n may possibly give a physical meaning to H_0 and n : for example the presence of a strong continuous background is expected to affect the value of n.

We proceeded to a systematic comparison of the relative intensities of the continuum and the molecular bands with the absolute magnitude H_0, the n-factor and the period P. Although no clear cut conclusion was reached the main results are summarized here.

In the case of comets on parabolic orbits there is a tendency toward a stronger continuous (solar reflected) spectrum at larger heliocentric distances. This tendency is illustrated in the following comparison based on 18 comets:

for $r > 1$, 6 comets show a strong continuum;
4 have a faint continuum;
for $r < 1$, 1 has a strong continuum;
7 show a faint continuum.

For comets of long period ($\geqslant$ 100 years) there appears to be no correlation between the period and the intensity of the continuous spectrum, whatever r may be ($<$ or >1). A group of three short period-comets ($3 < P < 10$ years) show a strong continuum for $r < 1$. Comet Encke ($P = 3.3$ years) seems to be an exceptional case: all through the range from $r = 0.7$ to 1.3 A.U., the continuum is absent or extremely faint.

There appears to be no correlation between the value of the n-exponent and the intensity of the continuum; this holds for $r < 1$ as well as for $r > 1$. The n values are grouped around a mean value between 3 and 4, irrespective of whether the continuum is strong or faint.

There seems to be a tendency for intrinsically brighter comets to possess a stronger continuum. The absolute magnitudes of the comets displaying a strong continuum average one magnitude brighter than the others. This may possibly be an effect of age (the brighter comets being on the average, fresher and younger objects). Or it may possibly mean that the gaseous emission is more or less independent of the dust content, which may be variable in a given comet.

These rather vague statistical results illustrate the difficulties involved in any theory on the origin, evolution and classification of comets. Possibly these difficulties will disappear partly when good monochromatic magnitudes become available.

Similarly a comparison of the spectra with the measurements of «diameters» reveals the vagueness of the concept of diameter. Considerable effort has been devoted to the «measurement» of «diameters», with the general result that the diameter reaches a maximum around $r = 1.4$ A.U. and decreases for both smaller and larger values of r. Most Atlas Plates show the very different extensions of different molecules into the head. What then is the diameter of the head ?

The head of a comet has no physical limit. Its intensity distribution fades out gradually. The intensity gradient is different for different molecules. A precise definition of the size of the head for a specific molecule would be the diameter of a region such that the intensity on the edge is a given fraction (say one half) of the intensity at the center. In such measurements which may be performed by various techniques corrections should be made for the superimposed continuous emission of the central region and for the sky background.

Comparison between the spectra of comets and the spectra of N-stars, aurorae, twilight glow, nightglow and combustion phenomena

The absorption bands of the late carbon stars belong to the same molecules as the main emissions of comets—that is CN, C_3, CH and C_2. Some of the unassigned Merrill-Sanford bands of N stars—which probably belong to a polyatomic C_2X molecule—coincide with unexplained cometary emissions [13]. The C_3-band extends probably shortward of the (0-0) band of CN in N-stars as well as in comets when λ 4052 is very strong. Two important differences between the spectra of N-stars and of comets—beside the obvious fact that in the N-stars the bands appear in absorption instead of in emission as in comets—are:

(*a*) the rotational and vibrational intensity distributions in carbon stars have a real meaning and correspond to the excitation temperature of the molecules;

(*b*) the late N-stars exhibit the strong violet continuum associated with C_3 while there is no trace of it in comets.

Aurorae have many points in common with comets. Among the strongest bands of the aurora is the N_2^+ system which is also present in comet tails. At one time or another various auroral emissions have been assigned to molecules which are present in comets, such as OH. In both cases the temperature would be relatively low. A detailed discussion of the identifications in the spectra of aurorae would be helped by a comparison with comets. This applies especially to the ultraviolet and red regions. It should be emphasized that the excitation mechanisms are different in aurorae (collisions) and comets (fluorescence). However in sunlit aurorae, fluorescence is probably active as in comets.

The twilight glow shows N_2^+- and Na-emissions which are also present in comets. In both cases fluorescence is the excitation process.

In discussions on the nightglow spectrum molecules have been considered which are observed in comets or aurorae. A detailed comparison will be fruitful.

The spectra of combustion phenomena such as flames reveal bands belonging to the same molecules as those of comets. This is illustrated by plate XXI. In particular the C_3-bands appear in certain flames as they do in comets; but unlike the comets the flames often show the continuum associated with C_3.

No detailed comparison will be carried out here. However it is hoped that the Atlas will be of help in the discussions on N-stars, aurorae, twilight, nightglow and combustion phenomena.

REFERENCES

(1) F. Baldet and G. de Obaldia, *Catalogue Général des Orbites de Comètes, de l'an* — 466 à 1952, Ann. Bureau Longitudes, Paris, 1950.

(2) J. Bouska and V. Vanysek, various papers in *Bull. Ast. Inst. Czekoslovakia*, vol. I, II, IV, V (1947 to 1954). Also: J. Bouska, in « La Physique des Comètes » *Mém. in* 8°, *Soc. R. Sc. Liège*, 4th Series, vol. 13, p. 25, 1953. (This volume contains the contributions presented at the Fourth International Astrophysical Symposium in Liège; it will hereunder be referred to as P. Co.).
V. Vanysek, P. Co., p. 30.
M. Beyer, A. N., numerous notes from 1933 to 1955.

(3) N. U. Mayall, *Pub. A.S.P.*, **53**, 340, 1941.
G. Herbig, *Pub. A.S.P.*, **58**, 61, 1946 (in H. M. Jeffers, *Comet Notes*).
R. Minkowski, private communication.

(4) P. Swings and T. L. Page, *Ap. J.*, **108**, 526, 1948; **111**, 530, 1950.

(5) T. L. Page, *P. Co.*, p. 49.

(6) P. Swings, note in «*Vistas in Astronomy*», Pergamon Press Ltd., 1955.

(7) P. Swings, *Lick Obs. Bull.*, **19**, 131, 1941.

(8) A. McKellar, *Rev. Mod. Phys.*, **14**, 179, 1942; *Ap. J.*, **98**, 1, 1943; *P. Co.*, p. 116.

(9) J. Hunaerts, *Ann. Obs. R. Belg.*, 3d Series, vol. V, p. 3, 1950.

(10) D. Barbier, *P. Co.*, p. 263.

(11) J. Hunaerts, *P. Co.*, p. 62.

(12) J. Hunaerts, *Ann. Obs. R. Belg.*, 3rd Series, vol. VI, fasc. 4, p.97, 1954.

(13) P. Swings, *Ann. Aph.*, **16**, 307, 1953.

(14) P. D. Jose and P. Swings, *Ap. J.*, **111**, 41, 1950.

(15) A. McKellar, *Ap. J.*, **99**, 162, 1944.

(16) P. Swings, C. T. Elvey and H. W. Babcock, *Ap. J.*, **94**, 320, 1941.

(17) P. Swings, *Ap. J.*, **95**, 270, 1942.

(18) A. McKellar, *Ap .J.*, **99**, 162, 1944.

(19) N. T. Bobrovnikoff, *Pub. A.S.P.*, **42**, 119, 1930; *Ap. J.*, **99**, 173, 1944.

(20) A. S. King and P. Swings, *Ap. J.*, **101**, 6, 1945.

(21) N. H. Kiess and H. P. Broida, Private communication.

(22) R. Copeland and J. G. Lohse, *Copernicus* (Dublin), **2**, 225, 1882.
P. Swings, *La physico-chimie des comètes*, confér. Palais de la Découverte, p. 15, 1951.
P. Ledoux, private communication.

(23) F. L. Whipple, *Ap. J.*, **111**, 375, 1950; **113**, 464, 1951; *P. Co.*, p. 281.

(24) L. Haser, *Comptes rendus*, Paris, **241**, 742, 1955.

(25) P. Swings, *Report of Chairman of Commission* 15, *Draft Reports of the I.A.U.*, p. 120, 1955.

IMPORTANT DATA CONCERNING THE LABORATORY SPECTRA OF MOLECULES WHICH ARE OBSERVED IN COMETS

OH

In the laboratory the electronic spectrum of OH is known between λ 2400 and λ 3600 Å. All the bands observed in this region belong to a $A^2\Sigma^+ \rightleftarrows X^2\Pi_i$ transition. They are degraded to the red and have four heads (R_1, R_2, Q_1, Q_2). On spectrograms taken with low resolution only the R_1 head is conspicuous.

In addition, the vibrational-rotational spectrum has been observed in the infra-red (1).

Several bands which have been tentatively ascribed to OH can be excited in special types of discharges in the λ 4200 - λ 5500 Å region (2), (3), (4).

Table I gives the wave lengths of all the known bands of the $A^2\Sigma^+ - X^2\Pi_i$ system, according to (5), and the transition probabilities according to (8).

TABLE I

OH-Bands

v' / v''	0	1	2	3	4	5
0	3063.56 (0.907)	2811.32 (0.086)	2609 (0.006)	2444 (0.000)		
1	3428.02 (0.089)	3121.64 (0.716)	2875.30 (0.169)	2677 (0.023)	2517 (0.003)	
2	(0.003)	3483.74 (0.186)	3184.69 (0.514)	2944.96 (0.237)	2753 (0.054)	(0.007)
3		(0.012)	(0.280)	3253.87 (0.321)	3022 (0.253)	
4			(0.032)	(0.329)	3331	

Note to Table I:

The wavelength data in the earlier literature vary considerably from one author to an other, mainly on account of the lack of resolution of the individual lines. The data listed in Table I are taken from the very complete recent high dispersion work by Dieke and Crosswhite (5), where an extensive list of molecular constants may be found. When the second decimal place is given the wave length is that of the R_1 line nearest to the head. For the other (mostly weak) bands only the approximate position of the head can be given. For a possible extension of this table towards higher v'-values see (4b).

Table II gives the wave lengths of the lines corresponding to K= 1 to 5 for the (0-0) and (1-1) bands, the only transitions observed in comets (6). The other bands are either too faint or located outside the observable range.

The data in Table II are taken from (5). Details of the identifications are given in (7).

The transition probabilities for the vibrational and rotational transitions in the OH bands have been studied in detail in (5), where a complete review of earlier theoretical and experimental investigations in this field may be found. New calculations have been made by W. R. Jarmain, P. A. Fraser, and R. W. Nicholls (8).

It is interesting to note that the bands with $v' > 1$ are relatively weak in the laboratory in spite of their theoretically high intensity. This may perhaps be explained by a weak predissociation studied by A. G. Gaydon and H. G. Wolfhard (9). Concerning the intensity anomalies of the OH bands in emission see (10).

A Spectrophotometric Atlas of the Bands of OH taken with high resolution between λ 2610 and λ 3520 has recently been published by A. M. Bass and H. P. Broida (11).

REFERENCES

(1) W. S. Benedict, E. K. Plyler and G. J. Humphreys, *J. Chem. Phys.*, **21**, 398, 1953.

(2) H. Schlüer and L. Reinebeck, *Zs. f. Naturf.*, **4a**, 560, 1949.

(3) S. Leach, *C. R.*, **228**, 1006, 1949.

(4a) S. Benoist, *C. R.*, **238**, 883, 1954.

(4b) S. Benoist, *Ann. de Phys.*, **10**, 25, 1955.

(5) G. H. Dieke and H. M. Crosswhite, *The Ultraviolet Bands of OH*, Fundamental Data, The Johns Hopkins University, Bumblebee Series Report No. 87, Nov. 1948.

(6) P. Swings, C.T. Elvey and H. W. Babcock, *Ap. J.*, **94**, 320, 1941, and **95**, 218, 1942.
P. Swings and T. L. Page, *Ap. J.*, **111**, 530, 1950.

(7) J. Hunaerts, *Mém. Soc. Roy. Sc. Liège*, **13**, 59, 1953.

(8) W. R. Jarmain, P. A. Fraser and R. W. Nicholls, *Ap. J.*, **122**, 55, 1955.

(9) A. G. Gaydon and H. G. Wolfhard, *Proc. Roy. Soc.*, A, **208**, 63, 1951.

(10) A. G. Gaydon and H. G. Wolfhard, *Revue Instit. Franç. du Pétrole*, **4**, 405, 1949.
A. G. Gaydon and H. G. Wolfhard, *Flames*, Chapman and Hall Ltd, 1953.

(11) A. M. Bass and H. P. Broida, *A Spectrophotometric Atlas of the $^2\Sigma^+ - {}^2\Pi_i$ Transition of OH*, Nat. Bur. of Stand. Circular 541, June 1953.

TABLE II

First Lines of the (0-0) and (1-1) Bands

First lines of the (0-0) *transition*

P_1		Q_1		R_1	
J	λ	J	λ	J	λ
1.5	3081.665	1.5	3078.440	1.5	3072.009
2.5	3086.390	2.5	3079.951	2.5	3070.318
3.5	3091.186	3.5	3081.541	3.5	3068.704
4.5	3096.124	4.5	3083.278	4.5	3067.240
5.5	3101.229	5.5	3085.196	5.5	3065.976

P_2		Q_2		R_2	
J	λ	J	λ	J	λ
0.5		0.5	3090.473	0.5	3084.050
1.5	3096.349	1.5	3089.861	1.5	3080.231
2.5	3099.593	2.5	3089.861	2.5	3077.028
3.5	3103.342	3.5	3090.364	3.5	3074.369
4.5	3107.553	4.5	3091.361	4.5	3072.199

$^{O}P_{12}$		$^{P}Q_{12}$		$^{Q}P_{21}$	
J	λ	J	λ	J	λ
0.5		0.5	3093.722	1.5	3078.468
1.5	3099.593	1.5	3096.349	2.5	3080.006
2.5	3106.017	2.5	3099.538	3.5	3081.620
3.5	3113.075	3.5	3103.267	4.5	3083.374
4.5	3120.578	4.5	3107.457	5.5	3085.317

$^{Q}R_{12}$		$^{R}Q_{21}$		$^{S}R_{21}$	
J	λ	J	λ	J	λ
0.5	3090.449	1.5	3072.063	1.5	3062.523
1.5	3089.861	2.5	3070.392	2.5	3057.727
2.5	3089.861	3.5	3068.799	3.5	3053.051
3.5	3090.270	4.5	3067.356	4.5	3048.565
4.5	3091.186	5.5	3066.114	5.5	3044.325

TABLE II *(continued)*

First Lines of the (0-0) and (1-1) Bands

First lines of the (1-1) *transition*

P_1		Q_1		R_1	
J	λ	J	λ	J	λ
1.5	3137.749	1.5	3134.578	1.5	3128.224
2.5	3142.522	2.5	3136.174	2.5	3126.674
3.5	3147.410	3.5	3137.894	3.5	3125.236
4.5	3152.454	4.5	3139.791	4.5	3123.945
5.5	3157.712	5.5	3141.909	5.5	3122.958

P_2		Q_2		R_2	
J	λ	J	λ	J	λ
		0.5	3147.112	0.5	3140.731
1.5	3152.967	1.5	3146.560	1.5	3137.056
2.5	3156.241	2.5	3146.631	2.5	3133.989
3.5	3160.067	3.5	3147.274	3.5	3131.469
4.5	3164.394	4.5	3148.752	4.5	3129.532

$^{O}P_{12}$		$^{P}Q_{12}$		$^{Q}P_{21}$	
J	λ	J	λ	J	λ
		0.5	3150.314	1.5	3134.599
1.5	(3156.14)	1.5	3152.947	2.5	3136.227
2.5	3162.609	2.5	3156.184	3.5	3137.969
3.5	3169.613	3.5	3159.989	4.5	3139.886
4.5	3177.227	4.5	3164.297	5.5	3142.023

$^{Q}R_{12}$		$^{R}Q_{21}$		$^{S}R_{21}$	
J	λ	J	λ	J	λ
0.5	3147.112	1.5	3128.281	1.5	3218.879
1.5	3146.504	2.5	3126.745	2.5	3214.262
2.5	3146.560	3.5	3125.329	3.5	3209.801
3.5	3147.195	4.5	3124.094		
4.5	3148.309	5.5	3123.096		

In the laboratory the emission spectrum of NH has been observed in various flames and discharges. Four transitions are known:

1. $A^3\Pi_i \rightleftarrows X^3\Sigma^-$ in the region λ 3300 - λ 3500 Å, without conspicuous heads. References: (1), (2), (3).

2. $c^1\Pi \rightarrow b^1\Sigma^+$ in the region λ 4500 - λ 4600 Å, degraded to the red, with a R (0-0) head at λ 4502.0 Å and a Q (0-0) head at λ 4523.2 Å. Reference: (4).

3. $c^1\Pi \rightarrow a^1\Delta$ in the region λ 3240 - λ 3650 Å, degraded to the red, with the strongest R (0-0) head at λ 3240.1 Å and the Q (0-0) head at λ 3253.4 Å. References: (5), (6), (7), (11).

4. $d^1\Sigma \rightarrow c^1\Pi$ in the region below λ 2560 Å, degraded to the violet, P (0-0) head at λ 2557.3 Å, Q (0-0) head at λ 2530.2 Å. Reference: (8).

The ground level of the NH molecule is involved only in the $A^3\Pi_i \rightleftarrows X^3\Sigma^-$ transition; accordingly this is the only important transition for cometary investigations. In the laboratory it has been observed in emission as well as in absorption (3).

Table III contains the wave lengths of the first rotational lines of the (0-0) band. According to Hunaerts (9) the corresponding rotational levels are the only ones involved in the fluorescence mechanism. The values listed in table I are those observed in the laboratory by Funke in emission or absorption (1) (3).

The molecular constants of NH as given in (1), (10) or (11) are not very reliable. Additional work is required in order to obtain a greater precision.

TABLE III

First Rotational Lines of the $A^3\Pi_i - X^3\Sigma^-$ *Transition of* NH

(0 — 0) *band*

K''	R_1	R_2 (1)	R_3 (2)	Q_1 (3)	Q_2 (4)	Q_3 (5)	P_1 (6)	P_2 (7)	P_3
0	3357.8								
1	3353.6	3350.8	3349.6	3361.7					
2	3349.6	3347.6	3346.4	3361.0	3357.8	3355.5	3369.1		
3	3345.6	3344.2	3343.2	3360.6	3358.4	3356.5	3372.1		3367.7
4	3341.8	3340.8	3339.9	3360.3	3358.8	3357.3	3373.4	3373.4	3372.2

(1) not separated from $^RQ_{21}$
(2) » » » $^RQ_{32}$ and $^RP_{31}$
(3) » » » $^QR_{12}$
(4) » » » $^QR_{23}$ and $^QP_{21}$
(5) » » » $^QP_{32}$
(6) » » » $^PQ_{12}$ and $^PR_{13}$
(7) » » » $^PQ_{23}$

REFERENCES

(1) G. W. Funke, *Zs. f. Physik*, **96**, 787, 1935.
(2) G. W. Funke, *Dissertation*, Stockholm, 1936.
(3) G. W. Funke, *Zs. f. Physik*, **101**, 104, 1936.
(4) R. W. Lunt, R. W. B. Pearse and E. C.W. Smith, *P.R.S.*, A, **151**, 602, 1935.
(5) R. W. B. Pearse, *P.R.S.*, A, **143**, 112, 1933.
(6) G. Nakamura and T. Shidei, *Japan. J. Phys.*, **10**, 5, 1934.
(7) R. Florent and S. Leach, *J. Phys. Rad.*, **13**, 377, 1952.
(8) R. W. Lunt, R.W.B. Pearse and E.C.W. Smith, *P.R.S.*, A. **155**, 173, 1936.
(9) J. Hunaerts (private communication).
(10) G. Herzberg, *Spectra of Diatomic Molecules*, 1950.
(11) Tables de Constantes (B. Rosen, edit.) vol. 4, 1951.

CH

In the laboratory the emission spectrum of CH has been observed in various flames and discharges under a wide range of conditions. Three electronic transitions of CH are known:

I) Transition $A^2\Delta - X^2\Pi$.
Region λ 4135 Å to λ 4950 Å.
Most characteristic band heads (degraded to the violet):
Q (0 — 0) head near λ 4315 A;
Q (0 — 1) head near λ 4890 A.
References: (1), (2), (3).

II) Transition $B^2\Sigma^- - X^2\Pi$.
Region λ 3600 Å to λ 4120 Å.
Most characteristic band heads (degraded to the red):
Q (0 — 0) head near λ 3889.2 Å;
R (0 — 0) head near λ 3871.7 Å;
R (1 — 0) head near λ 3627.3 Å;
R (1 — 1) head near λ 4025.3 Å.
References: (1), (2).

III) Transition $C^2\Sigma^+ - X^2\Pi$.
Region λ 3080 Å to λ 3230 Å.
Most characteristic feature: group of closely packed lines of the Q branches near λ 3143.5 Å.
References: (1), (2), (4), (5).

The identification of the A — X system of CH in cometary spectra was first made by M. Nicolet (6), that of the B — X system by J. Dufay (7). The problem of the CH-cometary emission has been studied in detail by P. Swings, C. T. Elvey and H. W. Babcock (8) and by A. McKellar (9). A recent review of this question has been published by J. Hunaerts (10), where details concerning the identification of lines, the transition probabilities and the mechanism of fluorescence may be found.

Tables IV, V and VI contain the wave lengths of the first rotational lines of the three band systems of CH.

The spectroscopic molecular constants may be found in (11) and (12). Some new data are listed in (3).

TABLE IV

First Rotational Lines of the $A^2\Delta - X^2\Pi$ *Transition of* CH, *(0 — 0) Band*

J''	R_1	R_2	Q_1	Q_2	P_1	P_2	$^{R}Q_{21}$	$^{Q}P_{21}$	$^{Q}R_{12}$	$^{P}Q_{12}$
0.5		4300.325								
1.5	4303.952	4296.621		4312.709			4303.625		4313.032	
		.660								
2.5	4297.995	4291.118	4314.210	4312.596		4328.834	4297.774	4313.886	4312.900	4329.150
		.223		.709		.919	.			.241
3.5	4292.050	4285.377	4313.591	4312.159	4329.944	4333.846	4291.900	4313.278		4334.209
	.123	.531	.662	.296	4330.005	4334.004				
4.5	4286.007	4279.482	4312.901	4311.503	4334.662	4338.631				
	.199	.711	4313.032	.728	.782	.849				
5.5	4280.032	4273.487	4312.083	4310.690	4339.259	4338.631				
	.221	.791	4313.032	.993	.454	.494				
6.5	4273.931	.4267.395	4311.159	4309.699	4343.696	4347.531				
	4274.196	.805	.437	4310.097	.969	.965				
7.5	4267.763	4261.232	4310.097	4308.578	4347.965	4351.725				
	4268.116	.781	.491	4309.105	4348.340	4352.258				
8.5	4261.537	4255.000	4308.905	4307.314	4352.080	4355.718				
	.999	.636	4309.382	.958	.562	4356.379				
9.5	4255.256	4248.740	4307.583	4305.909	4356.017	4359.515				
	.832	4249.483	4308.171	4306.690	.621	4360.304				
10.5	4248.949	4242.447	4306.147	4304.396	4359.759	4363.109				
	4249.653	4243.346	.848	4305.319	4360.502	4364.052				
11.5	4242.624	4236.110	4304.585	4302.761	4363.322	4366.528				
	4243.465	4237.164	4305.453	4303.833	4364.206	4367.623				

The higher rotational lines are not separated from the corresponding main branches.

Note: In this table wavelength values given in (2) are used. According to (13) they seem to be more reliable than those given in (1).

TABLE V

First Rotational Lines of the $B^2\Sigma^- - X^2\Pi$ *Transition of* CH, *(0 — 0) Band, according to* (2)

J''	R_1	R_2	Q_1	Q_2	P_1	P_2
0.5		3878.772		3886.414		
1.5	3881.486	3877.460	3889.117	3888.912	3892.929	3896.531
2.5	3878.417	3875.312	3889.852	3890.559	3897.491	3901.966
3.5	3875.961	3873.556	3891.192	3892.588	3902.620	3907.774
4.5	3874.054	3872.288	3893.073	3985.081	3908.274	3914.014
5.5	3872.696	3871.546	3895.461	3898.076	3914.427	3920.724
6.5	3871.897	3871.367	3898.395	3901.604	3921.078	3927.945

TABLE VI

First Rotational Lines of the $C^2\Sigma^+ - X^2\Pi$ *Transition of* CH, *(0 — 0) Band, according to* (2)

J''	R_1	R_2	Q_1	Q_2	P_1	P_2
0.5		3137.4				
1.5	3139.31	3135.78	3144.9		3147.77	3149.84
2.5	3136.36	3133.10			3150.42	3152.76
3.5	3133.47	3130.37			3153.15	3155.60
4.5	3130.65	3127.64			3155.89	3158.42
5.5	3127.85	3124.92			3158.63	3161.20

Note. — The Q branches are not resolved for small J.

REFERENCES

(1) E. Fagerholm, *Arkiv för Mat. Astr. och Fysik*, **27**, nº 19, 1941.
(2) K. Gerö, *Zeitschr. f. Physik*, **118**, 27, 1941.
(3) N. H. Kiess, *National Bureau of Standards Reports*, nº 3975, 1955.
(4) T. Hori, *Zeitschr. f. Physik*, **59**, 91, 1929.
(5) T. Heimer, *Zeitschr. f..Physik*, **78**, 771, 1932.
(6) M. Nicolet, *Zeitschr. f. Astroph.*, **15**, 154, 1938.
(7) J. Dufay, *Ap. J.*, **91**, 91, 1940.
(8) P. Swings, C. T. Elvey and H. W. Babcock, *Ap. J.*, **95**, 218, 1942.
(9) A. McKellar, *Ap. J.*, **98**, 1, 1943.
(10) J. Hunaerts, *Ann. Obs. Roy. Belg.*, **6**, 97, 1954.
(11) *Table des constantes* (B. Rosen, Edit.), 1951.
(12) G. Herzberg, *Spectra of Diatomic Molecules*, 1950.
(13) M. Nicolet, *Inst. R. Mét. Belg.*, Misc., fasc. 20, 1945.

CN

The spectrum of the CN molecule can easily be excited in various flames and discharges. The following six systems are actually known and have been studied in detail:

I) Transition $A^2\Pi_i - X^2\Sigma^+$ (red system), observed from λ 4300 Å to λ 15,000 Å.

II) Transition $B^2\Sigma^+ - X^2\Sigma^+$ (violet system), observed from λ 3150 Å to λ 4600 Å.

III) Transition $H^2\Pi - B^2\Sigma^+$, observed from λ 2800 Å to λ 3100 A.

IV) Transition $F^2\Delta - A^2\Pi_i$, observed from λ 2000 Å to λ 2400 Å.

V) Transition $D^2\Pi_i - A^2\Pi_i$, observed from λ 2200 Å to λ 3000 Å.

VI) Transition $D^2\Pi_i - X^2\Sigma^+$, observed from λ 2700 A to λ 3700 A.

Details of these systems:

I) Table VII gives the wave lengths of the most prominent (R_2) heads (*) (degraded to the red) according to ([1]), ([2]) and ([3]), and the relative vibrational transition probabilities (in parenthesis) according to ([4]). New bands with higher v' and v'' values have been listed in ([5]).

(*) For most of the bands included in Table I the Q_1, R_1, R_2, and $^5R_{21}$ heads have been measured, the R_2 head being the most conspicuous particularly on low dispersion spectrograms.

TABLE VII

R_2 *Heads of the* $A^2\Pi_i - X^2\Sigma^+$ *Transition of* CN

v' / v''	0	1	2	3	4	5	6	7
0	10 933	9 148.3	7 876.4	6 927.1	6 192.1	5 607.6	5 130.4	
	(0.499)	(0.321)	(0.126)	(0.040)	(0.011)	(0.003)	(0.000)	
1	14 074	11 247	9 392.5	8 067	7 091	6 333.6	5 731.1	
	(0.370)	(0.046)	(0.242)	(0.195)	(0.094)	(0.036)		
2		14 545			8 272	7 261	6 480.0	5 859.4
	(0.111)	(0.348)	(0.012)	(0.100)	(0.184)			
3			15 050			8 485	7 435	6 632.9
	(0.018)	(0.223)	(0.209)	(0.089)				
4								
	(0.002)	(0.055)	(0.288)					
5								
	(0.000)	(0.007)						
6								
	(0.000)							

Important references: ([1]), ([2]), ([5]). Improved values for the molecular constants given in ([6]) and ([7]) may be found in ([5]) and ([8]). For data on the rotational fine structure of the strongest $A^2\Pi_i - X^2\Sigma^+$ bands see ([1]). The presence of these bands in comets has been discussed in ([9]). This question is not definitely settled.

II) Transition $B^2\Sigma^+ - X^2\Sigma^+$ (violet system).

Table VIII gives the wave lengths of the most prominent heads (degraded to the violet) according to ([5]) and ([8]), and the relative vibrational transition probabilities (in parentheses) according to ([4]).

TABLE VIII

P-Heads of the Violet System

v' / v''	0	1	2	3	4	5
0	3 883.38	3 590.38				
	(0.920)	(0.073)				
1	4 216.01	3 871.43	3 585.88			
	(0.074)	(0.787)	(0.137)			
2	4 606.15	4 197.20	3 861.96	3 583.9		
	(0.005)	(0.121)	(0.691)	(0.180)		
3		4 577.97	4 180.96	3 854.73		
		(0.014)	(0.147)	(0.625)		
4			4 553.15	4 167.76	3 851.31	
				(0.625)		
5				4 531.9	4 158.05	
6					4 514.8	4 152.39
7						4 502.2

TABLE IX

First Rotational Lines of the $B^2\Sigma^+ - X^2\Sigma^+$ *Transition of* CN, (0 — 0) *band*

P - branch		R - branch	
K''		K''	
1	—	0	3874.612
2	3876.319	1	74.001
3	76.843	2	73.373
4	77.353	3	72.738
5	77.836	4	72.050
6	78.302	5	71.369
7	78.753	6	—
8	79.186	7	69.916
9	79.580	8	69.180
10	—	9	68.408
11	80.330	10	67.622
12	—	11	66.815
13	80.995	12	65.989
14	81.300	13	65.155
15	81.575	14	—
	81.626	15	63.399
16	81.871	16	62.484
17	82.078	17	—
18	82.307	18	60.605
19	82.523	19	59.671
20	82.696	20	58.686
21	82.859		58.597
22	82.989	21	57.685
—	—	22	56.668
28	83.387	23	55.631
	band head	24	54.562
			54.497
		25	53.497
		26	52.410

Important references: (4), (5), (8), (10) and (11). For the «tail bands», see (11) and (12). Improved values for the molecular constants given in (6) and (7) may be found in (5) and (8). For details on the calculation of the transition probabilities see (14) and (15).

Table IX gives the first rotational lines of the (0-0) vibrational transition (excerpt from (8)).

Measurements of the rotational lines of the strongest bands of the violet system of $C^{13}N^{14}$ are given in (11).

III) Transition $H^2\Pi - B^2\Sigma^+$,

The strongest heads are $R_2(0 - 0)$ at λ 2842.9 Å and $R_2(0 - 1)$ at λ 3025.6 Å.

Reference (5).

IV) Transition $F^2\Delta - A^2\Pi_i$.

The strongest heads are:

$R_{21}(0 - 1)$, λ 2047.9 Å;
$R_{21}(0 - 2)$, λ 2123.6 Å;
$R_{21}(0 - 3)$, λ 2204.9 Å;
$R_{21}(0 - 4)$, λ 2291.4 Å;
$R_{21}(0 - 5)$, λ 2383.5 Å.

Reference (5).

V) Transition $D^2\Pi_i - A^2\Pi_i$.

The bands have an open structure and the band heads are not obvious.

Reference (5).

VI) Transition $D^2\Pi_i - X^2\Sigma$.

The band heads are not prominent.

Reference (5).

REFERENCES

(1) F. A. Jenkins, Y. K. Roots and R.S. Mulliken, *Phys. Rev.*, **39**, 16, 1932.
(2) G. Herzberg and J. G. Phillips, *Ap. J.*, **108**, 163, 1948.
(3) R. K. Asundi and J. W. Ryde, *Nature*, **124**, 57, 1929.
(4) P. A. Fraser, W. R. Jarmain and R. W. Nicholls, *Ap. J.*, **119**, 286, 1954.
(5) A. E. Douglas and P. M. Routly, *Ap. J.*, Suppl. Series, **1**, 295, 1955.
(6) G. Herzberg, *Molecular Spectra*, 1, 1950.
(7) *Tables de Constantes* (B. Rosen, Edit.), 1951.
(8) J. Weinard, *Ann. d'Astrophysique*, 1956 (in press).
(9) A. S. King and P. Swings, *Ap. J.*, **101**, 6, 1945.
P. Swings and T. L. Page, *Ap. J.*, **108**, 526. 1948.
P. Swings and T. L. Page, *Ap. J.*, **111**, 530, 1950.
(10) W. Jevons, *Proc. Roy. Soc.*, A, **112**, 407, 1926.
(11) F. A. Jenkins and D. E. Woolidge, *Phys. Rev.*, **53**, 137, 1938.
(12) F. A. Jenkins, *Phys. Rev.*, **31**, 539, 1928.
(13) M. W. Feast, *Proc. Phys. Soc.*, London, A, **62**, 121, 1949.
(14) W. R. Jarmain and P. A. Fraser, *Proc. Phys. Soc.*, London, A, **66**, 1153, 1953.
(15) P. A. Fraser and W. R. Jarmain, *Proc. Phys. Soc.*, London, A, **66**, 1145, 1953.

C_2

The emission spectrum of C_2 is easily excited in a wide variety of flames and discharges; it covers the range λ 2300 - λ 9300 Å. Although the C_2-radical is certainly present in most flames containing carbon its observation in absorption is difficult; it is only by the application of the photoflash method that the C_2-radicals have recently been observed with certainty in absorption in the laboratory (1). On the contrary the Swan-bands of C_2 are prominent in absorption in the spectra of many late type stars.

Five electronic transitions are known, of which only the Swan system has been observed in astronomical bodies.

I) Transition $A^3\Pi_g \rightleftarrows X^3\Pi_u$ (Swan bands). This system extends in the laboratory from λ 3400 to λ 7900 Å. The main bands are degraded toward the violet, while the «tail bands» are degraded toward the red.

Table X gives the wave lengths of the observed heads, and the vibrational transition probabilities.

A comparison of the «theoretical profiles» of the C_2-sequences in comets with the laboratory intensity distributions is of great interest. J. Hunaerts (7) has determined theoretical profiles for the C_2-bands excited by a fluorescence mechanism. He predicts weak secundary peaks within the sequences which agree fairly well with certain observed maxima in cometary spectra; his results are in favor of a pure fluorescence excitation. He assumes a Boltzmann distribution of the molecules corresponding to T= 3000 °K. These calculations have been supplemented by A. McKellar and J. L. Climenhaga (15). However it should be pointed out that similar secondary maxima have been observed under various discharge conditions by R. Herman (16) and by B. Rosen, and the agreement between the cometary- and laboratory-maxima is generally satisfactory. Accordingly the argument in favor of fluorescence is not convincing in the case of C_2. Moreover it seems that anomalies appear in the intensity distribution, for example in the (1 — 0) sequence. Such anomalies which are present in laboratory- as well as in cometary spectra deserve further scrutiny. Actually it seems that the whole question of the interpretation of the «high pressure bands» deserves to be carefully reconsidered.

The Swan bands of $C^{12}C^{13}$ and $C^{13}C^{13}$ are of considerable importance in the N-stars where they have been especially studied in detail by A. McKellar (18). The $C^{12}C^{13}$ bands are always weak in comets.

II) Other electronic systems of C_2:

a) $B^3\Pi_g - X^3\Pi_u$ (Fox-Herzberg system), region λ 2370 - λ 3280;

b) $b^1\Pi_u - a^1\Sigma_g^+$ (Phillips system), region λ 7700 - λ 9300;

c) $c^1\Pi_g - b^1\Pi_u$ (Deslandres-d'Azambuja system), region λ 3400 - λ 4100;

d) $d^1\Sigma_u^+ - a^1\Sigma_g^+$ (Mulliken system), region λ 2300 - λ 2325.

These bands are not observed in comets. All the desirable data may be found in (19) and (20).

REFERENCES

(1) R. G. W. Norrish, G. Porter and B. A. Thrush, *Proc. Roy. Soc.*, A, **216**, 165, 1953.
(2) R. C. Johnson, *Phil. Trans. Roy. Soc.*, A, **226**, 157, 1927.
(3) R. C. Johnson and R. K. Asundi, *Proc. Roy. Soc.*, A, **124**, 668, 1929.
(4) J. G. Phillips, *Ap. J.*, **108**, 434, 1948.
(5) J. D. Shea, *Phys. Rev.*, **30**, 825, 1927.
(6) A. Budo, *Zs. f. Phys.*, **98**, 437, 1936.
(7) J. Hunaerts, *Ann. Obs. Uccle*, Ser. 3, **5**, No. 1, 1950.
(8) R. B. King, *Ap. J.*, **108**, 429, 1948.
(9) A. A. Wyller, *Mém. Soc. Roy. Liège*, **13**, 97, 1953.
(10) M. E. Pillow, *Proc. Phys. Soc.*, **64** A, 772, 1951, and *Mém. Soc. Roy*, **13**, 105, 1953.
(11) A. McKellar and W. Buscombe, *Publ. Dom. Ap. Obs.*, **7**, 361, 1948.
(12) A. McKellar and N. R. Tawde, *Ap. J.*, **113**, 440, 1951.
(13) P. A. Fraser, W.R. Jarmain and R. W. Nicholls, *Ap. J.*, **119**, 286, 1954.
(14) C. Manneback, *The Computation Laboratory*, Problem Report No. 27. (Harvard University, (1952).
(15) A. McKellar and J. L. Climenhaga, *Mém. Soc. Roy. Liège*, **13**, 116, 1953.
(16) R. Herman, *Journal de Physique et le Radium*, **8**, 7_s, 1947. (Séance Soc. Franç. Phys. 1947, febr. 13.)
(17) B. Rosen, (unpublished).
(18) A. McKellar, *Publ. Dom. Ap. Obs.*, **7**, 1949.
(19) G. Herzberg, *Molecular Spectra I*, 1950.
(20) *Tables de Constantes* (B. Rosen, editor), 1951.

TABLE X

The Swan Bands of C_2

v' / v''	0	1	2	3	4	5	6 (*)	7	8	9	10	11	12	13
0	5165.2	4737.1	4382.5				3418.9							
	(0.731)	(0.237)	(0.024)	(0.001)	(0.000)	(0.000)	(0.000)							
1	5635.5	5129.3	4715.2	4371.4			3619.5							
	(0.211)	(0.363)	(0.356)	(0.060)	(0.003)	(0.000)	(0.000)							
2	6191.2	5585.5	5097.7	4697.6	4365.2									
	(0.042)	(0.280)	(0.162)	(0.405)	(0.097)	(0.006)								
3		6122.1	5540.7		4684.8		4680.1							
	(0.007)	(0.088)	(0.280)	(0.057)	(0.427)									
4			6059.7	5501.9		4678.6	4368.8							
	(0.001)	(0.020)	(0.124)	(0.263)										
5			6677.3	6004.9	5470.3		4680.1							
	(0.000)	(0.005)	(0.030)											
6				6599.2	5958.7				4395					
									(o)					
7					6533.7	5923.4	5435.0							
8						6480.5	5899.4			4734				
										(o)				
9							6442.3				4770.1			
											(t)			
10							7083					4836.1		
												(t)		
11							7853						4911.0	
													(t)	
12														4996.7
														(t)

(*) «High pressure bands».
(o) Origin of band.
(t) «Tail bands».

Notes to Table X:

The wave lengths of the main bands are from the work of R. C. Johnson [2]. The «high pressure bands» (corresponding to $v' = 6$) are taken from Herzberg [3] and the «tail bands» ($v' > 6$) from J. G. Phillips [4]. The data of table I are reliable only for the main heads in each sequence. Measurements are difficult for heads with high v' and v'', on account of the superpositions and of the presence of the «returning branches» of the sequences. Moreover the highest v' - levels are perturbed [4].

The rotational structure of the Swan bands has been measured and analysed by many investigators, particularly by R.C. Johnson [2], J. D. Shea [5], and J. G. Phillips [4]; important theoretical considerations are due to A. Budo [6]. J. Hunaerts [7] has prepared a useful compilation of the available data between λ 4676 and λ 5635 A.

The vibrational transition probabilities of the strongest Swan bands have been calculated by various authors [8] to [14]. The figures given in table I are the relative values obtained by P. A. Fraser, W. R. Jarmain and R. W Nicholls [13]. The theoretical values obtained by the different authors agree satisfactorily for the strongest bands, but considerable discrepancies appear for higher v' - values.

C_3

The C_3 spectrum (λ 4050 group) may be excited in emission in various flames and discharges [1][2][3] and in a King furnace [4][5]. In absorption it has been obtained by applying the photoflash technique [6]. In most sources it extends approximately from λ 3975 to λ 4100; however N. H. Kiess [7] finds that it extends into the ultraviolet down to approximately λ 3600 on strong exposures. The main bands are degraded toward the red.

It was shown by A. E. Douglas [8] and confirmed by K. Clusius and A. E. Douglas [9] that C_3 is a linear molecule. The rotational structure of the strongest band near λ 4050 (according to [1]: P-head at λ 4049.76 and origin at λ 4051.13) has been studied by A. Monfils and B. Rosen [10], R. Etienne [11] A. E. Douglas [8], and N. H. Kiess and A. M. Bass [3]. A list of wave lengths of the rotational lines may be found in references [8] and [3].

On account of the complex structure of the spectrum a vibrational analysis is difficult and uncertain; a tentative vibrational classification of the strongest heads has been suggested in reference [2] on the basis of the wave lengths given by R. Herman [12] and R. Etienne [11], with some help from the cometary wave lengths.

The relations between the C_3 bands in the laboratory, the comets and the late carbon stars have been discussed in several recent papers [1] [2] [13].

Under most experimental conditions which however have not yet been clearly defined a continuous spectrum extending approximately from λ 3400 to λ 5000 is superimposed on the discrete C_3 emission. This continuum has been extensively investigated recently [3] [5] [14] [15]. It appears to be related somehow to the 4050 group. It is not observed in comets.

REFERENCES

[1] B. Rosen, *Mém. Soc. Roy. Sc. Liège*, **13**, 187, 1953 (*P. Co.*) and **15**, 332, 1955; these papers contain an extensive list of references to related investigations.
[2] B. Rosen and P. Swings, *Ann. d'Astroph.*, **16**, 82, 1953.
[3] N. H. Kiess and A. M. Bass, *Journ. Chem. Phys.*, **22**, 569, 1954.
[4] W. R. S. Garton, *Proc. Phys. Soc., A*, **66**, 848, 1953.
[5] J. G. Phillips and L. Brewer, *Mém. Soc. R. Sc. Liège*, **15**, 341, 1955.
[6] R. G. W. Norrish, G. Porter and B. A. Thrush, *Proc. Roy. Soc., A*, **216**, 165, 1953 and private communication (1955).
[7] N. H. Kiess and H. P. Broida, private communication (June 1955).
[8] A. E. Douglas, *Ap. J.*, **114**, 466, 1951.
[9] K. Clusius and A. E. Douglas, *Can. Journ. Phys.*, **32**, 319, 1954.
[10] A. Monfils and B. Rosen, *Nature*, **164**, 713, 1949.
[11] R. Etienne, *Thesis*, Liège, 1950 (unpublished).
[12] R. Herman, *Comptes rendus*, Paris, **223**, 281, 1946.
[13] P. Swings, A. McKellar and K. N. Rao, *M.N.R.A.S.*, **113**, 427, 1953.
[14] R. Herman and L. Herman, *Comptes rendus*, Paris, **238**, 664, 1954.
[15] G. V. Marr and R. W. Nicholls, *Can. J. Res.*, **33**, 394, 1955.

NH_2

A strong open band structure (many-line spectrum) observed throughout the visible region (λ 4000 - λ 8300 Å) in the ammonia flame and in various kinds of discharges through streaming ammonia has been suspected for a long time to be due to a decomposition product of NH_3, probably NH_2. This spectrum was commonly designated as the α-ammonia band. Swings, McKellar and Minkowski [1] accepted tentatively the assignment of the α-ammonia band to the NH_2 radical. Observing these bands in absorption Herzberg and Ramsay [2], [3] have given strong support in favor of this assignment, and some additional evidence has been given recently by Leach and Pannetier [4]. Detailed recent measurements in the λ 4000 - λ 6500 Å region of the discharge spectra may be found in [5] and [6]. Gaydon [7] observed the structure up to λ 8300 Å. Earlier the λ 4500 - λ 6500 Å region had been measured by Rimmer [8].

Table XI gives according to [3] and [9] the centers of the strongest α-ammonia bands observed in absorption by the use of the flash photolysis technique.

The values listed in table XI correspond to the longward edges of the clearly defined Q branches, which are accompanied by somewhat irregular and much more widely spaced P and R branches; these centers can not be defined with a precision greater than $\pm 20\ cm^{-1}$. A detailed analysis of these complex bands has not yet been performed, the difficulty being probably due to the fact that the molecule is a strongly asymmetric top and that more than one transition are involved. On the other hand the investigation of the isotopic effect indicates that the origin of the system probably lies near λ 10,400 Å, well beyond the observed part of the spectrum [3].

TABLE XI

Approximate Centers of the NH_2 *— Ammonia Bands*
(*according to* [3])

λ 7354 Å (*w*)	λ 5708 Å (*s*)	λ 4718 Å (*w*)
λ 6619 Å (*m*)	λ 5429 Å (*m*)	λ 4524 Å (*w*)
λ 6302 Å (*s*)	λ 5166 Å (*s*)	
λ 5977 Å (*s*)	λ 4925 Å (*m*)	

(*w*= weak; *m*= medium; *s*= strong).

In the absence of a detailed analysis it is very difficult to select a representative list of individual lines of the α-ammonia bands. In the two wavelength columns of Table XII we have listed side by side the lines which are strongest in the two recent series of measurements of the discharge spectra made by Chauvin [5], Proisy [6] and by Swings, McKellar and Minkowski [1]. The relative intensities are given in the corresponding column. To make clearer the correspondence between both series of measurement less intense lines have been added in a few cases.

Both series of measurements used in Table XII have been made on discharge spectra. The agreement between them as well as with the older measurements by Rimmer [8] is generally within the limit of the normal error for complex incompletely resolved spectra taken with relatively low dispersion. The utmost precaution is required in any comparison of cometary emissions with the wave lengths listed in Table II or in the more extensive lists published in [5], [6] and [8]. The situation is as unsatisfactory if cometary spectra are compared with flame spectra which are usually taken with a very low dispersion (see for instance [1]). Considering the great differences in relative intensities in the discharge and in the flame, and taking into account the possibility of superposition of different systems, the analysis of the spectrum will require high dispersion spectra obtained with the different available sources. The absorption spectra obtained by Herzberg and Ramsay [2], [3] will probably give the best information, but no list of absorption lines has been published as yet.

D. A. Ramsay [9] reports that the analysis of the α-ammonia bands is proceeding satisfactorily.

REFERENCES

[1] P. Swings, A. McKellar and R. Minkowski, *Ap. J.*, **98**, 142, 1943.
[2] G. Herzberg and D. A. Ramsay, *J. Chem. Phys.*, **20**, 347, 1952.
[3] G. Herzberg and D. A. Ramsay, *Faraday Soc. Disc.*, No. 14, p. 11, 1952.
[4] S. Leach and G. Pannetier, *J. Phys. Rad.*, **15**, 413, 1954.
[5] H. Chauvin, *Diplôme d'Etudes Supérieures*, Paris, 1950, quoted in (4).
[6] P. Proisy, *Ann. de Phys.*, **1**, 5, 1953.
[7] A. G. Gaydon, *P.R.S.*, A., **81**, 197, 1942.
[8] W. B. Rimmer, *P.R.S.*, A, **103**, 696, 1923.
[9] D. A. Ramsay (private communication, december 1955).

TABLE XII

Wave Lengths of the Strongest Lines of the α-Ammonia Band (according to (5), (6) and (1))

according to (5)	according to (6)	according to (1)
	4502.0 (6)	
4511.0 (3)	4511.7 (5)	
	4531.7 (5)	
	4536.4 (5)	
	4542.2 (5)	
	4706.6 (6)	
4722.4 (4)	4722.3 (6)	
4925.8 (4)	4925.6 (4)	
4954.5 (4)	4954.1 (4*)	
5070.6 (3)	5071.5 (6)	
5076.4 (3)	5075.7 (5)	
5081.6 (4)	5081.4 (6)	
5110.7 (3)	5110.2 (6)	
5156.5 (3)	5156.5 (5)	
5166.5 (5)	5166.1 (6)	
5177.6 (4)	5177.1 (5)	
5182.0 (4)	5181.5 (5)	
5185.9 (4)	5185.4 (5*)	
5203.1 (4)	5203.1 (5)	
5239.4 (4)	5238.8 (5)	
5256.1 (4)	5255.5 (5)	
5259.0 (4)	5258.3 (5)	
5263.6 (4)	5262.9 (5)	
5317.5 (5)	5317.2 (5*)	
5384.2 (6)	5384.3 (6)	
5428.2 (7)	5427.1 (6*)	
5524.6 (5)	5525.3 (4)	
5527.1 (5)	5527.1 (4)	
5560.2 (6)	5560.1 (6)	
5562.7 (6)	5562.6 (6)	
5677.3 (6)	5677.4 (4)	
5682.2 (5)	5681.4 (3)	
5696.2 (5)	5695.9 (3)	5696.9 (1 d)
5702.7 (5)	5703.0 (4)	
5706.7 (9)	5706.9 (6)	
		5713.8 (4)
5731.4 (5)	5731.5 (4)	
5740.7 (5)	5740.8 (5)	5741.4 (1/2)
5752.3 (7)	5752.3 (6)	5753.5 (1/2)
		5781.3 (1/2 *d*)
		5792.7 (1/2 *d*)

TABLE XII *(continued)*

Wave Lengths of the Strongest Lines of the α-Ammonia Band (according to (5), (6) and (1))

according to (5)	according to (6)	according to (1)
5810.8 (5)	5812.0 (5)	5809.4 (1/2 *d*)
		5870.7 (1/2 *d*)
5881.6 (5)		
	5887.5 (5)	
		5891.7 (1/2 *d*)
		5898.4 (1)
5915.2 (4)		5917.5 (1/2)
5931.2 (3)		5929.1 (1/2)
		5953.8 (1/2)
5960.0 (4)		5963.8 (1 *d*)
5975.1 (10)	5976.4 (6)	5978.6 (4)
5994.3 (5)	5995.3 (*)	5998.6 (1/2)
6010.0 (3)	6009.5 (5)	6011.8 (1/2)
6018.4 (7)	6019.3 (*)	6021.2 (1)
		6027.8 (1)
6031.6 (7)	6031.7 (5)	6031.4 (2)
6047.3 (4)	6046.8 (5)	6048.1 (2)
		6054.3 (3)
	6078 (*)	
6096.3 (5)		6097.5 (1/2)
		6109.3 (1/2)
6120.1 (6)	6120.8 (4)	6121.0 (1 *d*)
		6143.3 (1/2)
		6168.3 (1/2)
		6181.9 (1/2)
6187.5 (5)	6188.4 (4)	6188.8 (3)
		6314.4 (1/2 *d*)
6230.7 (4)		6232.6 (2)
6261.4 (4)		6262.5 (1 *d*)
6286.2 (3)		6287.5 (1)
6297.7 (8)	6299.5 (6)	6299.5 (8)
		6321.8 (2)
6326.4 (5)		
6332.8 (5)	6332.9 (4)	6332.6 (4)
6345.7 (2)		6345.8 (1)
		6356.0 (1)
6369.3 (3)		6369.9 (1)
6390.1 (0)		6390.0 (1/2)
		6409.4 (2 *d*)
6431.7 (0)		6432.3 (1 *d*)
		6447.5 (1/2 *d*)

TABLE XII *(continued)*

Wave Lengths of the Strongest Lines of the α-Ammonia Band (according to (5), (6) and (1))

according to (5)	according to (6)	according to (1)
		6478.6 (1 *d*)
		6497.7 (1/2 *d*)
		6529.4 (1)
		6547.5 (1 *d*)
		6560.3 (1)
		6571.3 (1)
		6587.6 (1)
		6601.5 (4)
		6620.1 (8)
		6630.4 (1/2 *d*)
		6646.8 (5)
		6656.6 (1)
		6672.1 (1)
		6688.7 (2 *d*)
		6704.0 (1)
		6713.5 (1)
		6734.2 (2 *d*)
		6749.5 (1 *d*)
		6770.8 (1)
		6780.1 (2)
		6799.8 (2 *d*)
		6829.6 (1 *d*)
		6846.8 (1 *d*)
		6864 (1 *d*)

(*) center of broad feature
(*d*) diffuse line.

CH^+

The singlet system $^1\Pi - {}^1\Sigma$ of CH^+ appears in the region λ 3730 - λ 4800 Å; it may be excited in an electrodeless discharge through helium with a trace of benzene [1]. The band heads are given in Table XIII.

TABLE XIII

Band Heads of CH^+

v′ / v″	0	1	2
0	4225.26	3954.37	3743.68
1	4775.88		

The bands are degraded to the red; they have a simple open structure with one R, one Q and one P branch. Table XIV gives the wave lengths of the first rotational lines of the (0 — 0) and (1 — 0) bands [1]. These bands have been identified in cometary spectra by P. Swings [4].

An other band system observed by F. C. McDonald [2] and by L. Gerö and R. F. Schmid [3] in the region λ 2200 - λ 2300 Å has been tentatively assigned to CH^+; the origin of the most prominent band is at λ 2264 Å.

REFERENCES

[1] A. E. Douglas and G. Herzberg, *Can. J. Res.*, **20**, 71, 1942.
[2] F. C. McDonald, *Phys. Rev.*, **29**, 212, 1927.
[3] L. Gerö and R. F. Schmid, *Phys. Rev.*, **60**, 363, 1941.
[4] P. Swings, *Ap. J.*, **95**, 270, 1942.

TABLE XIV

First Rotational Lines of the $^1\Pi - {}^1\Sigma$ *Transition of* CH^+

J″	(0 — 0) band			(1 — 0) band		
	R	Q	P	R	Q	P
0	4232.54	—	—	3957.71	—	—
1	4229.32	4237.56	—	3955.49	3962.07	—
2	4227.06	4239.37	4247.57	3954.37	3964.26	3970.82
3	4225.69	4242.11	4254.38	3954.37	3967.54	3977.38
4	4225.26	4245.77	4262.13	3955.49	3971.94	3985.04
5	4225.80	4250.38	4270.78	3957.71	3977.47	3993.82

OH^+

The $A^3\Pi_i - X^3\Sigma^-$ system of OH^+ may be excited in an electrodeless discharge through water vapor at low pressure [1], [2]. The most prominent band heads are given in Table XV [2].

TABLE XV

Band Heads of OH^+

v′ / v″	0	1
0	3565	3382
1	3893	3695

Each band contains nine main branches, plus numerous weaker bands of which nine have been measured. Table XVI gives the wave lengths of the first rotational lines of the (0 — 0) band [3].

The presence of the OH^+ band in the spectrum of 1941 I was first suggested by P. Swings [4]. This assignment was later discussed by J. Hunaerts [3] and by R. Herman and L. Herman [5].

REFERENCES

[1] W. H. Rodebush and M. H. Wahl, *J. Chem. Phys.*, **1**, 696, 1933.
[2] F. W. Loomis and W. H. Brandt, *Phys. Rev.*, **49**, 55, 1936.
[3] J. Hunaerts, *Bull. Astr. Obs. Roy. Belg.*, **3**, 320, 1945.
[4] P. Swings, *Ap. J.* **95**, 270, 1942.
[5] R. Herman and L. Herman, *Ann. d'Astroph.*, **12**, 52, 1948.

CO^+

Three electronic transitions of CO^+ have been observed in discharges through CO, CO_2 and mixtures with noble gases; the first two are present in cometary spectra.

1) $A^2\Pi_i - X^2\Sigma$ (Comet tail system), bands degraded toward the red, region λ 3080 - λ 6360.

2) $B^2\Sigma - A^2\Pi_i$ (Baldet-Johnson system), bands degraded toward the violet, region λ 3330 - λ 4845.

3) $B^2\Sigma - X^2\Sigma$ (First negative system), bands degraded toward the red, region λ 1975 - λ 3155.

Tables XVII and XVIII give the wave lengths of the most prominent heads of the C.T.- and B.J. systems respectively [1]. At low resolution both systems show sequences of double heads. In the C. T. system these are the $Q_1 + R_1$ and $Q_2 + R_2$ heads. In the B.J. system the doublets are formed by the $Q_1 + P_1$ and $Q_2 + P_2$ branches. The transition probabilities in Table I are taken from [5].

TABLE XVI

Wave Lengths of the First Rotational Lines of the $A^3\Pi_i - X^3\Sigma^-$ *System of* OH^+, (0 — 0) *Band*

K''	P_1	Q_1	R_1	$^PQ_{12}$	$^QR_{12}$	
1	3596.32			3596.63		
2	3600.50	3587.75		3500.84	3588.15	
3	3605.90	3589.00	3576.27	3606.24	3589.35	
4	3612.37	3591.24	3574.44	3612.75	3591.56	
5	3619.86	3594.50	3573.52	3620.26	3594.87	

K''	P_2	Q_2	R_2	$^RQ_{21}$	$^PQ_{23}$	$^QR_{23}$	$^QP_{21}$
1	3585.14		—				
2	3591.56	3579.26		3570.38	3591.24	3578.86	3578.86
3	3598.74	3582.06	3569.24	3568.94	3598.42	3581.76	3581.76
4	3606.41	3585.64	3568.17	3568.21	3606.24	3585.47	3585.28
5	3614.83	3589.86	3568.54	3568.21	3614.64	3589.66	3589.50

K	P_3	Q_3	R_3	$^RQ_{32}$	$^QP_{32}$	
1	3578.86	3569.37	—	—		
2	3586.22	3572.62	3565.25		3572.91	
3	3594.14	3576.41	3564.69	3565.02	3576.82	
4	3602.60	3580.64	3564.76	3565.02	3580.86	
5	3611.56	3585.47	3565.35	3565.60	3585.63	

Recent investigations by K. N. Rao [2] have led to a new numbering of the vibrational transitions.

The cometary emissions due to the C.T. system have been extensively described by F. Baldet [3] and others, as they appear on objective-prism plates. The first observation of the Baldet-Johnson system on the basis of slit spectrograms was reported by P. Swings and T. L. Page [4].

TABLE XVIII

CO^+ Bands (Baldet-Johnson System)

v''	v'	0	1	2	3
0	Q_1	3973.5	3724.9	3511.7	3329.0
	Q_2	3953.6	3707.4	3496.7	3314.8
1	Q_1	4231.6			
	Q_2	4209.1			
2	Q_1		4201.5		
	Q_2		4179.1		

REFERENCES

[1] R. W. B. Pearse and A. C. Gaydon, *The Identification of Molecular Spectra*, Chapman and Hall Ltd., pp. 97 and 98, 1950.
[2] K. N. Rao, *Ap.J.*, **111**, 50 and 306, 1950; *P. Co.* p. 141, 1953.
[3] F. Baldet, *Thesis*, Paris, 1926.
[4] P. Swings and T. L. Page, *Ap. J.*, **111**, 530, 1950.
[5] W. R. Jarmain, P. A. Fraser and R. W. Nicholls, *Ap. J.*, **122**, 55, 1955.

N_2^+

The N_2^+ molecule is isoelectronic with CN and has a similar spectrum which is observed in low pressure discharges through noble gases containing a trace of N_2.

All three band systems of N_2^+ which are known in the laboratory involve the ground state:

1) $A^2\Pi - X^2\Sigma$ (Meinel system), bands degraded toward the red, region λ 5500 - λ 9250.

TABLE XVII

CO^+ Bands (Comet Tail System)

v''	v'	0	1	2	3	4	5	6	7	8	9	10	11
0	R_2	4138.9	4565.8	4272.0	4017.7	3795.8	3600.8	3427.9	3273.9	3135.5			
	R_1	4879.5	4539.4	4248.9	3997.3	3777.8	3584.2	3413.3	3260.4	3123.2			
		(0.042)	(0.113)	(0.166)	(0.180)	(0.159)	(0.122)	(0.085)	(0.055)	(0.034)			
1	R_2	5499.9	5072.1	4711.2	4403.3	4138.9	3908.0	3705.3	3525.6	3366.1	3222.4	3093.3	
	R_1	5461.4	5039.7	4683.4	4378.9	4117.3	3888.6	3688.1	3510.3	3351.7	3209.7	3081.5	
		(0.149)	(0.191)	(0.099)	(0.015)	(0.004)	(0.041)	(0.078)					
2	R_2	6238.7	5693.6		4865.8							3314.2	3180.3
	R_1	6189.4	5652.6		4836.6	4518.0	4244.1					3300.7	3168.1
		(0.246)	(0.083)	(0.002)	(0.071)	(0.096)	(0.051)						
3	R_2			5900.4					4151.9				
	R_1			5856.5					4130.4				

2) $B^2\Sigma$— $X^2\Sigma$ (Negative system), single headed bands degraded toward the violet, region λ 3000 - λ 5860.

3) $C^2\Sigma$— $X^2\Sigma$, bands degraded toward the red, region λ 1720 - λ 2060.

The Meinel system [1] [2] which is a prominent feature in aurorae is probably not present in comets. There are cometary emissions near λ 8000 coinciding roughly with Meinel bands. However the cometary emissions near λ 8000 are confined in the central region of the head, while the 0-0 band of the negative system of N_2^+ extends far out into the tail. Moreover the coincidences in wave length and profile do not appear satisfactory. Yet this assignment has been advocated by S. M. Poloskov [3].

Table XIX gives the wave lengths of the band heads of the negative system [4], and the transition probabilities calculated by W. R. Jarmain, P. A. Fraser and R. W. Nicholls [5]. Several of these N_2^+-bands have been observed in comets [6], [7] the strongest being (0-0) at λ 3914.

REFERENCES

[1] F. W. Dalby and A. E. Douglas, *Phys. Rev.*, **84**, 843, 1951.
[2] A. E. Douglas, *Ap. J.*, **117**, 380, 1953.
[3] S. M. Poloskov, *Problems of Cosmogony*, 1955 (in Russian).
[4] R. W. B. Pearse and A. G. Gaydon, *The Identification of Molecular Spectra*, Chapman and Hall, Ltd., p. 176, 1950.
[5] W. R. Jarmain, P. A. Fraser and R. W. Nicholls, *Ap. J.*, **118**, 228, 1953.
[6] Baldet, *Thesis*, Paris, 1926.
[7] P. Swings and T. L. Page, *Ap. J.*, **111**, 530, 1950.

TABLE XIX

N_2^+ *Band Heads*

v′ / v″	0	1	2
0	3914.4	3582.1	3308.0
	(0.666)	(0.289)	(0.043)
1	4278.1	3884.3	3563.9
	(0.250)	(0.234)	(0.399)
2	4709.2	4236.5	3857.9
	(0.065)	(0.288)	(0.048)
3	5228.3	4651.8	4199.1
	(0.015)	(0.130)	(0.231)

C_2^+O

The CO_2^+-ion has two electronic systems involving the ground state $^2\Pi_g$:

$^2\Pi_u \rightarrow {}^2\Pi_g$, extending from λ 2800 to λ 5000;

$^2\Sigma_u^+ \rightarrow {}^2\Pi_g$, double band at λ 2883 - λ 2986.

These bands may be excited in the hollow cathode or in ordinary discharges through CO or CO_2.

The strong double band at λ 2883 - λ 2896 has been analysed by F. Bueso-Sanllehi [1], the other system by S. Mrozowski [2]. The CO_2^+-bands of the $^2\Pi_u \rightarrow {}^2\Pi_g$ system have a fairly simple structure. The CO_2^+ molecule is linear in both $^2\Pi$ states. All the strong bands observed in the laboratory may be attributed to symmetrical vibrations, ν_1, the CO_2^+ molecules remaining in their lowest states of ν_2 (bending) and ν_3 (antisymmetrical) vibrations. In the laboratory a typical band consists of two narrow subbands $^3\Pi_{1.5} \rightarrow {}^2\Pi_{1.5}$ and $^2\Pi_{0.5} \rightarrow {}^2\Pi_{0.5}$, which are degraded toward the red. In the $^2\Pi_{1.5} \rightarrow {}^2\Pi_{1.5}$ subband the origin practically coincides with an accumulation of lines due to the Q branch; the head of the R branch is displaced 0.4 to 0.7 Å shortward of the origin; the P branch extends toward the red. The structure is similar in the $^2\Pi_{0.5} - {}^2\Pi_{0.5}$ subband, except that the Q branch is not observed. The $^2\Pi_{1.5}$, $v'' = 1$ level is split by perturbation into two sublevels, 1^a and 1^b, so that the (0 — 1) transition has actually three components: (0 — 1^a) and (0 — 1^b) of $^2\Pi_{1.5} - {}^2\Pi_{1.5}$, and (0 — 1) of $^2\Pi_{0.5} - {}^2\Pi_{0.5}$. For the higher values of v' and v'' the bands are complicated by perturbations. Numerous weak bands can not be interpreted by assuming only symmetric vibrations; bending or asymmetric vibrations are probably involved in those cases.

Table XX gives the wave lengths of the origins of the CO_2^+ bands; the R-heads are approximately 0.5 Å to the violet of the origins. The estimated relative intensities are from ref. [2].

For the identification of CO_2^+ in comet-tail spectra, it appears safe to adopt the mean laboratory wave lengths of the origins for the wave lengths of the subbands. Moreover one should not expect the two (or three) subbands corresponding to each vibrational transition to be resolved on the spectrograms of cometary tails. A synthetic profile has been calculated by J. Hunaerts [4].

TABLE XX

Origins of the CO_2^+ *Bands*

Subbands 1.5 — 1.5

v′ / v″	0	1	2	3	4
0	3503.7	3370.6	3247.7	3133.6	3027.4
	(4)	(5)	(5)	(3)	(1)
1^a	3663.2	3517.9	—	—	3151.4
	(4)	(0)			(3)
1^b	3669.3	—	3389.5	3265.5	3150.2
	(3)		(3)	(4)	(4)
2	3839.8	3680.5	3534.4	—	—
	(5)	(3)	(4)		
3	4030	3856.8	—	3549.7	—
	(2)	(4)		(2)	

Subbands 0.5 — 0.5

v′ / v″	0	1	2	3	4
0	3511.6	3378.0	3254.8	3140.6	3034.6
	(4)	(5)	(5)	(4)	(3)
1	3675.1	—	3394.7	3270.7	3155.9
	(5)		(3)	(4)	(4)
2	3853.1	3692.9	3546.0	—	—
	(5)	(4)	(4)		
3	4047	3871.6	—	3563.0	—
	(2)	(4)		(3)	

The first identification of CO_2^+ in comet tails is due to P. Swings and T. L. Page [3].

REFERENCES

[1] F. Bueso-Sanllehi, *Phys. Rev.*, **60**, 556, 1941.
[2] S. Mrozowski, *Phys. Rev.*, **60**, 730, 1941; **62**, 270, 1942; **72**, 682, 1947; **72**, 691, 1947. *Rev. Mod. Physics*, **14**, 216, 1942.
The first paper contains references to the numerous previous attempts at clarifying the CO_2^+ or CO_2 bands.
[3] P. Swings, *Bull. Acad. Roy. Belg.*, Cl. Sc., **36**, 113, 1950 (with bibliography).
P. Swings and T. L. Page, *Ap. J.*, **111**, 530, 1950.
[4] J. Hunaerts, *Comm. Obs. Roy. Belg.*, No. 35, 1951.

PLATE I

Slit Spectrograms of Comet Cunningham (1940 c, 1941 I) in the Spectral Region λ 3800-λ 6420 (Glass Prisms).

List of spectrograms.

No.	r(A.U.)
1	1.16
2	1.14
3	1.01
4	0.99
5	0.85
6	0.73
7	0.71
8	0.69
9	0.67
10	0.57
11	0.52

Spectrograph: McDonald Observatory Cassegrain spectrograph; glass prisms and *f*/1 camera; original dispersion 89 A/mm at λ 3880; comparison spectrum: iron arc.

Except for spectrum 9, the image of the central condensation of the head was kept on the center of the slit.

Notes:

(1) Very different extensions of specific molecules in head, CN giving the longest lines, CH and NH_2 the shortest. Decreasing order of extension in head: CN, C_2, C_3, CH — NH_2.

(2) Variations of relative intensities with increasing *r*: increase of C_3/C_2 , CN/C_2 , CN/CH , CH/C_2 , C_3/NH_2 and C_3/CN with increasing *r*. The increase of the intensity ratio C_3/C_2 with increasing *r* is especially striking (compare, for example, sp. 1 and 11). On sp. 3, 4, 5 and 6, the R branch of the $^2\Delta$ — $^2\Pi$ system of CH is stronger than the (2,0) sequence of C_2; on sp. 11, the opposite is true.

(3) Presence of the sodium D-lines in emission on sp. 10 and 11.

(4) Presence of the $^2\Delta$ — $^2\Pi$ system of CH on all spectrograms and of the $^2\Sigma$ — $^2\Pi$ system on sp. 3 to 10.

(5) Transitions between low rotational and vibrational levels only are observed for the heteronuclear molecules CN and CH, whereas in the case of the homonuclear molecule C_2 transitions occur between levels of fairly high vibrational quantum number [See plates XXI and XXII for comparison with laboratory spectra].

(6) Variations in the profiles of the CN, CH and C_2 emission bands, in the sense of a shift of the maxima toward higher rotational quantum numbers for a decreasing heliocentric distance. No appreciable change in the profile of the C_3-emission.

(7) Presence of several as yet unidentified emissions between C_2(0-0) and C_2(1-0).

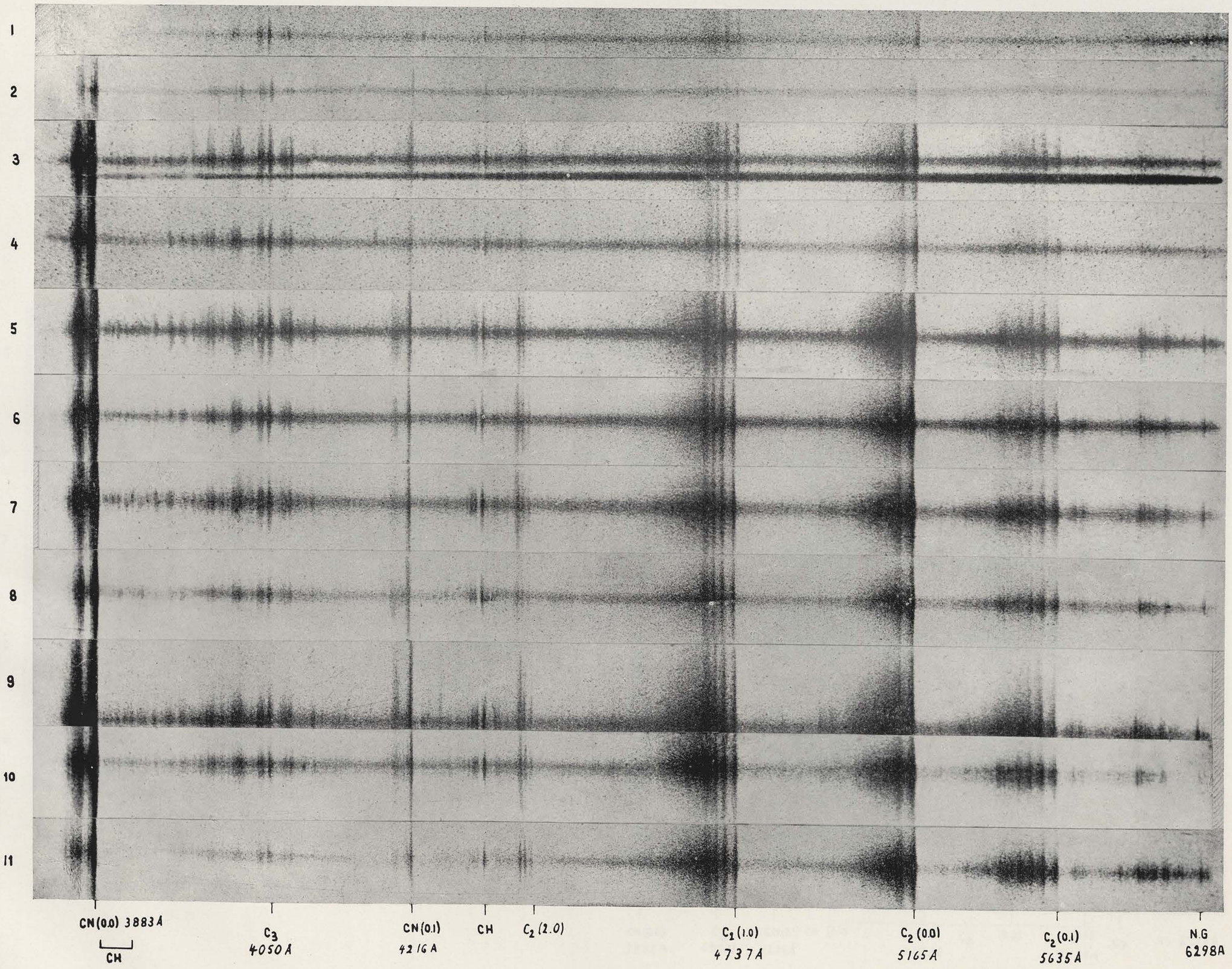

Slit spectrograms of Comet Cunningham (1940 c - 1941 l)
in the spectral region λ3800-λ6420 (glass prisms).

PLATE II

Slit Spectrograms of Comet Cunningham (1940 c, 1941 I) in the Spectral Region λ 3000-λ 6400 (Quartz Prisms)

List of spectrograms.

No.	*r* (A.U.)
1	2.24
2	1.85
3	1.47
4	1.18
5	1.03
6	0.87
7	0.75
8	0.63
9	0.50
10	0.48

Spectrographs: for sp. 1, McDonald Observatory nebular spectrograph, quartz prisms, *f*/1 camera;
for sp. 2 to 9, McDonald Observatory Cassegrain spectrograph; quartz prisms, *f*/1 camera, original dispersion 137 A/mm at λ 3360;
for sp. 10, same spectrograph with *f*/2 camera, dispersion 68 A/mm at λ 3360.

On sp. 8, the appearance of the NH band is slightly marred by a defect in the plate.

Notes;

(1) Presence of OH- and NH- bands in ultraviolet region; also of CN (1-0) (first cometary spectrograms giving the rotational resolution of the OH and NH bands, enabling the first identification of these two radicals in comets).

(2) Different extensions of OH and NH (in this comet, OH is more concentrated toward the center than NH; see however plate no. IV, spectrum no. 4 of Comet 1943 I, on which OH extends farther into the head than NH).

(3) Increase of intensity ratios $\frac{OH}{NH}$ and $\frac{OH}{CN}$ with increasing *r*; intensity ratio $\frac{NH}{CN}$ approximately constant.

(4) Spectra 3, 9 and 10 are perturbed by twilight (solar spectrum: see G-band in solar absorption near CH-cometary emission; also solar H- and K- absorption lines).

(5) Presence of strong nightglow- or twilight- emissions.

(6) Details on individual spectra.
sp. 1 and 2: the main features (excluding the nightglow emissions) are the continuum and CN(0-0); traces of C_3 and NH_2; absence of C_2. Notice strength of H- and K- solar absorption lines (indicating that there is no continuous emission in the blue-violet region).
sp. 3: Perturbed by moonlight; CN, C_3 and NH_2 intense; NH present; C_2 present, but weaker that C_3; trace of CH, $^2\Delta - {}^2\Pi$; possible «emissions» shortward of CN(0-0).
sp. 4: Weak exposure; NH and NH_2 present; CH absent; C_3 stronger than (1-0) of C_2 and than (0-1) of CN.
sp. 5: CN(0-0) overexposed; C_2 and C_3 strong; OH, NH and CH present; NH shows a lower rotational temperature than on later spectra.
sp. 6: first trace of CN(1-0), also present on sp. 7 and 8.
sp. 7 to 10: many strong emissions; trace of tail spectrum on sp. 8; long D-lines of twilight superposed on short cometary D-lines on sp. 9 and 10 (enhacement in central condensation).

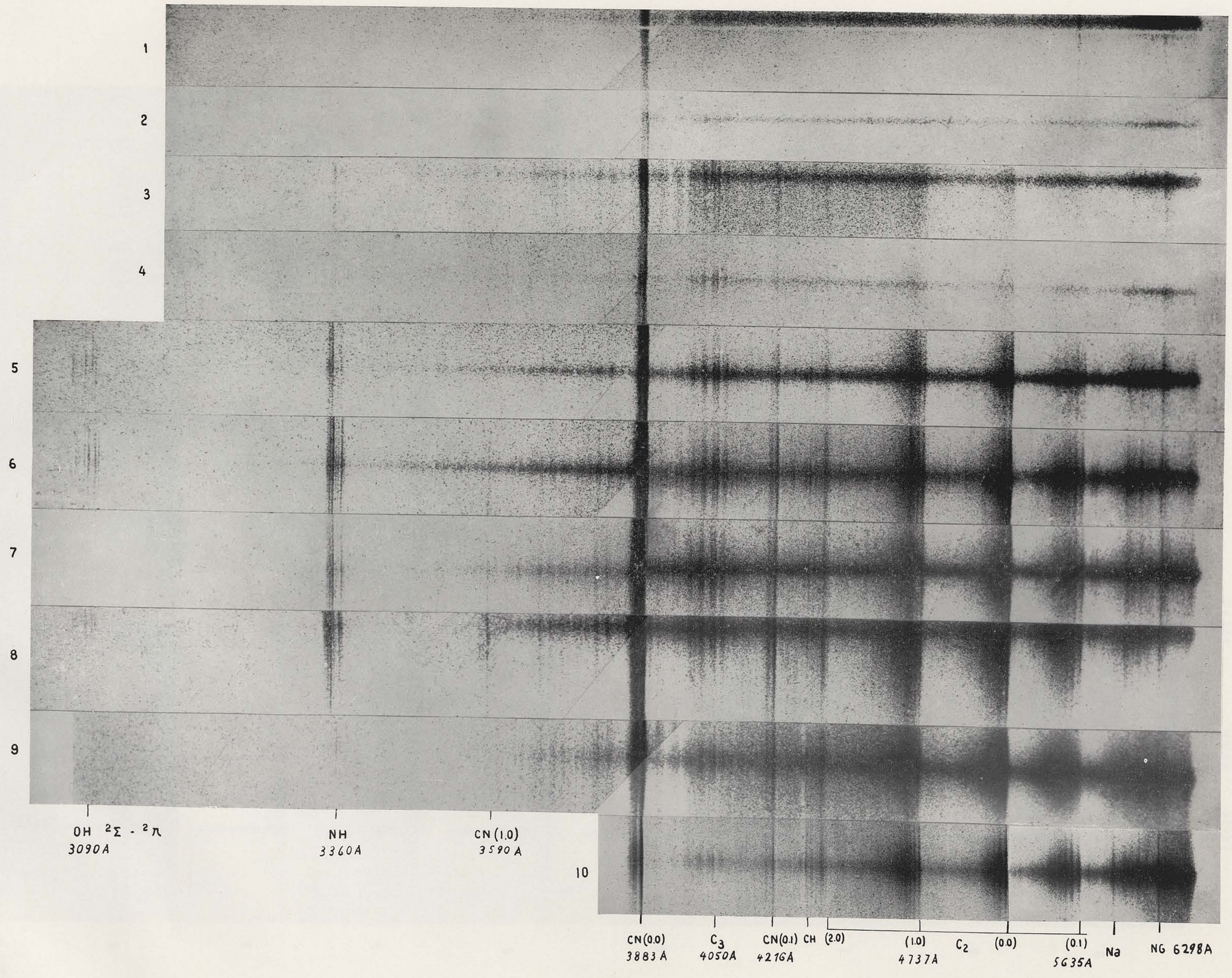

Slit spectrograms of Comet Cunningham (1940 c - 1941 I)
in the spectral region λ3000-λ6400 (quartz prisms).

PLATE III

Slit Spectrograms of the Head of Comet Bester (1947 k, 1948 I) in the Spectral Region λ 3460-λ 6700 (Grating)

List of spectrograms.

No.	r (A.U.)
1	0.805
2	0.812
3	0.837
4	0.845
5	0.864
6	0.884
7	0.915
8	1.274
9	1.301

Spectrograph: B grating spectrograph at prime focus of McDonald Observatory 82'' reflector; camera f/0.65 (see T. L. Page, La Physique des Comètes, pp. 49-52). Original dispersion: 330 A/mm. Comparison spectrum: Ne- bulb, plus Cd- Pb spark.

Except for spectrum 1 the central condensation was placed at one end of the slit, and the guiding was done as accurately as possible. Two slit spectrograms of the tail are given in Plate XXIIIa.

Notes:

(1) Very different extensions of different molecules in the head; decreasing order of extension: CN, C_2, C_3, CH — NH_2.

(2) Variations of relative intensities with increasing r: increase of $\frac{C_3}{C_2}$, $\frac{CN}{C_2}$, $\frac{CN}{CH}$, $\frac{C_2}{CH}$, $\frac{C_3}{CN}$.

(3) Presence of the nightglow [OI] emissions.

(4) The bands of CO^+, N_2^+ and CO_2^+ emitted by the tail are shown better on plate XXIII *a*.

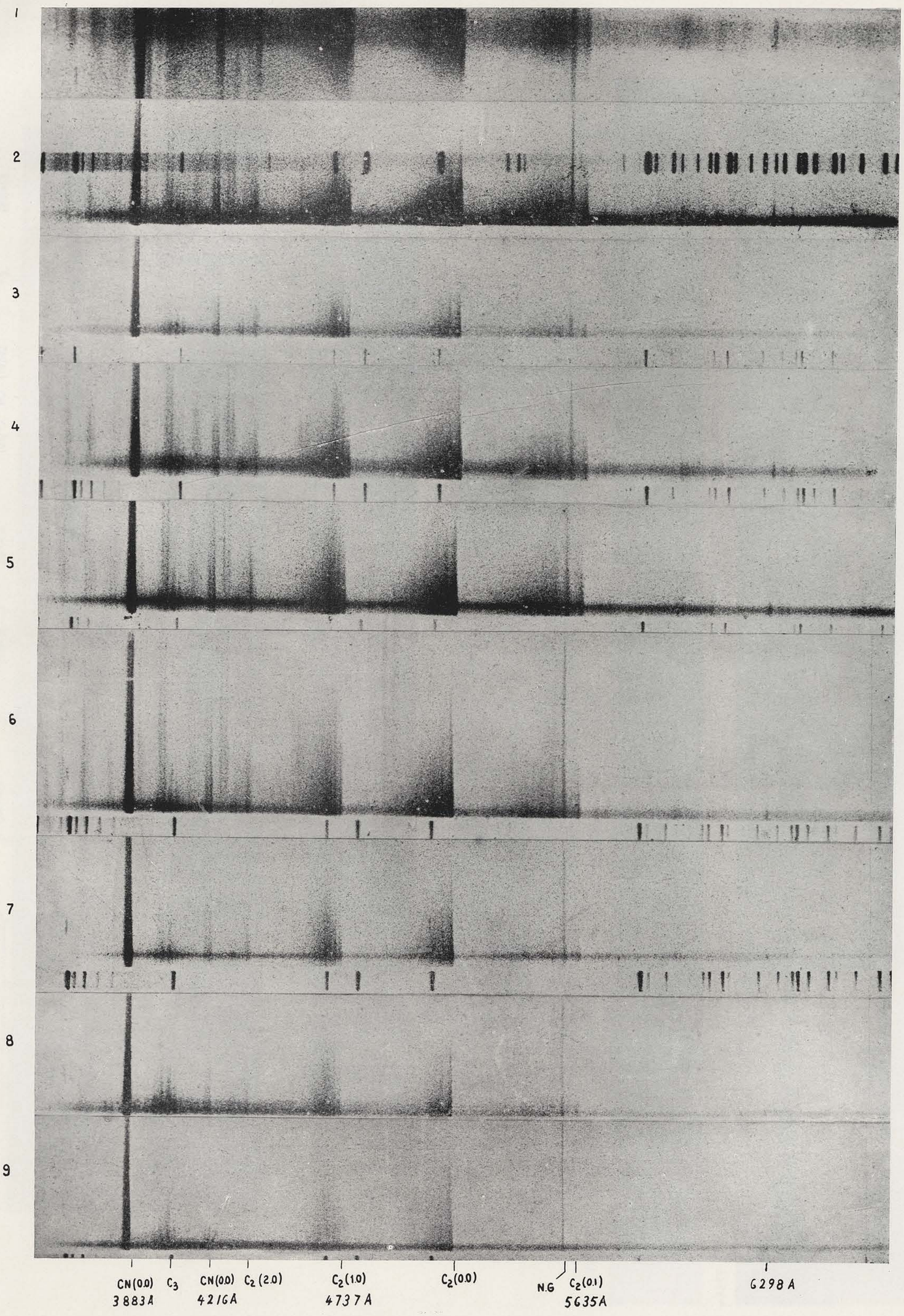

Slit spectrograms of the head of Comet Bester (1947 *k* - 1948 I) in the spectral region λ3460-λ6700 (grating).

PLATE IV

The General Aspect of Comet Head Spectra obtained with Slit (Prism and Grating) Spectrographs and with an Objective Prism.

List of spectrograms.

No.	Comet	r (A.U.)	Instrument	See also plate no.
1	1941 I	0.73	Slit, glass prisms, *f*/1 camera, McDonald	I, sp. 6
2	1948 XI	0.78	Slit, glass prisms, *f*/2 camera, McDonald	XI, sp. 4
3	1941 I	0.87	Slit, quartz prisms, *f*/1 camera, McDonald	II, sp. 6
4	1943 I	1.55	Slit, quartz prisms, *f*/2 camera, Haute Provence (Barbier)	VIII*b*, sp. 3
5	1948 I	0.84	Slit, grating, *f*/0.65 camera, McDonald	III, sp. 3
6	1947 XII	0.59	Id., covering red region	XIIa, sp. 2
7	1911 V	1.08	Glass objective prism, Lick	
8	1937 V	0.88	Glass objective prism, Meudon (Baldet)	

This plate illustrates the respective advantages of the different dispersing systems: high resolution given by a grating in the red region, clear spatial distribution of emissions on objective-prism spectra, desirability of slit instruments for resolution.

Notes:

(1) On spectrogram 2, compare CH cometary emission and CH solar absorption; notice the asymmetric distribution of CH; rotational structure of CN(0-0).

(2) On spectrograms 3 and 4, compare structures, extensions and relative intensities of OH and NH. The quartz prisms reveal the structures of the OH- and NH- bands, but not of CN, C_2 or CH.

(3) On spectrogram 6, good definition in visual region: presence of NH_2 and C_2, possibly also of the red system of CN. Doubling of head apparent in visual region.

(4) On objective prism plates 7 and 8, notice extension of different molecules in head. Trace of tail spectrum on sp. 8.
On sp. 7, asymmetric extension of CN and C_2.

(5) Nightglow or twilight lines on spectrograms 2, 3 and 6.

PLATE IV

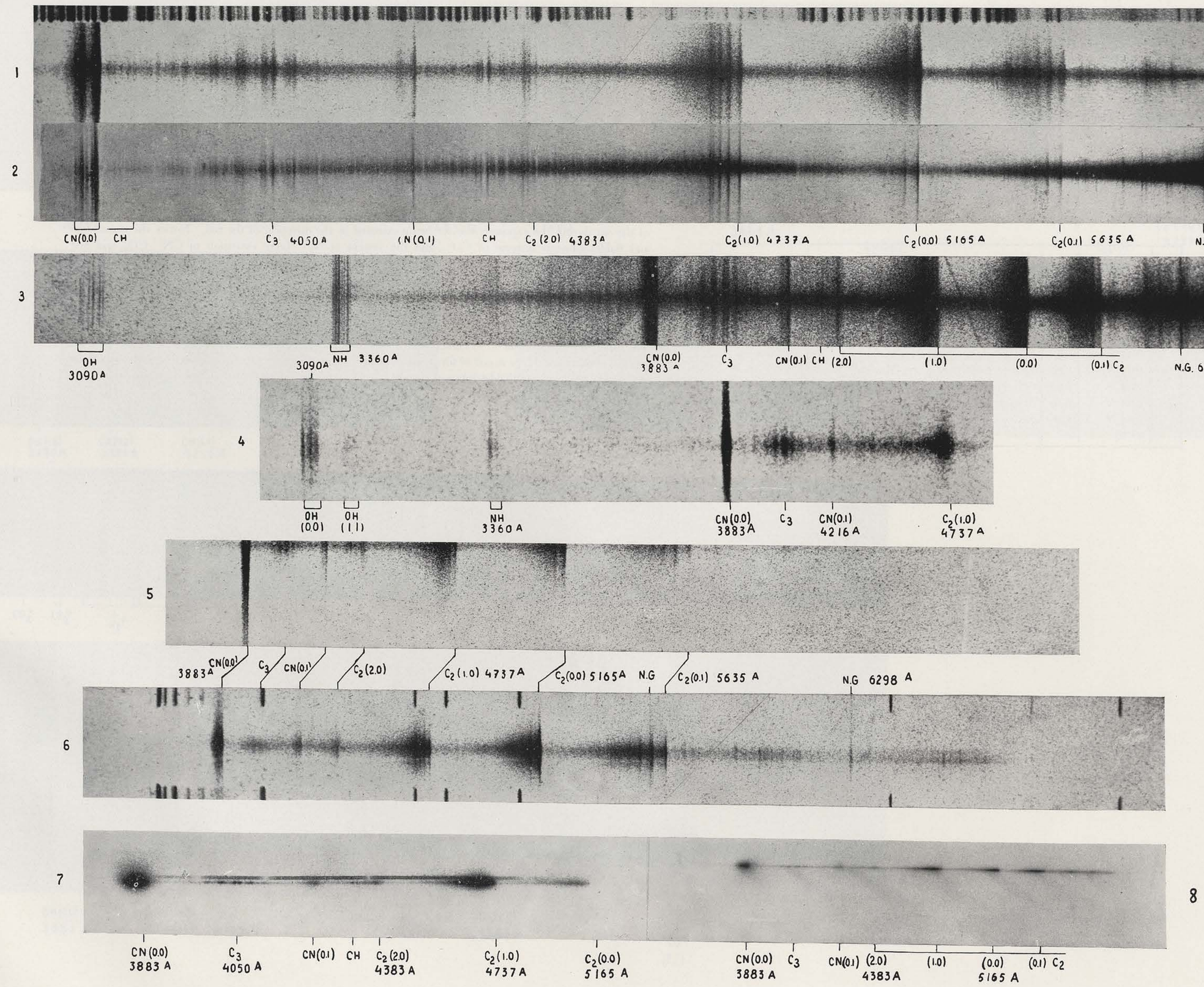

The general aspect of comet head spectra obtained with slit (prism and grating) spectrographs and with an objective prism.

PLATE V

General Aspect of Spectrograms of Comet Heads and Tails obtained with Various Types of Instruments

List of spectrograms.

No.	Comet	r (A.U.)	Instrument	See also plate no.
1	1911 V	0.50	Objective prism, Lick	VIIIa, sp. 4
2	1908 III	1.14	Objective prism (Baldet)	VI*b*, sp. 3
3	1948 I	0.97	Slit, grating, *f*/0.65, McDonald	XXIII*a*, sp. 1
4	1911 V	0.50	Quartz Objective prism, Meudon	VIII*a*, sp. 6
5	1948 I	0.88	Slit, grating, *f*/0.65, McDonald	III, sp. 6
6	1911 V	0.50	Slit, glass prisms, Lick	
7	1911 V	0.49	Slit, glass prisms, Lick	

Notes:

(1) On spectrogram 1, notice the broadening of the curved CO^+-tail away from the central region of the head. A CO^+-emission coincides almost with the (1-0) sequence of C_2; in the past this may have been a source of misinterpretation (carbon tails!). Similarly a CO^+ emission falls very near the C_3 band at λ 4010.

(2) Spectrograms 3 and 5 show the tail spectrum. The image of the central condensation was kept at one end of the slit during the exposure, the slit being oriented in the direction of the tail. Notice the comet tail- and Baldet-Johnson systems of CO^+, and the system of N_2^+. Long extension of CN. CO_2^+ was first identified in cometary spectra on these plates. Spectrogram 5 extends farther into the red: notice the very short NH_2-emissions and long nightglow lines.

(3) On slitless spectrogram 4, the dots (marked on original) indicate streamers in the tail.

(4) The glass prism spectrogram 6 was taken with a wide slit. It shows the doublet character of the CO^+ bands. Central condensation kept at end of slit. Spectrogram 7 taken with the same instrument, but with a narrower slit, shows a trace of the Baldet-Johnson system of CO^+; the central condensation was kept near the center of the slit.

PLATE V

1

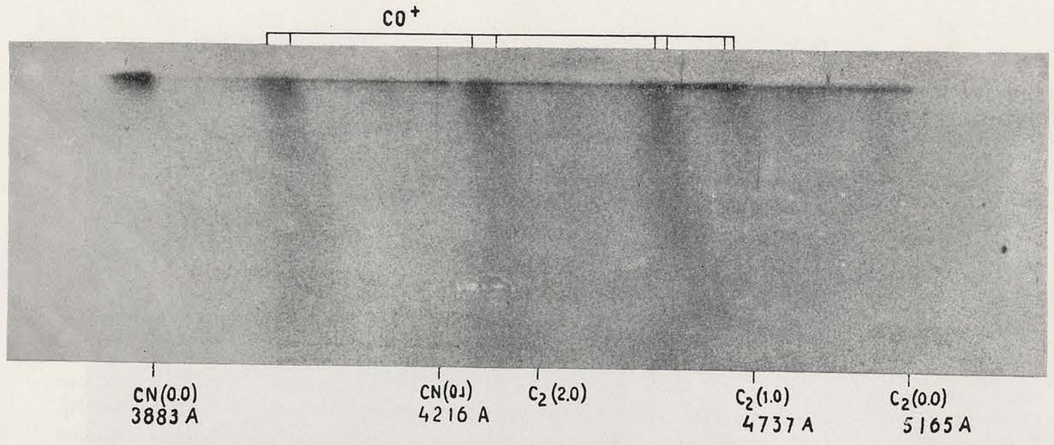

2

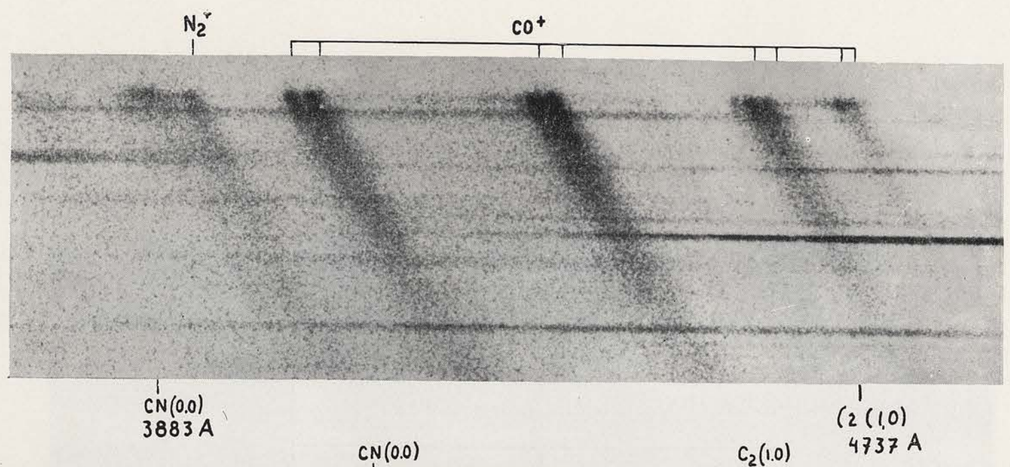

3

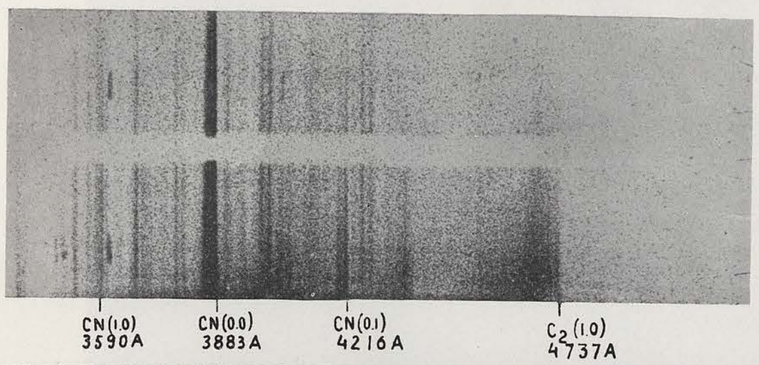

4

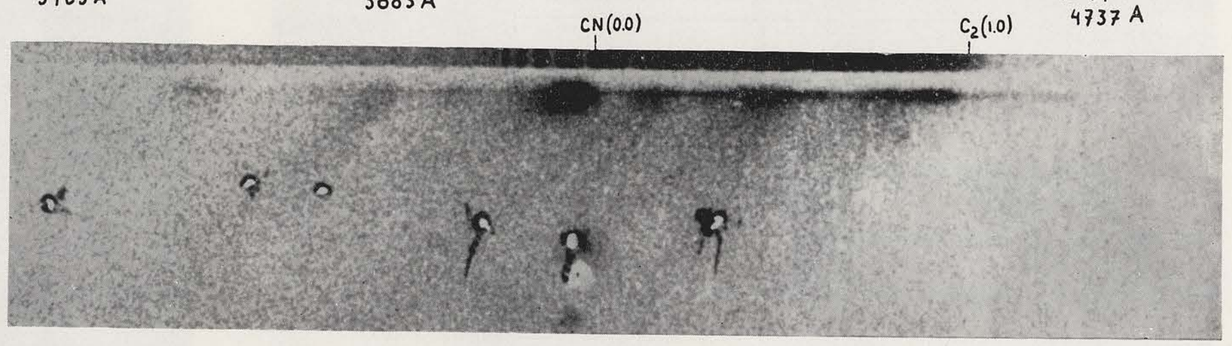

5

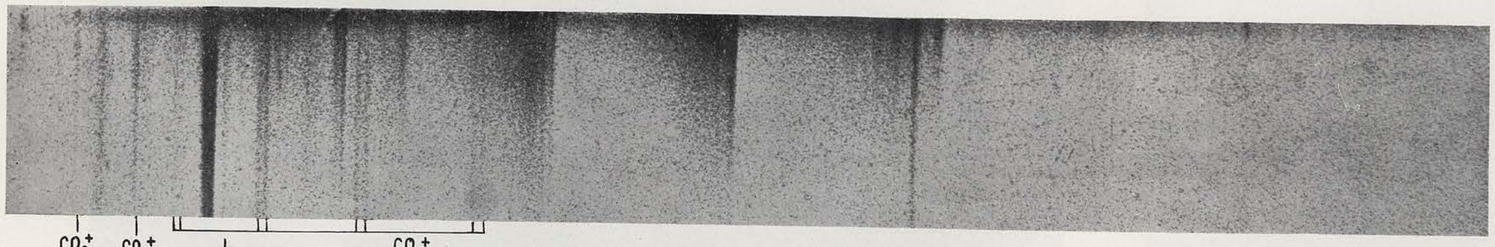

6

7

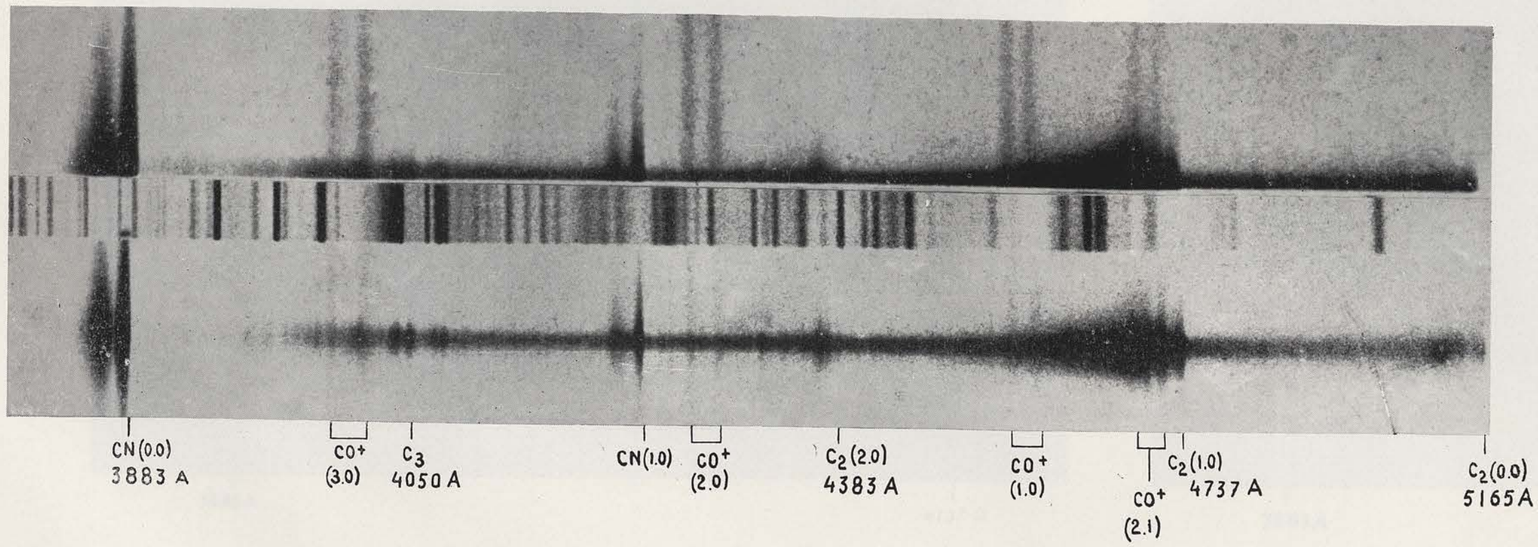

General aspect of spectrograms of comet heads and tails obtained with various types of instruments.

PLATE VI *a*, *b*.

*Objective Prism Spectrograms of Comet Morehouse (*1908 *c*, 1908 *III)*

List of spectrograms.

VI *a*		VI *b*	
No.	*r* (A.U.)	No.	*r* (A.U.)
1	1.51	1	1.43
2	1.49	2	1.37
3	1.48	3	1.14
4	1.44	4	1.07
5	1.43		

Instrument: objective prisms (Dr. F. Baldet); no comparison star centered.

Notes:

(1) Comet Morehouse had a peculiarly strong tail; the CO^+- and N_2^+-tail emissions were already intense at $r = 1.51$.

(2) The usual head spectrum is very weak; only CN(0-0) is conspicuous; the continuum is very weak.

(3) The doublet character of the CO^+-bands appears strikingly, although the appearance of the CO^+ emissions is complicated on sp. 5, 6 and 7, on account of the geometrical structure of the tail. The CO^+- and N_2^+ emissions are strong near the nucleus and extend slightly toward the sun in addition to their long extension away from the sun.

(4) Compare this plate with plate III (Comet Bester).

PLATE VI*a*

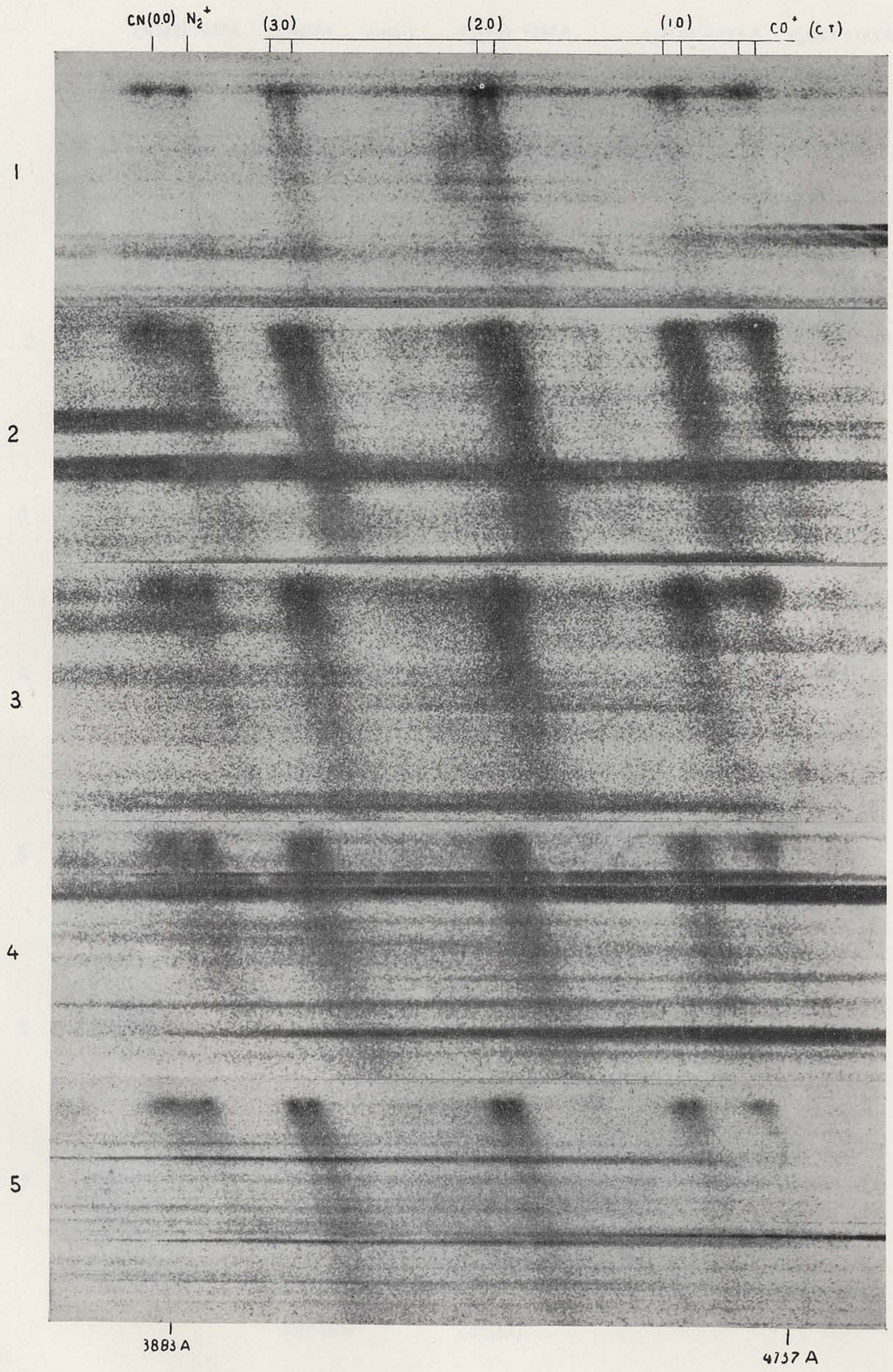

PLATE VI*b*

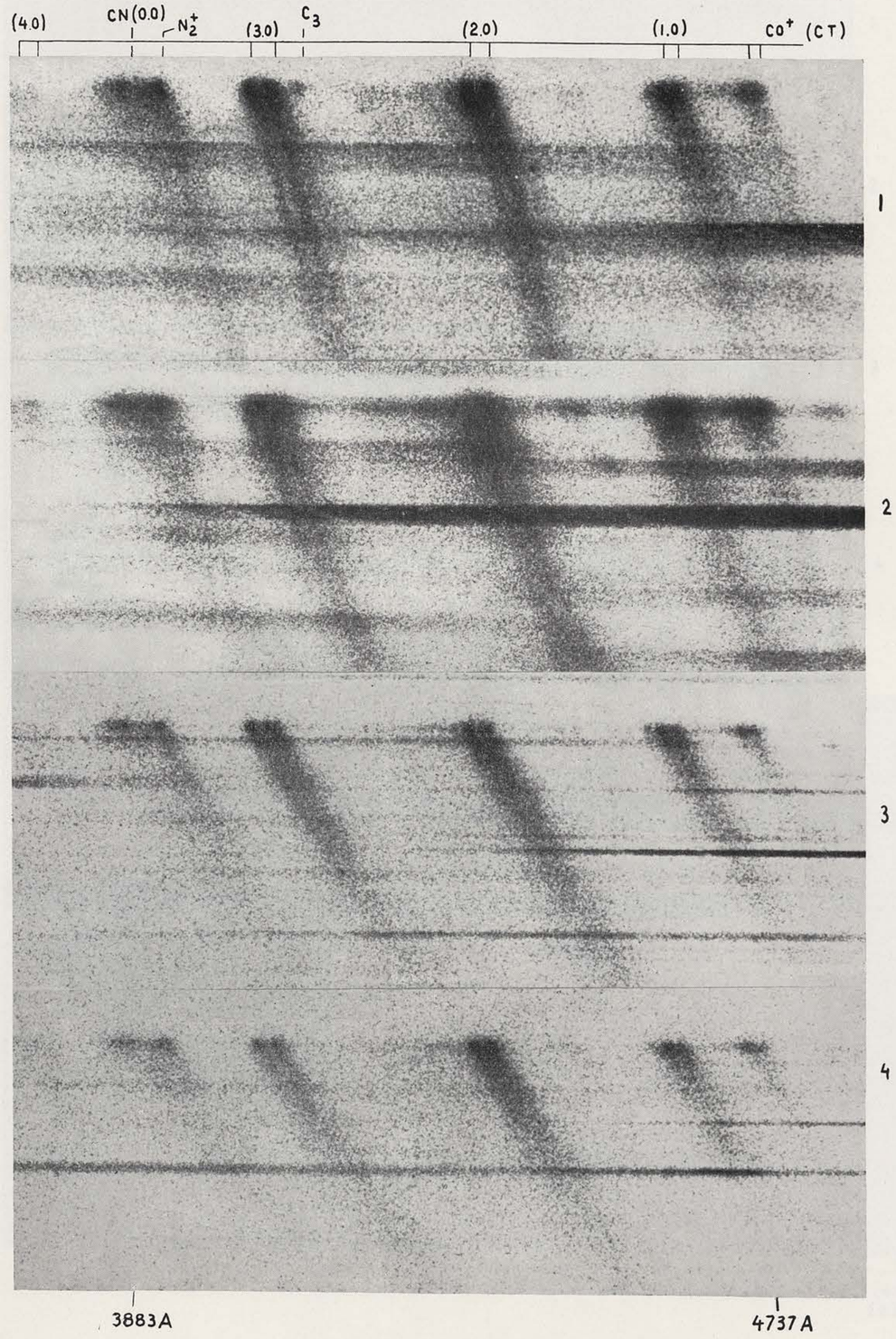

VI *a*, *b* Objective prism spectrograms of Comet Morehouse (1908 *c*, 1908 III).

PLATE VII *a*, *b*.

Head and Tail of Comet Brooks (1911 c-1911 *V*) *(Continued on Plate VIII a)*

List of spectrograms.

VII *a*		VII *b*	
No.	*r* (A.U.)	No.	*r* (A.U.)
1	1.42	1	0.90
2	1.38	2	0.89
3	1.30	3	0.85
4	1.10	4	0.85
5	1.06	5	0.82
6	1.04	6	0.81
7	0.94	7	0.63

Instruments: Objective prism spectrograms taken by Baldet:
on plate VII *a*: sp. 1, 2, 3, 5, 6, 7
on plate VII *b*: sp. 1, 2, 3, 5, 6, 7,
and at Lick Observatory:
on plate VII *a*, sp. 4
on plate VII *b*, sp. 4.
The spectrograms obtained by Baldet were generally more strongly exposed than the Lick Observatory plates.
Sp. 1, 2, 3, 5, 6, 7 of plate VII *a* have a comparison stellar spectrum (spectral class A). On plate VII *b*, sp. 5 and 6, the spectrum of a field star was not centered.

Notes:

(1) Tail appears at $r = 1.06$ (sp. 5), in sharp contrast with Comet Morehouse, where the tail was strong at $r = 1.51$ (see plate VI).

(2) Very different extensions of specific molecules in head (beware of effect of exposure time!). Decreasing order of extensions: CN, C_2, C_3, CH. The CN and C_2 emissions have asymmetric extensions (in direction of tail.)

(3) A CO^+-emission coincides with C_2; beware of erroneous assignment!

PLATE VII*a*

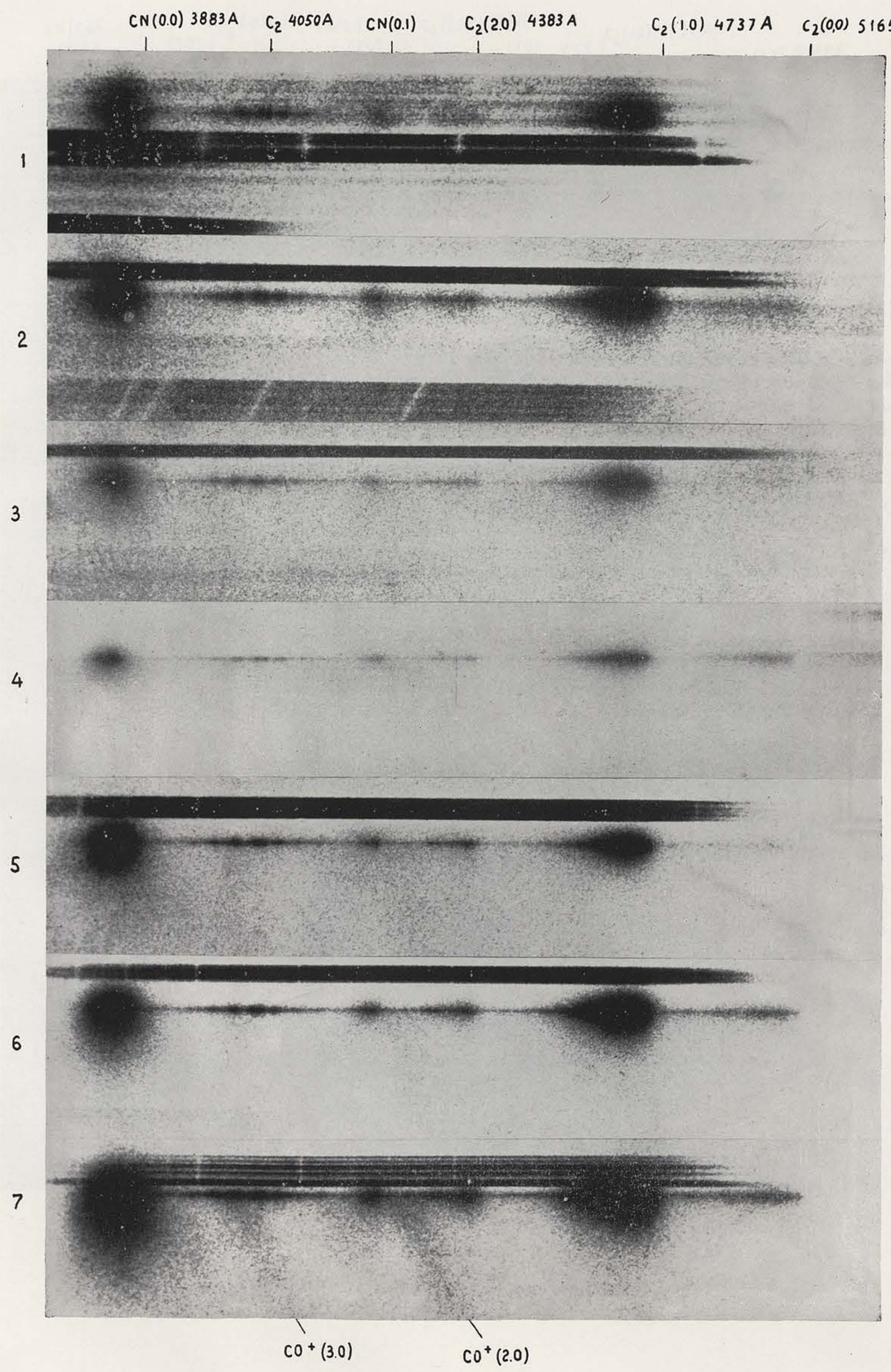

PLATE VII*b*

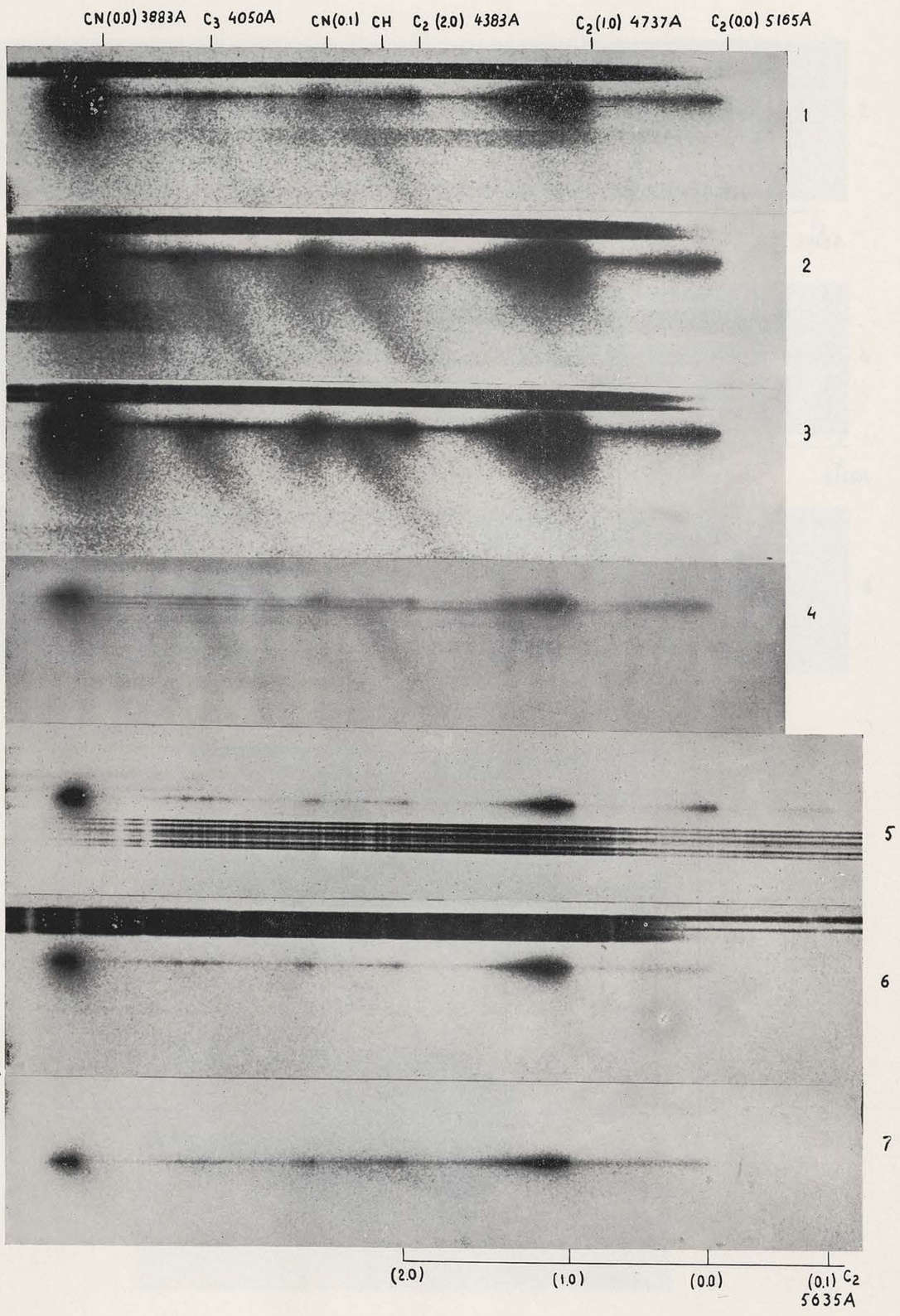

VII *a*, *b* Head and tail of Comet Brooks (1911 c - 1911 V) (continued on plate VIII *a*).

PLATE VIII *a*

Head and Tail of Comet Brooks (1911 c, 1911 *V*)
(Continued from Plate VII)

List of spectrograms.

No.	*r* (A.U.)	
1	0.53	
2	0.49	← perihelion
3	0.49	
4	0.50	
5	0.50	
6	0.50	

Instrument: Objective prism spectrograms taken by Baldet: sp. 3, 5, 6, and at Lick Observatory: sp. 1, 2, 4.

PLATE VIII *b*

General Aspect of Spectrograms of Low Resolution

List of spectrograms.

No.	Comet	*r* (A.U.)	Instrument
1	1937 II	0.65	Slit; glass prisms; Mt Wilson
2	1937 V	0.87	Slit; glass prisms; Lick
3	1943 I	1.54	Slit; quartz prisms; O.H.P. (Barbier)
4	1943 I	1.88	Slit; glass prisms; Mt Wilson
5	1951 I	2.57	6° O.P.; Curtis Telescope (103aO-emulsion)
6	1951 I	2.57	6° O.P.; Curtis Telescope (103aE, plus red Wratten 22 filter)
7	1948 IV	0.88	12° O.P.; 4″Ross; Michigan (103aO)
8	1952 III	1.22	6° + 4° O.P.; Curtis Telescope (103aE, plus red Wratten 22 filter)

Notes (Plate VIII *a*) :

(1) Notice variations in aspect of tail: curved on sp. 1 and 2; double on sp. 3, 4, 5, 6.

(2) Sp. 6 extends into ultraviolet; NH-emission in head.

Notes (Plate VIII *b*) :

(1) Low resolution spectrograms, such as those on plate VIII *b* reveal: the presence or absence of a continuous spectrum; the nature of the radicals which are present; the relative integrated band intensities'; the presence ot emissions of the tail. They also give some indication on the spatial distribution of the different emissions.

(2) These low resolution slit spectrograms (sp. 1 to 4) reveal some structure in the OH, NH and C_3 emissions; none or hardly any in CN, C_2 and CH.

(3) Compare sp. 5 and 7. On 5: almost pure continuum (confirmed on slit spectrograms, see plate XIV *a*, sp. 4); on 7: weak continuum, strong gaseous head emission and trace of tail (confirmed on slit spectrograms, see plate XII *b*).

(4) Sp. 6 and 8 give red part of spectrum.
Sp. 6: solar continuum;
sp. 8: solar continuum, plus weak contribution from NH_2 and C_2.

PLATE VIII*a*

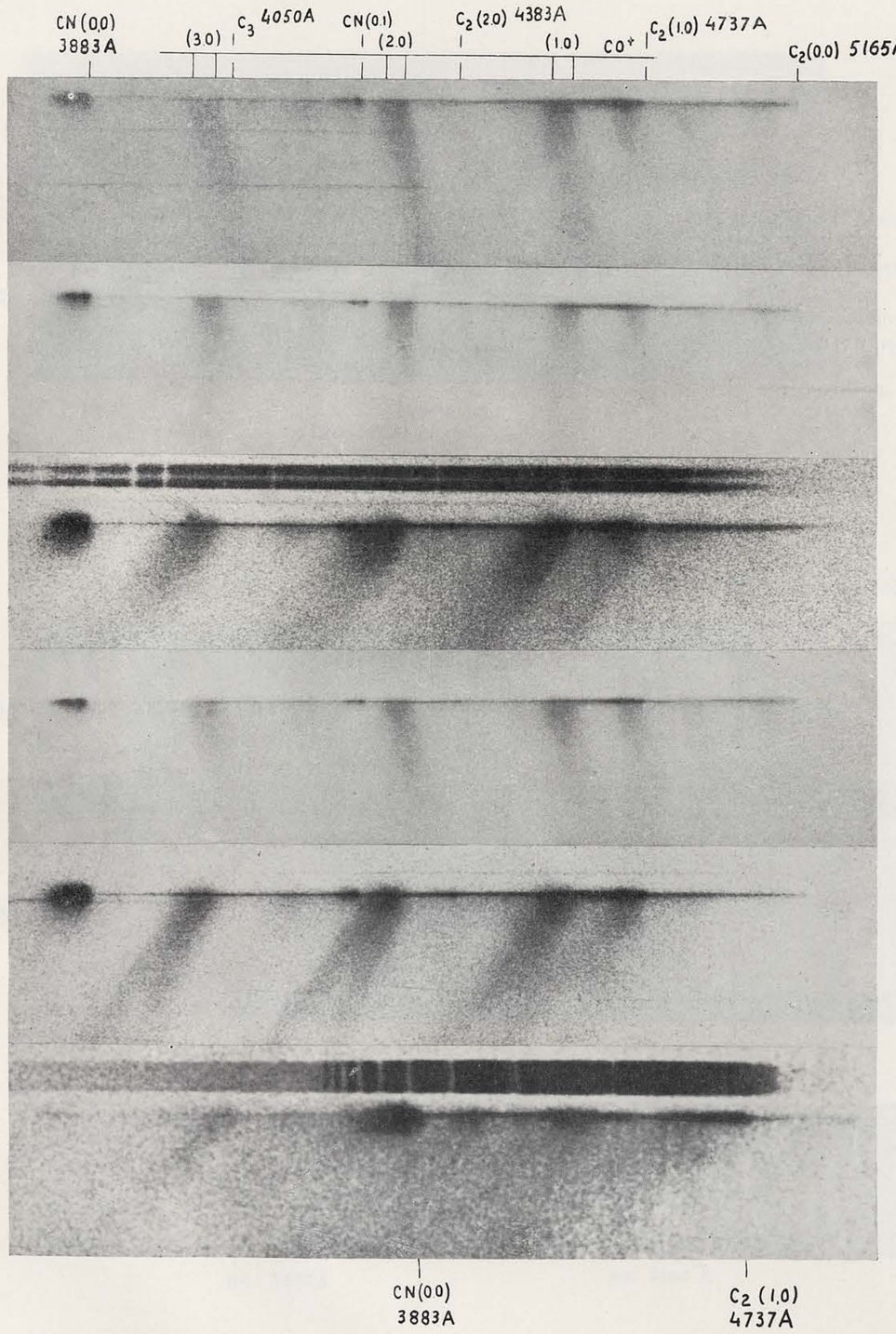

VIII a Head and tail of Comet Brooks (1911 *c* - 1911 V) (continued from plate VII).

PLATE VIII*b*

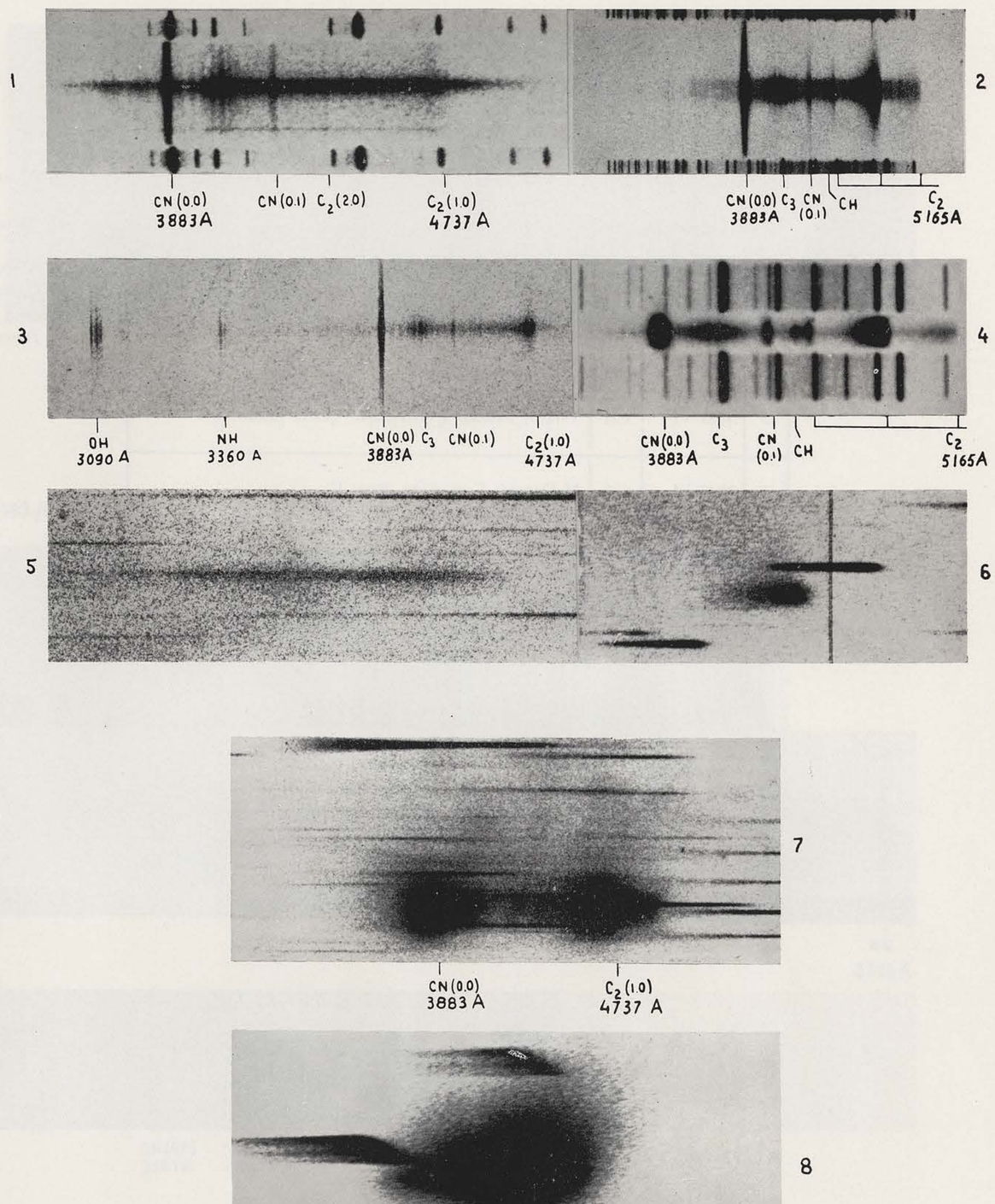

VIII *b* General aspect of spectrograms of low resolution.

PLATE IX

Spectrograms of Comet Encke Obtained at the 1937 and 1947 Apparitions

List of spectrograms.

No.	Comet	r (A.U.)	
1	1937 VI	0.95	O.P.; Lyons (Dufay).
2	1937 VI	0.83	O.P.; Lyons (Dufay).
3	1937 VI	1.31	Yerkes; Nebular spectrograph; quartz prisms; *f*/1.
4	1947 XI	1.13	McDonald; Cassegrain; glass; *f*/1.
5	1947 XI	1.02	McDonald; Cassegrain; glass; *f*/1.
6	1947 XI	1.06	McDonald; Cassegrain; quartz; *f*/1.

Remark: Original plate of sp. 5 is damaged between C_2(1-0) and C_2(2-0); the definition of the slit spectrograms is rather poor; presence of night glow.

Notes:

(1) A comparison of the two apparitions reveals that C_3 was definitely stronger in 1947 than in 1937.

(2) Asymmetry of emissions in head.

(3) Absence of solar continuum and of any other possible continuum in blue-violet region. The strong C_3-emission is *not* accompanied by a violet continuous emission.

(4) Presence of OH- and NH-bands, NH being stronger than OH.

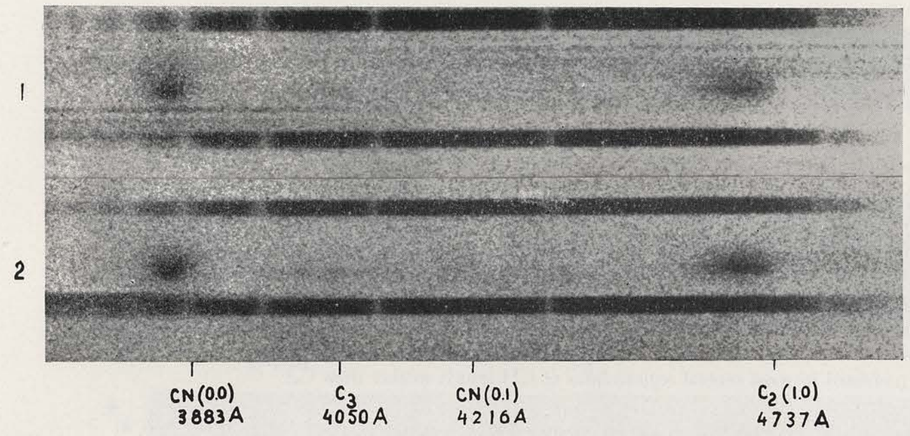

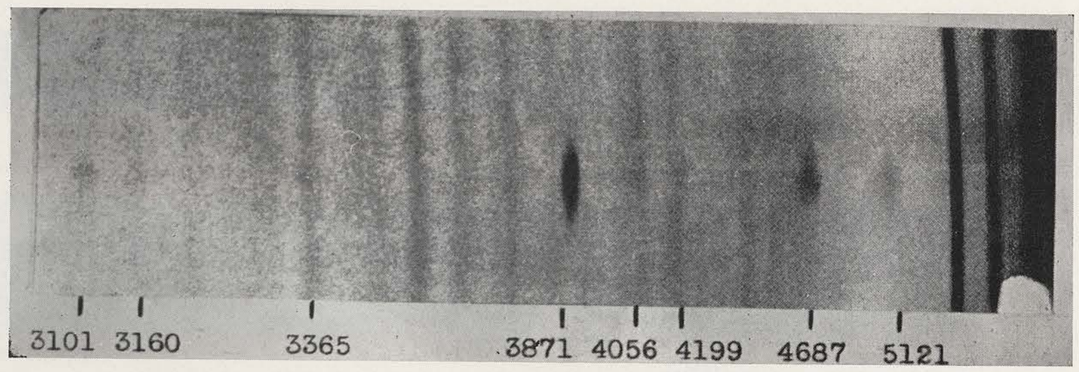

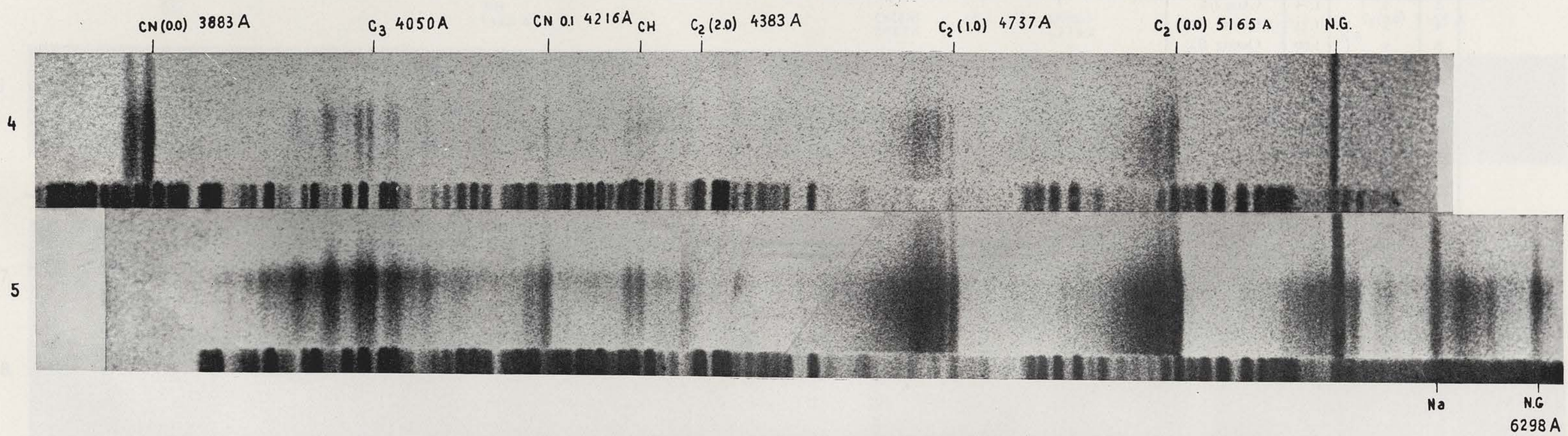

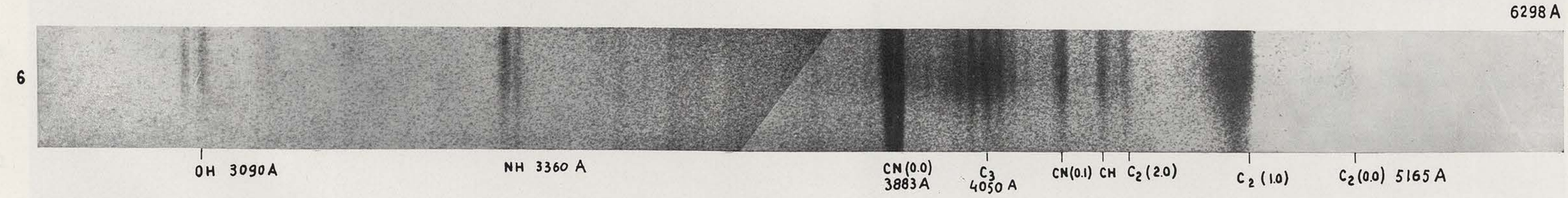

Spectrograms of Comet Encke obtained at the 1937 and 1947 apparitions.

PLATE X

Slit Spectrograms of Two Fairly Distant Comets: Whipple-Bernasconi-Kulin (1942 a, 1942 IV) and Van Gent (1941 d, 1941 VIII)

All spectrograms were taken with the McDonald Cassegrain spectrograph; several (6, 7, 9, 10) reveal nightglow lines of [OI].

List of spectrograms

No.	Comet	*r* (A.U.)	Instrument
1	1942 IV	1.76	Quartz *f*/2
2	»	1.75	Glass *f*/2
3	»	1.74	Glass *f*/2
4	»	1.73	Quartz *f*/2
5	»	1.60	Quartz *f*/2
6	1941 VIII	1.54	Glass *f*/1
7	»	1.52	Quartz *f*/1
8	»	1.27	Quartz *f*/1
9	»	1.26	Quartz *f*/1
10	»	1.25	Quartz *f*/1

Notes:

(1) Reflected solar spectrum very strong in 1942 IV, fairly strong in 1941 VIII; see depth of Fraunhofer lines; strong G- band in solar absorption in 1942 IV, near location of CH cometary emission which is extremely weak or absent.

(2) On 1942 IV, notice: the presence of strong CN, average C_3, weak C_2; the presence of OH and NH, the latter being relatively weak (only Q-branch).

(3) On 1941 VIII, notice: the appreciable extension of C_3; the great intensity of OH relative to NH; the presence of short (confined in most central region) lines of CH (much weaker than C_3).

(4) Structure of OH in 1942 IV and 1941 VIII should be compared with structure in 1941 I (Plate II, sp. 5, 6, 8) and 1948 I (Plate XVI *b*, sp. 3).

(5) Possibility of short emissions in 1941 VIII in region λ 3700-λ 3800.

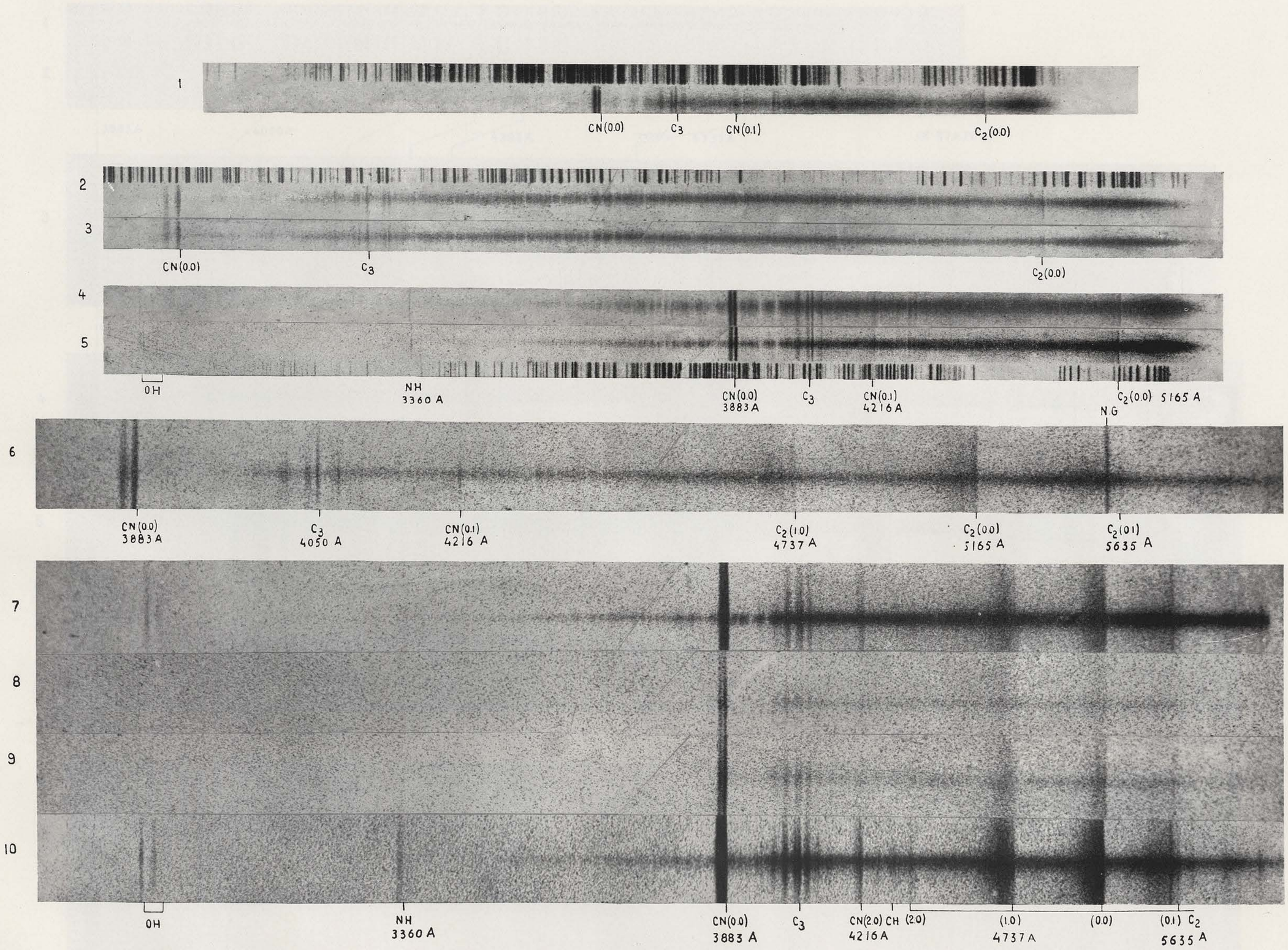

Slit spectrograms of two fairly distant comets: Whipple - Bernasconi - Kulin (1942 *a* - 1942 IV) and Van Gent (1941 *d* - 1941 VIII).

PLATE XI

Silt Spectrograms of Eclipse Comet (1948 1, 1948 XI)

List of spectrograms.

All spectrograms, except no. 1, were obtained with the McDonald Cassegrain spectrograph.

No.	r (A.U.)	Instrument
1	0.52	Cordoba; grating (Sahade)
2	0.65	Quartz; f/5 camera (CQ-designation)
3	0.73	Quartz; f/2
4	0.78	Glass; f/2
5	1.01	Glass; f/1
6	1.08	Glass; f/1
7	1.63	Quartz; f/1
8	2.22	Quartz; f/1

Notes:

(1) The intense reflected solar spectrum belongs to the central region of the head; the apparent variation in width of this solar continuum is due to the sensitivity curve of the emulsion. Notice the deep absorption lines. The solar absorption feature shortward of C_2(5-4)—see sp. 2—may perturb the appearance of the profile of the C_2-cometary sequence.

(2) Well developed structure of CN(0-0) on sp. 1, 2 and 4.

(3) At r= 2.22, only CN and C_3 remain.

(4) Nightglow emissions on sp. 3, 4, 5, 6.

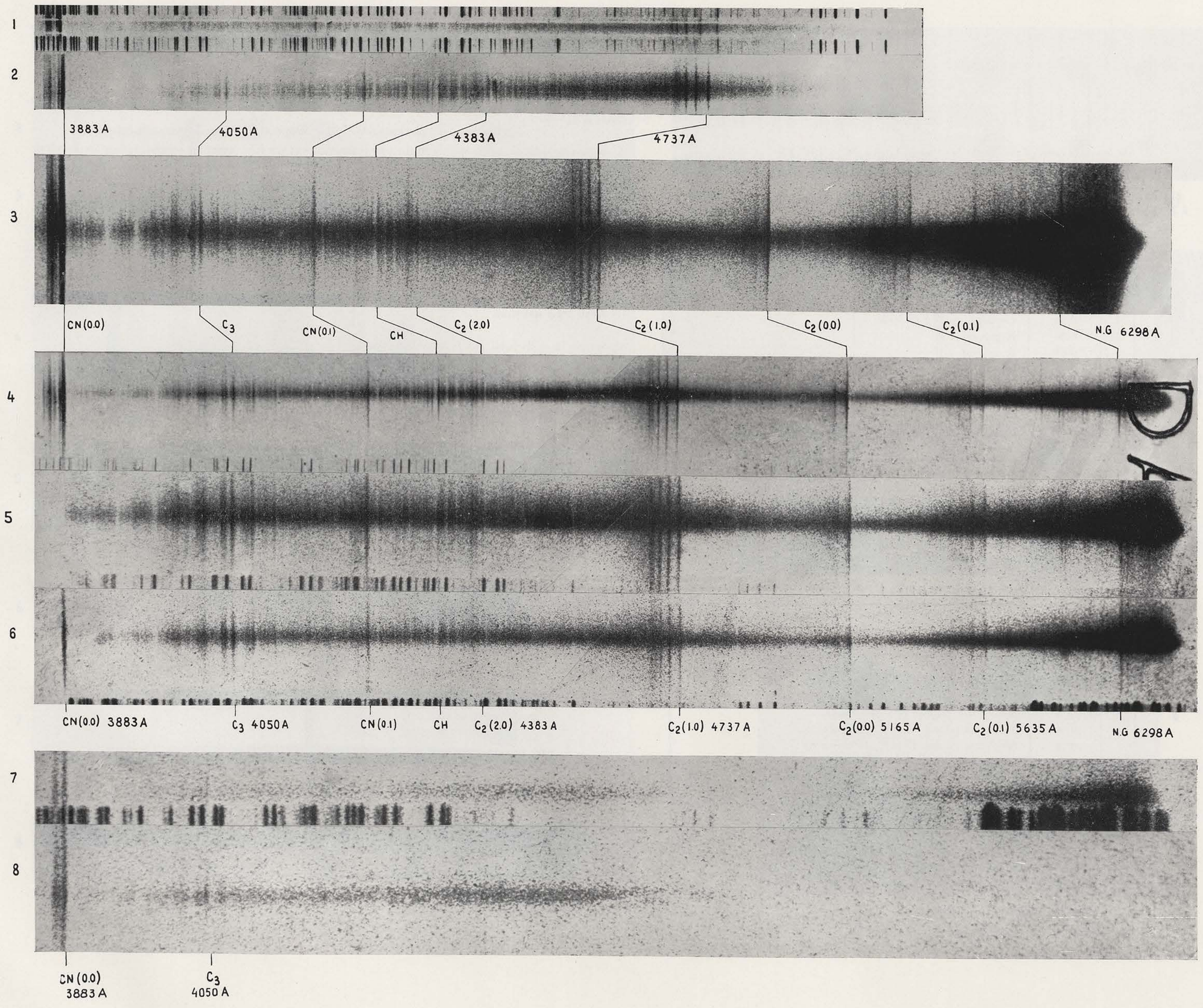

Slit spectrograms of Eclipse Comet (1948 *I* - 1948 XI).

PLATE XII *a*

Slit Spectrograms of the Bright Southern Comet (1947 *n*, 1947 XII)

List of spectrograms.

All spectrograms, except sp. 1, were obtained at McDonald Observatory: sp. 2 and 3 at the prime focus, 4 to 8 at the Cassegrain focus.

No.	*r* (A.U.)	Instrument
1	0.34	Cordoba, grating (Sahade)
2	0.59	B, grating
3	0.65	B, grating
4	0.78	Quartz, *f*/2
5	0.83	Glass, *f*/2
6	0.98	Glass, *f*/1
7	1.02	Quartz, *f*/1
8	1.07	Glass, *f*/1

Notes (Plate XII *a*) :

(1) Beginning with sp. 4, the spectra of the two components of the split comet are separated; they are identical.

(2) Comet 1947 XII is probably deficient in CH.

(3) Excellent resolution in visual region (NH_2) on sp. 2 and 3. Also for CN and C_2(1-0) on sp. 5.

PLATE XII *b*

Slit Spectrograms of Comet Honda-Bernasconi (1948 *g*, 1948 *IV*)

List of spectrograms.

No.	*r* (A.U.)	Instrument
1	0.67	Slit; glass prisms; O.H.P. (Fehrenbach).
2	0.69	Slit; glass prisms; O.H.P. (Fehrenbach).
3	0.74	Slit, quartz prisms; F/2, McDonald.
4	0.76	Slit; glass prisms; O.H.P. (Fehrenbach).
5	0.79	Slit; glass prisms; O.H.P. (Fehrenbach).
6	0.79	Objective prism, Sonneberg (Richter).
7	0.86	Objective prism, Sonneberg (Richter).

Comparison spectrum: iron + neon on sp. 1 and 2; iron on all others.

Notes (Plate XII *b*) :

(1) Weak solar spectrum.

(2) Strong $^2\Delta - {}^2\Pi$ band of CH at λ 4313.

(3) Strong emission and well defined structure of C_3 band on sp. 3; notice emissions shortward of CN(0-0).

(4) Long extension of CN(0-0) on sp. 6 and 7.

(5) Well developed resolution of sp. 1 and 2 in red region.

PLATE XIIa

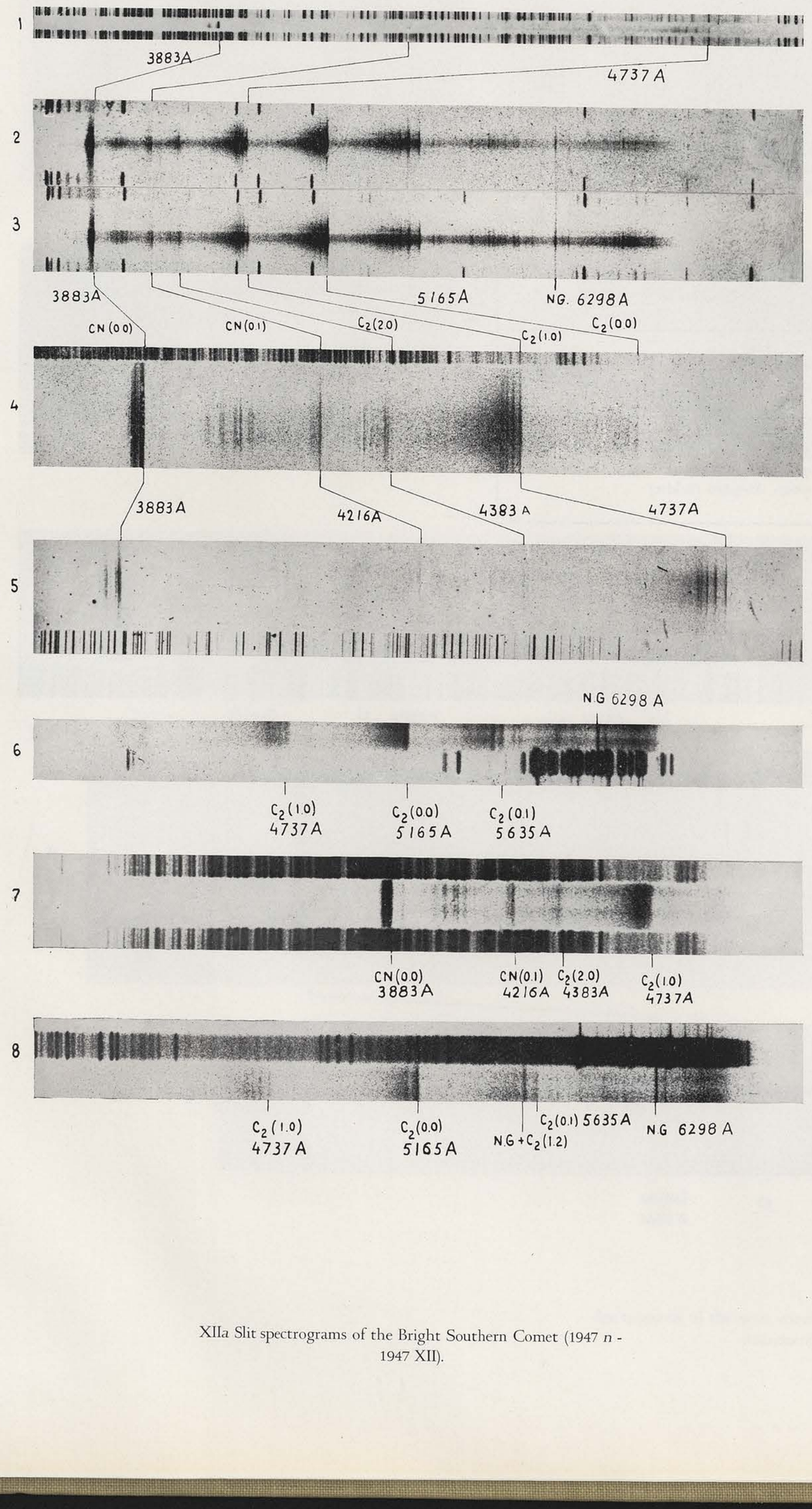

XIIa Slit spectrograms of the Bright Southern Comet (1947 *n* - 1947 XII).

PLATE XIIb

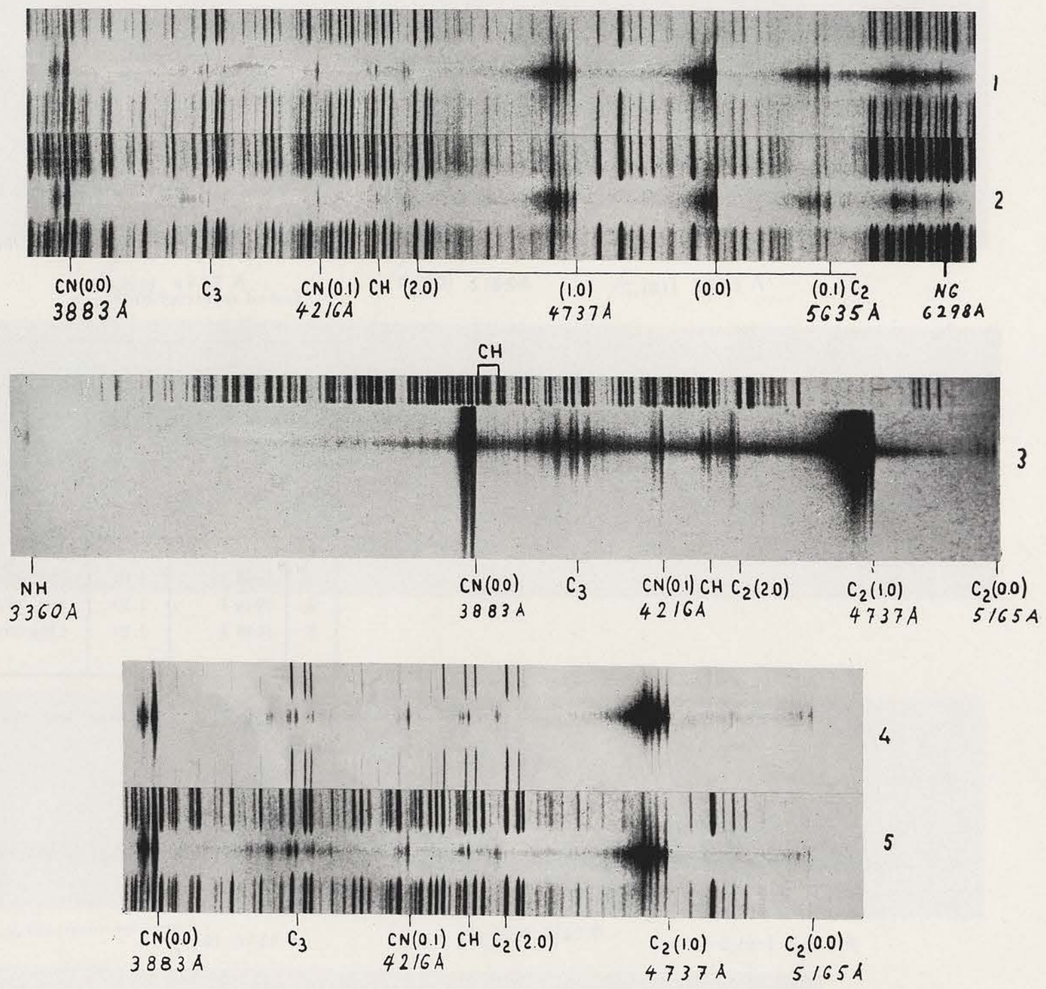

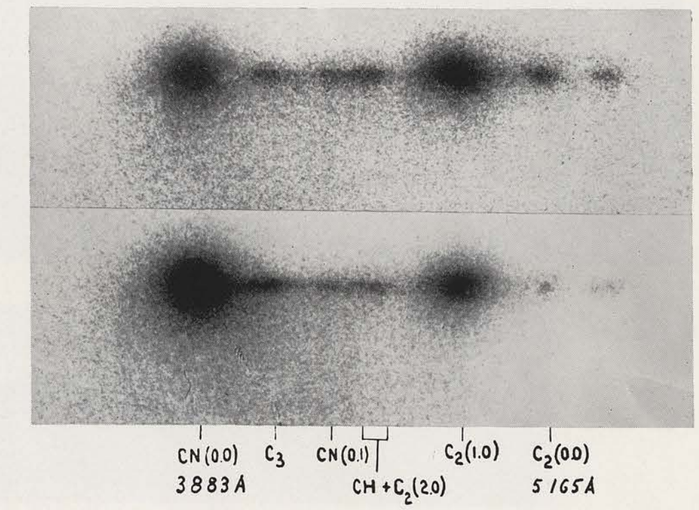

XII *b* Slit spectrograms of Comet Honda - Bernasconi (1948 *g* - 1948 IV).

PLATE XIII

Spectrograms of the same Comet Obtained with Different Instruments

List of spectrograms.

No.	Comet	r (A.U.)	Instrument
1	1937 V	0.89	Slit, prisms, Mt. Wilson
2	1937 V	0.87	Objective prism, Mt. Wilson
3	1948 I	1.16	Slit, glass prisms, F/1, McDonald
4	1948 I	1.30	Slit, grating, *f*/0.65, McDonald
5	1948 I	1.29	Objective prism, Meudon (Baldet)

The different resolutions and aspects are apparent.

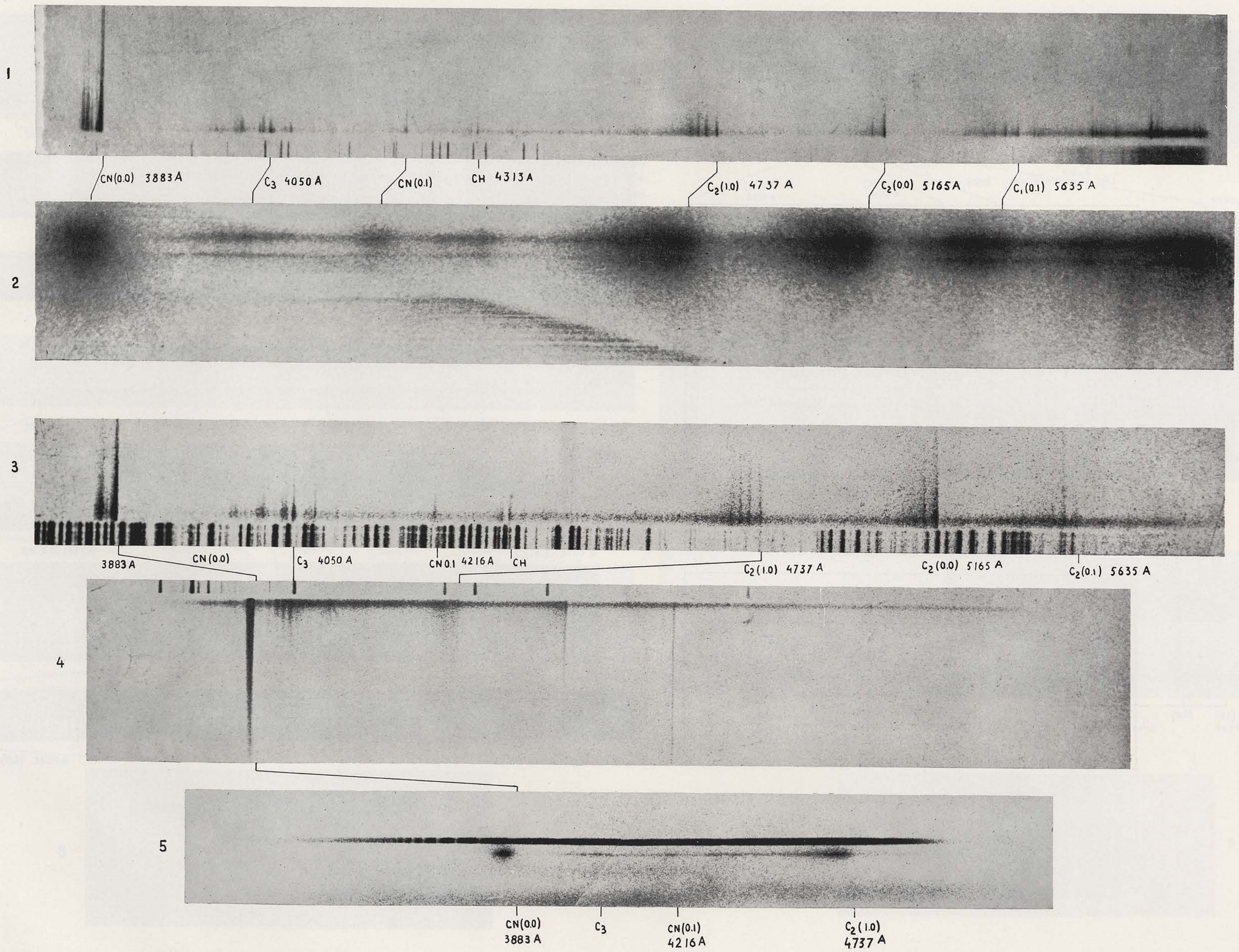

Spectrograms of the same comet obtained with different instruments.

PLATE XIV *a*

Appearance of the Solar Spectrum of the Central Condensation of a Comet's Head

List of spectrograms.

No.	Comet	*r* (A.U.)	Instrument
1	1910 II (Halley)	0.65	Slit, glass; Lick.
2	1941 I	2.24	Nebular spectrograph, quartz, *f*/1, McDonald.
3	1941 VIII	1.26	Quartz, *f*/1, Cassegrain, McDonald.
4	1951 I	2.64	Grating, *f*/0.65, Prime focus, McDonald (103aE).
5	1907 IV	0.59	Slit, glass, Lick.
6	1948 XI	0.73	Quartz, *f*/2, Cassegrain, McDonald.
7	1942 IV	1.73	Glass, *f*/2, Cassegrain, McDonald.
8	1951 I	2.64	Grating, *f*/0.65, Prime focus, McDonald (103aO).

PLATE XIV *b*

Effect of an Accidentally Superimposed Solar Spectrum due to Moonlight or Twilight

List of spectrograms.

No.	Comet	*r* (A.U.)	Instrument
1	1948 I	0.81	Grating, *f*/0.65, prime focus, McDonald.
2	1907 IV	0.52	Slit, glass, Lick.
3	1948 I	1.05	Quartż, *f*/1, Cassegrain, McDonald.
4	1951 I	2.66	Quartz, *f*/1, Cassergain, McDonald.
5	1941 I	0.50	Quartz, *f*/1, Cassegrain, McDonald.
6	1941 I	1.47	Quartz, *f*/1, Cassegrain, McDonald.
7	1951 I	2.66	Grating, *f*/0.65, prime focus, McDonald.

Note (Plate XIV *a*) :

Plate XIV *a* illustrates the fact that the central part of the head may exhibit a solar spectrum, irrespective of the heliocentric distance. There is no evidence for an additional continuum, such as a blue-violet continuum which would be associated to the λ 4050 group of C_3. See also plate IX (Comet Encke) where a strong C_3 emission appears on a perfectly dark background.

Notes (Plate XIV *b*) :

(1) Compare with XIV *a*; a solar spectrum due to moonlight or twilight extends over whole length of slit.

(2) Except in strong accidental exposures, OH is usually not perturbed.

(3) Plate XIV *b* illustrates the difficulty of identifying weak «emissions» in central condensation when a solar spectrum is present: spaces between absorptions may appear like emissions. The Fraunhofer lines are less crowded in the visual region.

PLATE XIV*a*

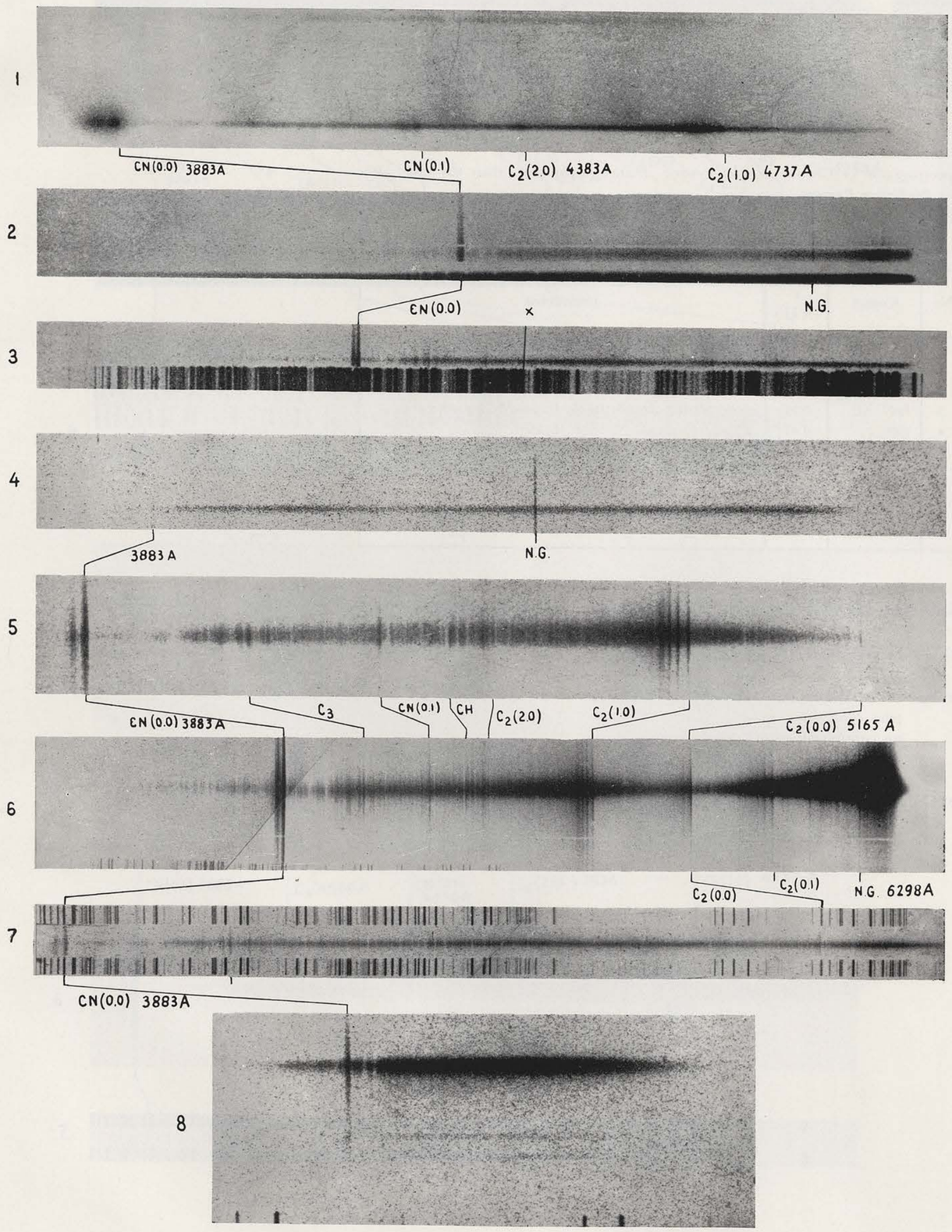

XIV *a* Appearance of the solar spectrum of the central condensation of a comet.

PLATE XIV*b*

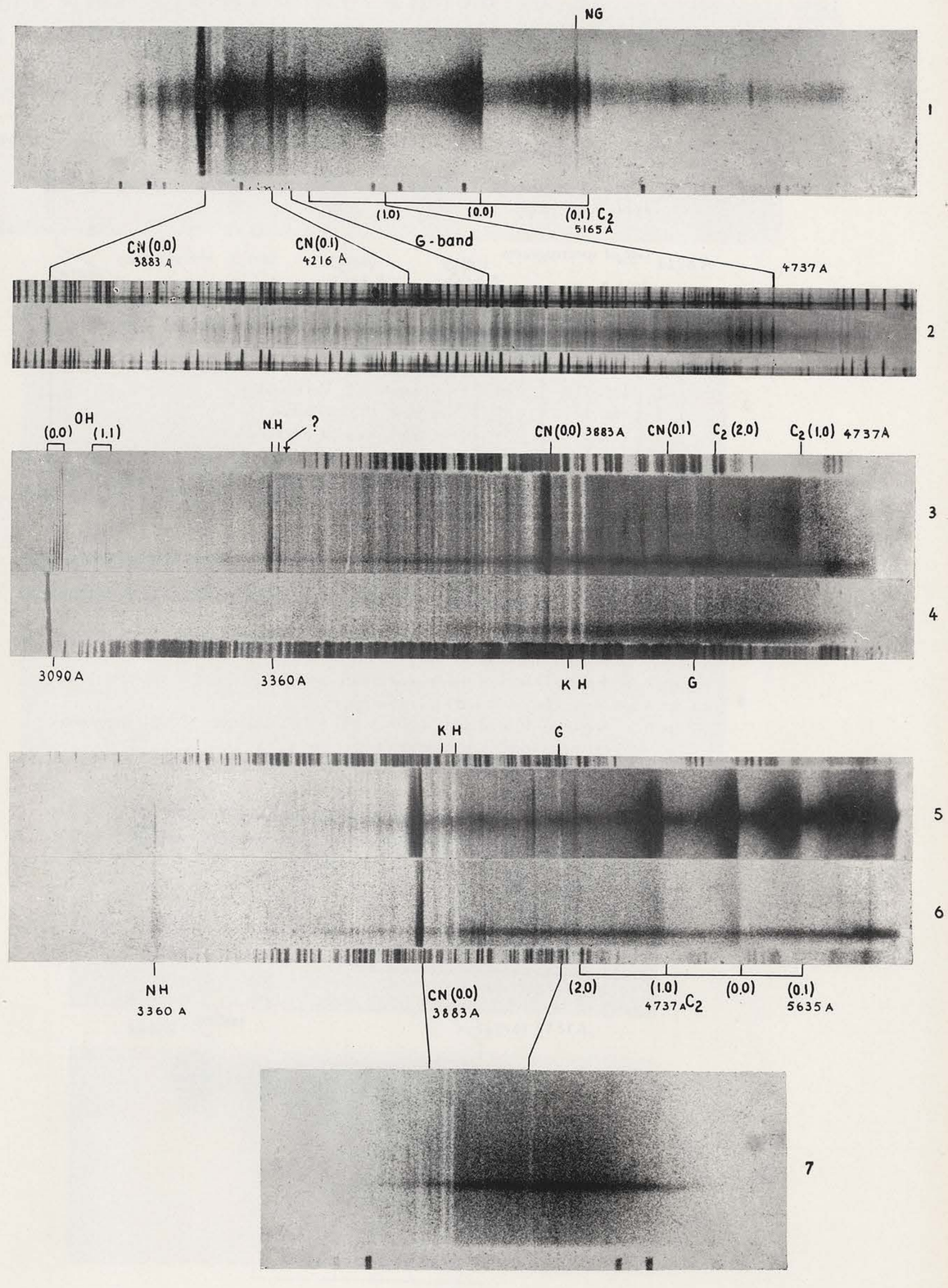

XIV *b* Effect of the accidentally superimposed solar spectrum due to moonlight or twilight.

PLATE XV *a*

Spectrograms of Comets at Heliocentric Distances Smaller than 0.6 A.U. before Perihelion Passage

List of spectrograms

No.	Comet	*r* (A.U.)	Instrument
1	1941 I	0.48	Slit, quartz, *f*/2, McDonald.
2	1941 I	0.57	Slit, glass, *f*/1, McDonald.
3	1941 I	0.55	Slit, glass, Victoria (McKellar).
4	1941 I	0.53	Slit, glass, Victoria (McKellar).
5	1911 V	0.53	Objective prism, Lick.
6	1907 IV	0.59	Slit, glass, Lick
7	1911 IV	0.34	Slit, glass, Lick.

Description:

sp. 1. — Sodium D-lines of comet and twilight are superposed; solar spectrum due to twilight; see plate II.
sp. 2. — Sodium D-lines of comet; see plate I.
sp. 3 and 4. — Only CN and C_2 are strong.
sp. 5. — Spectrum of head and of curved tail (CO^+, and trace of N_2^+); asymmetric extension of CN; coincidence of CO^+ and C_2 ($\Delta v = +1$).
sp. 6. — Strong continuum; compare with 1 and 2 (weak continuum), also with 7; effect of chromatic aberration of objective.

PLATE XV *b*

Spectrograms of Comets at Heliocentric Distances Smaller than 0.6 A.U. after Perihelion Passage

List of spectrograms.

No.	Comet	*r* (A.U.)	Instrument
1	1947 XII	0.34	Slit, grating, Cordoba (Sahade).
2	1947 XII	0.41	Slit, grating, Cordoba (Sahade).
3	1947 XII	0.59	Slit, grating, *f*/0.65, prime focus, McDonald.
4	1910 I	0.49	Objective prism, Meudon (Baldet).
5	1939 III	0.59	Slit, prisms, Victoria (McKellar).
6	1939 III	0.59	Objective prism, Meudon (Baldet).
7	1939 III	0.59	Objective prism, Hamburg (Beyer).
8	1948 XI	0.60	Objective prism, Cordoba (Sahade).

Notes (Plate XV *b*) :

(1) Good resolution of CN and C_2 on sp. 1 and 2.

(2) Sp. 4, 6, 7 and 8 illustrate various spectroscopic types of tail:
pure continuum, sp. 4;
no continuum, sp. 6-7;
partly continuum, partly CO^+, sp. 8.

(3) Compare sp. 2 and 3 (solar continuum) with 5, 6 ,7 (no continuum).

PLATE XV*a*

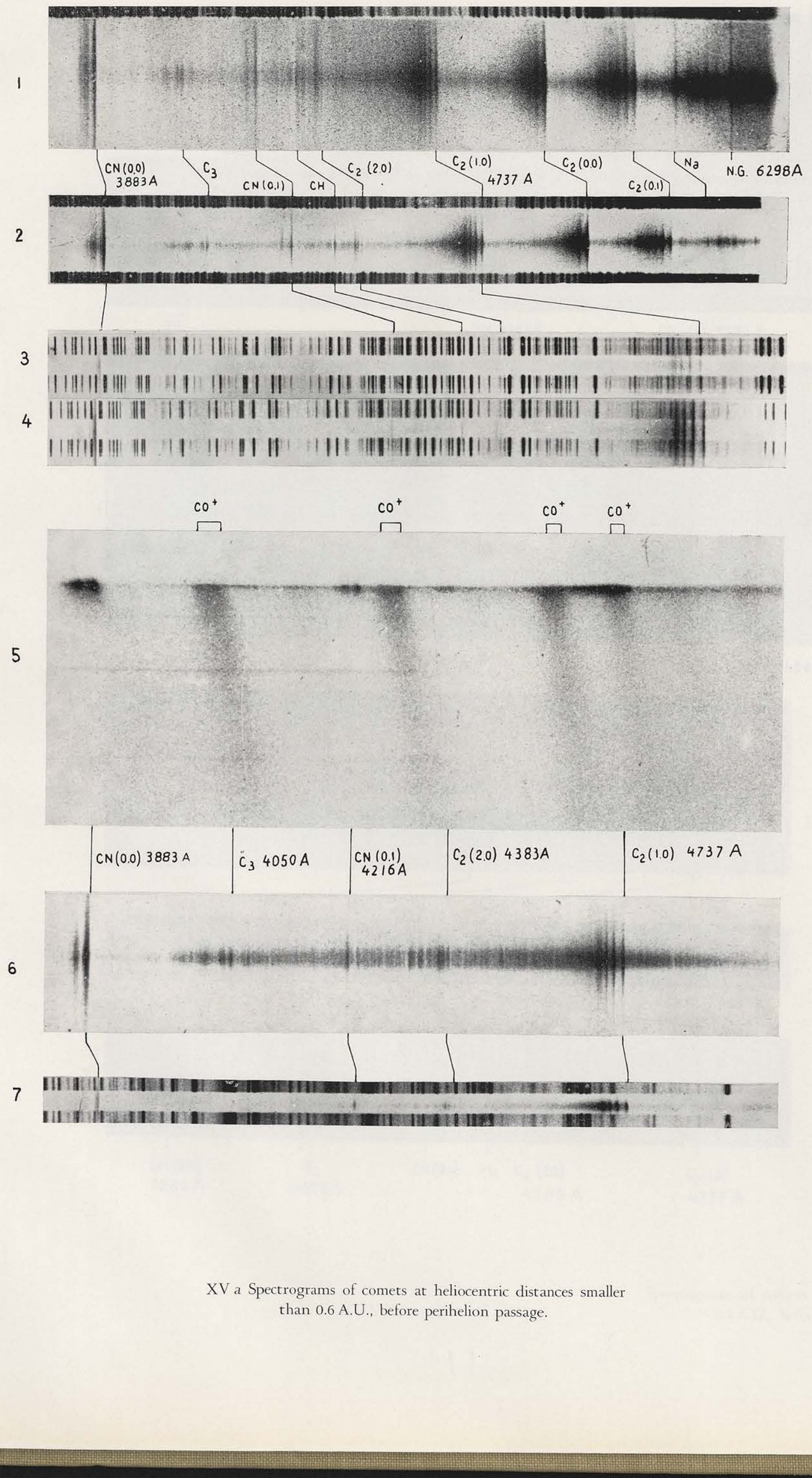

XV *a* Spectrograms of comets at heliocentric distances smaller than 0.6 A.U., before perihelion passage.

PLATE XV*b*

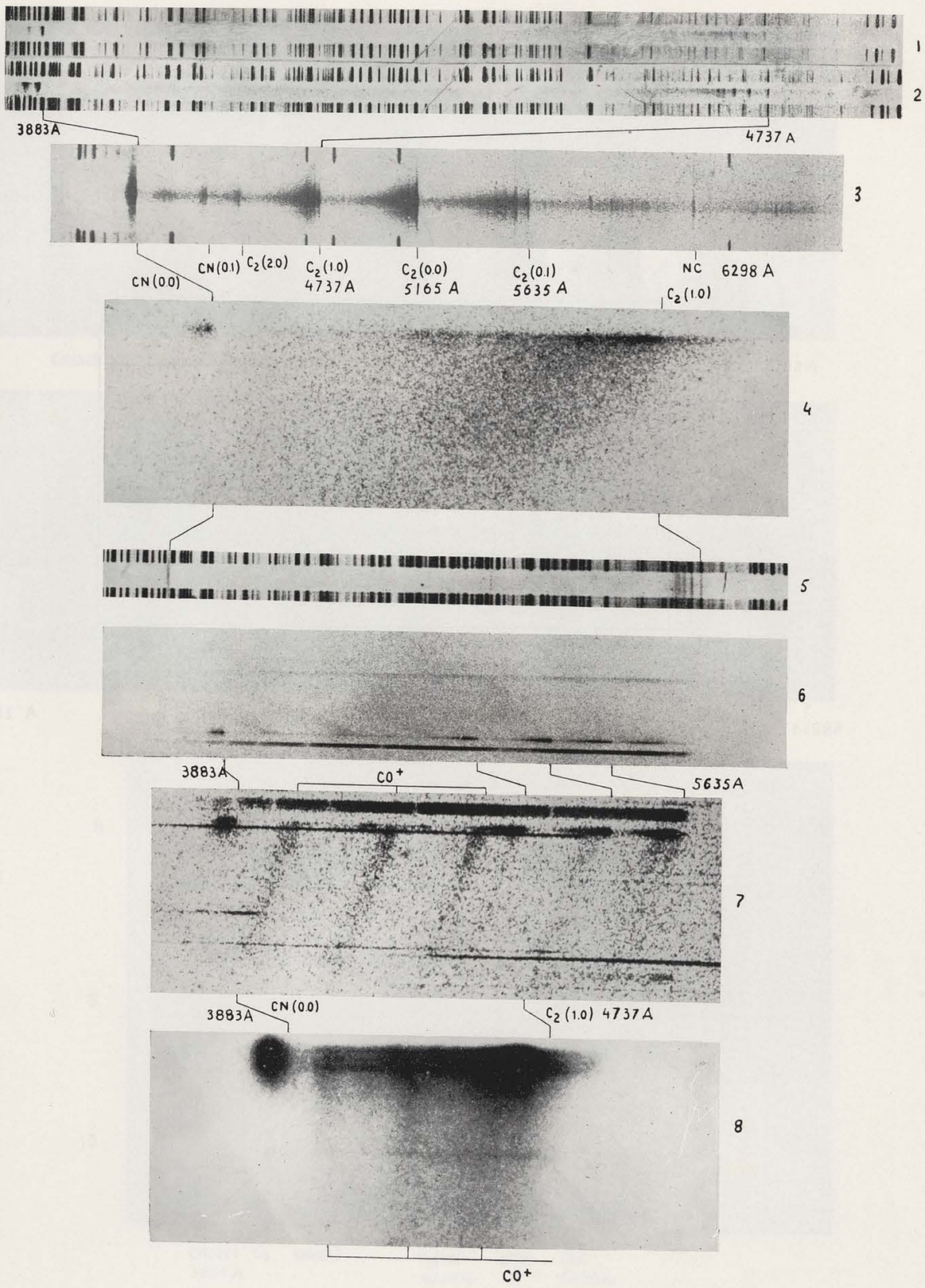

XV *b* Spectrograms of comets at heliocentric distances smaller than 0.6 A.U., after perihelion passage.

PLATE XVI

Spectrograms of Comets at Heliocentric Distances 0.6 *to* 0.8 *A.U. before Perihelion Passage*

List of spectrograms.

No.	Comet	r (A.U.)	Instrument
1	1941 I	0.75	Slit, quartz, f/1, McDonald.
2	1941 I	0.63	Slit, quartz, f/1, McDonald.
3	»	0.67	Slit, glass, f/1, McDonald.
4	»	0.69	Slit, glass, f/1, McDonald.
5	1903 IV	0.67	Slit, glass, Meudon (Baldet).
6	1947 XI	0.76	Slit, glass, f/1, McDonald.
7	1907 IV	0.71	Slit, glass, Lick.
8	1939 III	0.70	Objective prism, Lyons (Dufay).
9	1939 III	0.70	Objective prism, Lyons (Dufay).
10	1907 IV	0.70	Objective prism, Meudon (Baldet).

Notes :

(1) Continuous spectrum present on sp. 1, 2, 3, 4, 7, 10; absent on 5, 8 and 9, also on sp. 6 (Moon!).

(2) Strong tail on sp. 8 and 9; trace of tail on sp. 2 and 3.

(3) C_3 weak on sp. 8 and 9.

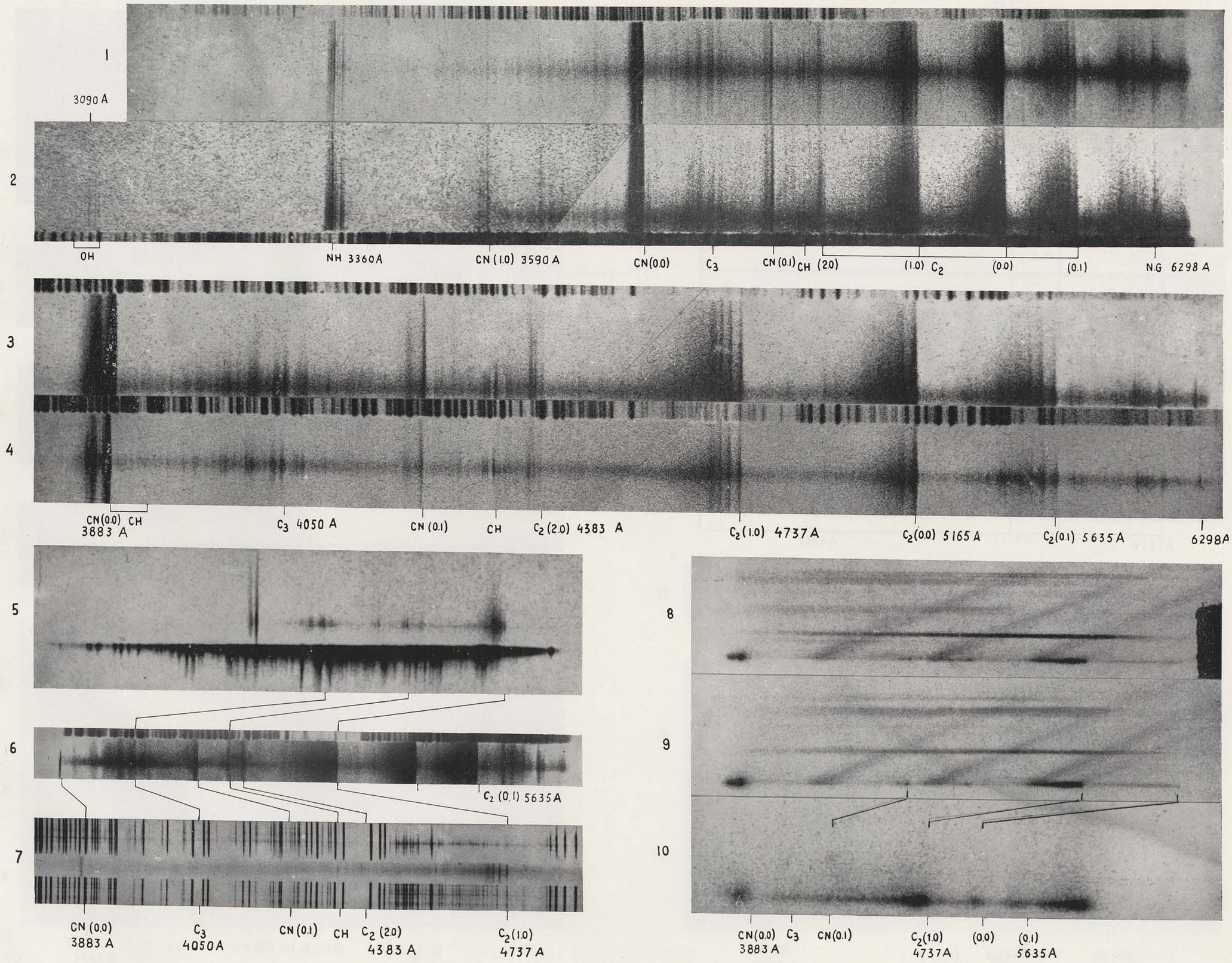

Spectrograms of comets at heliocentric distances 0.6 to 0.8 A.U., before perihelion passage.

PLATE XVII

Spectrograms of Comets at Heliocentric Distances 0.6 to 0.8 A.U. after Perihelion Passage

List of spectrograms

No.	Comet	*r* (A.U.)	Instrument
1	1948 XI	0.78	Slit, glass, *f*/2, McDonald.
2	1948 XI	0.65	Slit, quartz, *f*/5, McDonald.
3	1948 I	0.65	Slit, grating, *f*/0.65, McDonald.
4	1948 I	0.78	Slit, quartz, *f*/2, McDonald.
5	1910 II	0.64	Slit, glass, Lick.
6	1910 II	0.65	Objective prism, Lick.
7	1910 II	0.69	Objective prism, Lick.
8	1910 II	0.71	Objective prism, Lick.
9	1939 I	0.73	Objective prism, Lyons (Dufay).
10	1939 I	0.74	Objective prism, Lyons.
11	1939 I	0.74	Objective prism, Lyons.
12	1937 II	0.65	Slit, quartz, Lick.
13	1912 II	0.75	Objective prism, Meudon (Baldet).
14	1912 II	0.76	Objective prism, Meudon (Baldet).

Notes:

(1) The continuous spectrum is strong on sp. 1, 2, 3, 5, 6, 7, 8; weak on sp. 4, 9, 10, 11, 13, 14; absent on sp. 12.

(2) The intensity ratio of CH and C_2 (2-0) way be very different in different comets.

(3) The spectrum of the tail is present on sp. 6, 7, 8 (JHalley) and sp. 13, 14 (Gale).

(4) Sp. 13 and 14 show that CN has a much greater asymmetric extension than C_2; same on sp. 9, 10 and 11.

(5) Good resolution of CN on sp. 1 and 2.

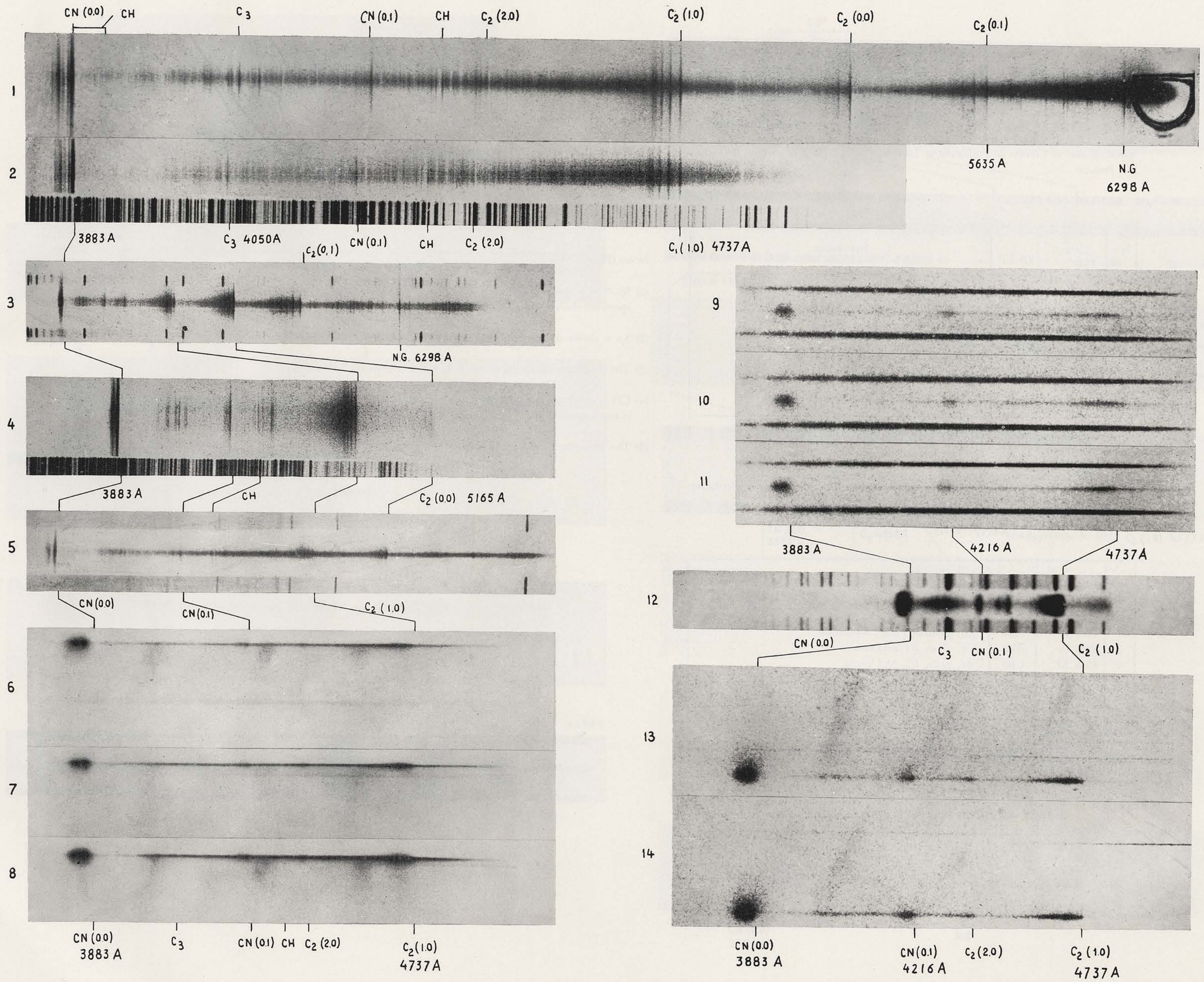

Spectrograms of comets at heliocentric distances 0.6 to 0.8 A.U., after perihelion passage.

PLATE XVIII *a*

Spectrograms of Comets at Heliocentric Distances 0.8 *to* 1.0 *A.U. before Perihelion Passage*

List of spectrograms

No.	Comet	*r* (A.U.)	Instrument
1	1937 V	0.88	Objective prism, Sonneberg (Richter).
2	1937 V	0.88	Objective prism, Lyons (Dufay)
3	1911 V	0.82	Objective prism, Meudon (Baldet).
4	1937 VI	0.83	Objective prism, Lyons Dufay).
5	1911 VI	0.85	Objective prism, Meudon (Baldet).
6	1911 V	0.85	Objective prism, Lick.
7	1941 I	0.85	Slit, glass, *f*/1, McDonald.

PLATE XVIII *b*

Spectrograms of Comets at Heliocentric Distances 0.8 *to* 1.0 *A.U. after Perihelion Passage*

List of spectrograms

No.	Comet	*r* (A.U.)	Instrument
1	1948 I	0.81	Slit, grating, *f*/0.65, McDonald.
2	1941 IV	0.80	Slit, glass, *f*/1, McDonald.
3	1948 XI	0.90	Slit, glass, *f*/2, McDonald.
4	1910 II	0.91	Slit, glass, Lick.
5	1912 II	0.91	Objective prism, Meudon (Baldet).
6	1947 XII	0.98	Slit, glass, *f*/1, McDonald (on 103aE).
7	1951 II	0.93	Slit, grating, *f*/0.65, McDonald.

Notes (Plate XVIII *a*) :

(1) CH stronger on sp. 7 (Cunningham) than on sp. 3 and 6 (Brooks).

(2) The $^2\Sigma - {}^2\Pi$ system of CH, visible on sp. 7, does not appear on objective prism spectrograms.

(3) NH_2 of approximately the same intensity on sp. 2 and 7.

Notes (Plate XVIII *b*) :

(1) Sp. 7 of Comet Pajdusakova (1951 II) is remarkable: despite the rather small heliocentric distance 0.93, the spectrum shows only CN emission in addition to the solar continuum (+ nightglow).

(2) Sp. 6 shows doubling of head, see plate XII *a*.

(3) The continuum is strong on sp. 1, 2, 4 and 7, weak on 3, 5 and 6.

(4) CH is much stronger on sp. 4 (Halley) than on any other on plate XVIII *b*. The intensity ratio C_3/CN is much greater on sp. 4 than on 2, 3 or 5.

(5) The intensity ratio C_2/CN is abnormally weak on sp. 2.

PLATE XVIIIa

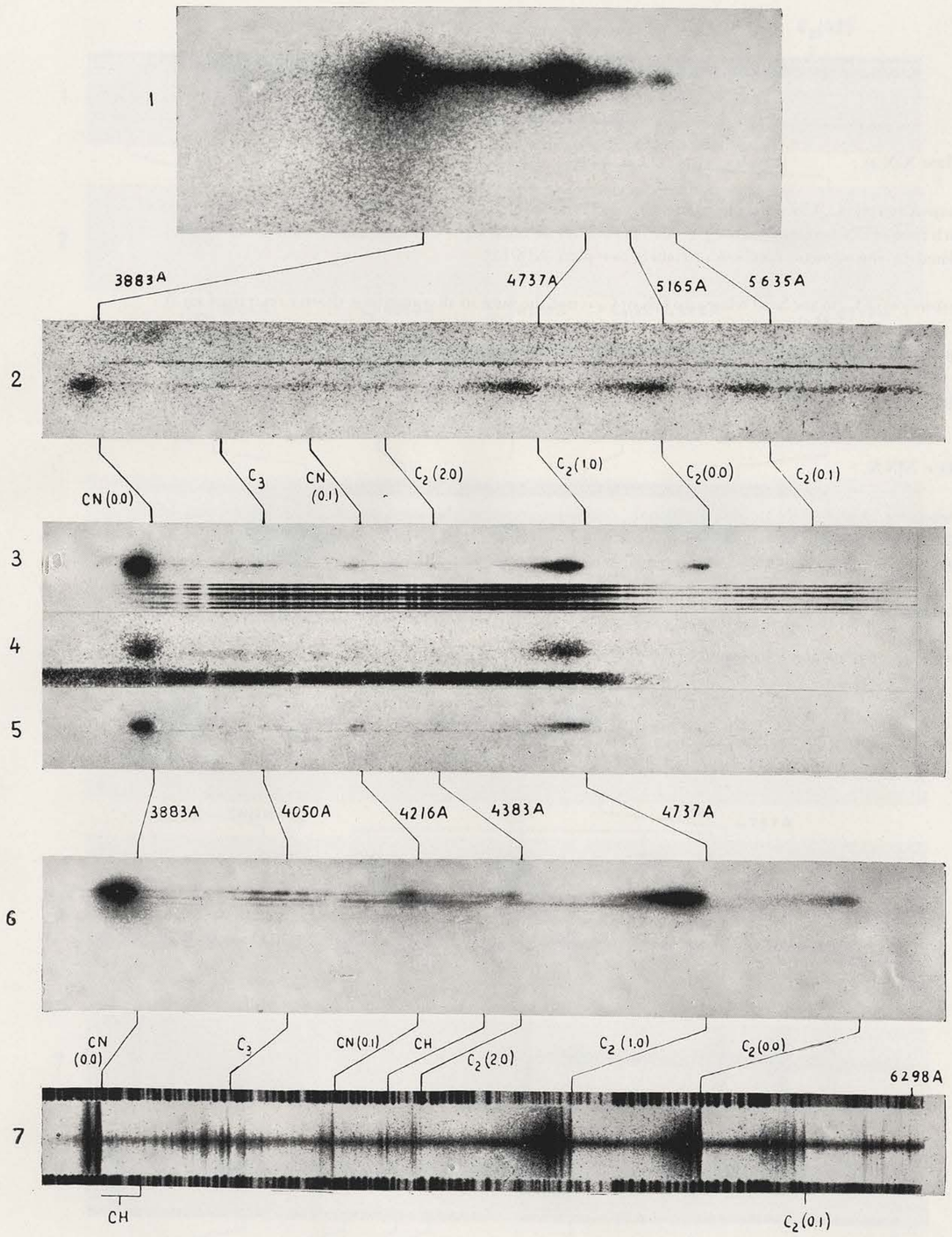

XVIII*a* Spectrograms of comets at heliocentric distances 0.8 to 1.0 A.U., before perihelion passage.

PLATE XVIII*b*

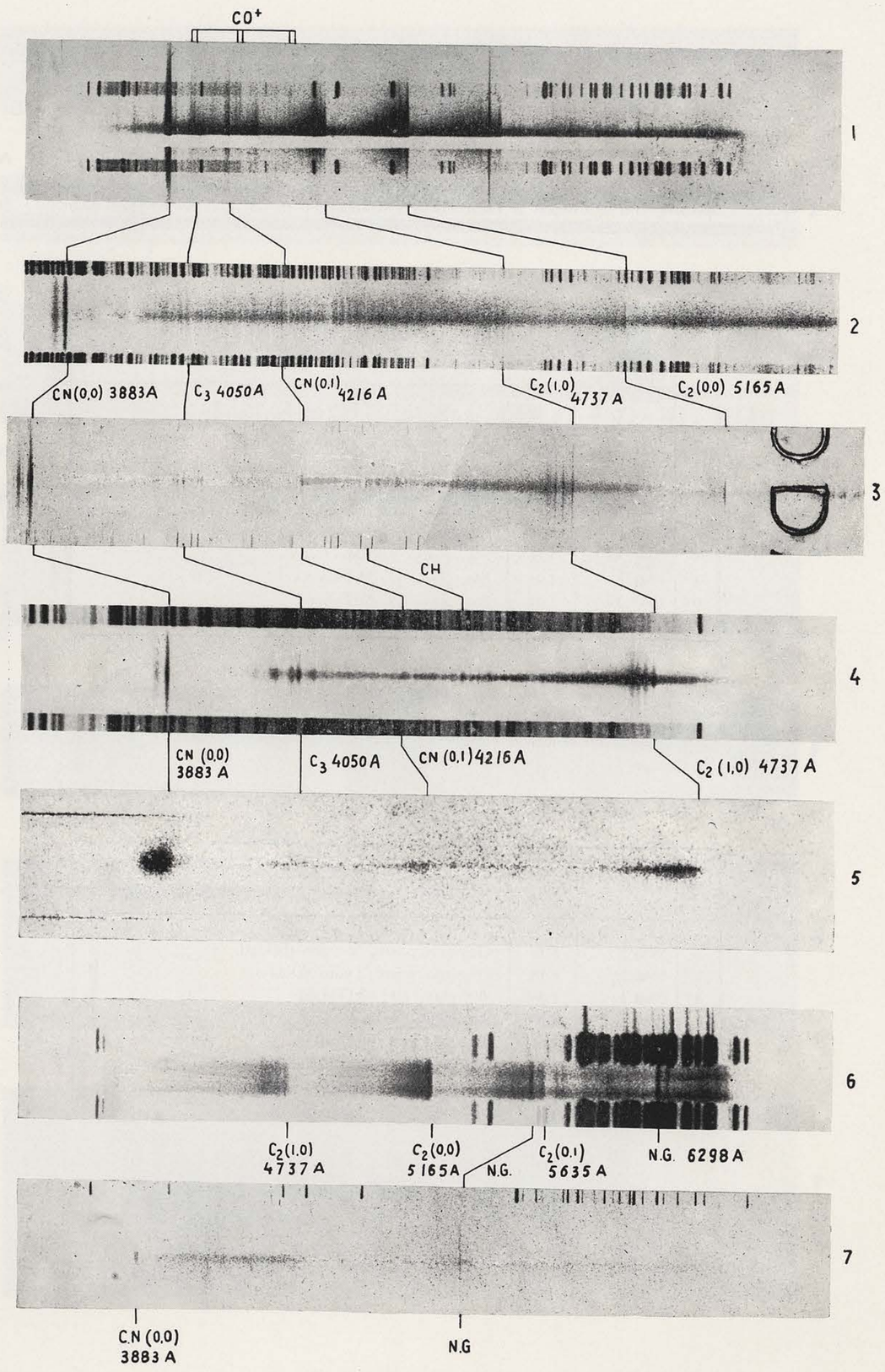

XVIII*b* Spectrograms of comets at heliocentric distances 0.8 to 1.0 A.U., after perihelion passage.

PLATE XIX *a*

Spectrograms of Comets at Heliocentric Distances 1.0 *to* 1.5 *A.U. before Perihelion Passage*

List of spectrograms.

No.	Comet	*r* (A.U.)	Instrument
1	1937 V	1.02	Objective prism, Meudon (Baldet) (panchro).
2	1911 VI	1.19	Objective prism, Meudon (Baldet).
3	1943 I	1.36	Objective prism, Lyons (Dufay).
4	1911 V	1.01	Objective prism, Meudon (Baldet).
5	1912 III	1.14	Objective prism, Meudon (Baldet).
6	1908 III	1.07	Objective prism, Meudon (Baldet).
7	1941 VIII	1.26	Slit, quartz, *f*/1, McDonald.
8	1941 I	1.01	Slit, glass, *f*/1, McDonald.
9	1947 XI	1.02	Slit, glass, *f*/1, McDonald.

PLATE XIX *b*

Spectrograms of Comets at Heliocentric Distances 1.0 *to* 1.5 *A.U. after Perihelion Passage*

List of spectrograms.

No.	Comet	*r* (A.U.)	Instrument
1	1936 II	1.10	Objective prism, Meudon (Baldet).
2	1946 II	1.15	Objective prism, Lyons (Dufay).
3	1948 I	1.06	Slit, glass, *f*/1, McDonald.
4	1910 II	1.08	Slit, glass, Lick.
5	1948 XI	1.01	Slit, glass, *f*/1, McDonald.
6	1948 I	1.27	Slit, grating, *f*/0.65, McDonald.
7	1952 III	1.25	Objective prism, Curtis telescope.

Notes (Plate XIX *a*) :

(1) The intensity ratio C_3/CN differs in different comets; comparing the intensity of the «central» part of λ 4052 C_3 with that of CN(0-1), one finds $C_3 <$ CN on 1, $C_3 =$ CN on 2, $C_3 >$ CN on 4 and 5. This behavior may be related to the «genetic families» of comets (see plate XIX *b*).

(2) The extension of C_3 in the head relative to CN or C_2 is not the same in all comets(it is shorter on 8 than on 7).

(3) Tail predominant on sp. 6 (Morehouse); weak on sp. 4; absent on others.

(4) On sp. 7, apparent emissions in central condensation, shortward of CN(0-0).

Notes (Plate XIX *b*) :

(1) The intensity ratio C_3/CN differs in different comets; comparing the intensity of the «central» part of λ 4052 C_3 with that of CN(0-1), one finds $C_3 <$ CN on sp. 1 and 2, and $C_3 \gg$ CN on sp. 3, 4, 6 and 7. This behavior may be related to the «genetic families» of comets (see plate XIX *a*).

(2) The continuum is weak on sp. 2, 3, 4 and 6; strong on sp. 1, 5 and 7.

(3) The weak short «emissions» longward of CN(0-0) may be due to C_3 instead of CH.

PLATE XIX *a*

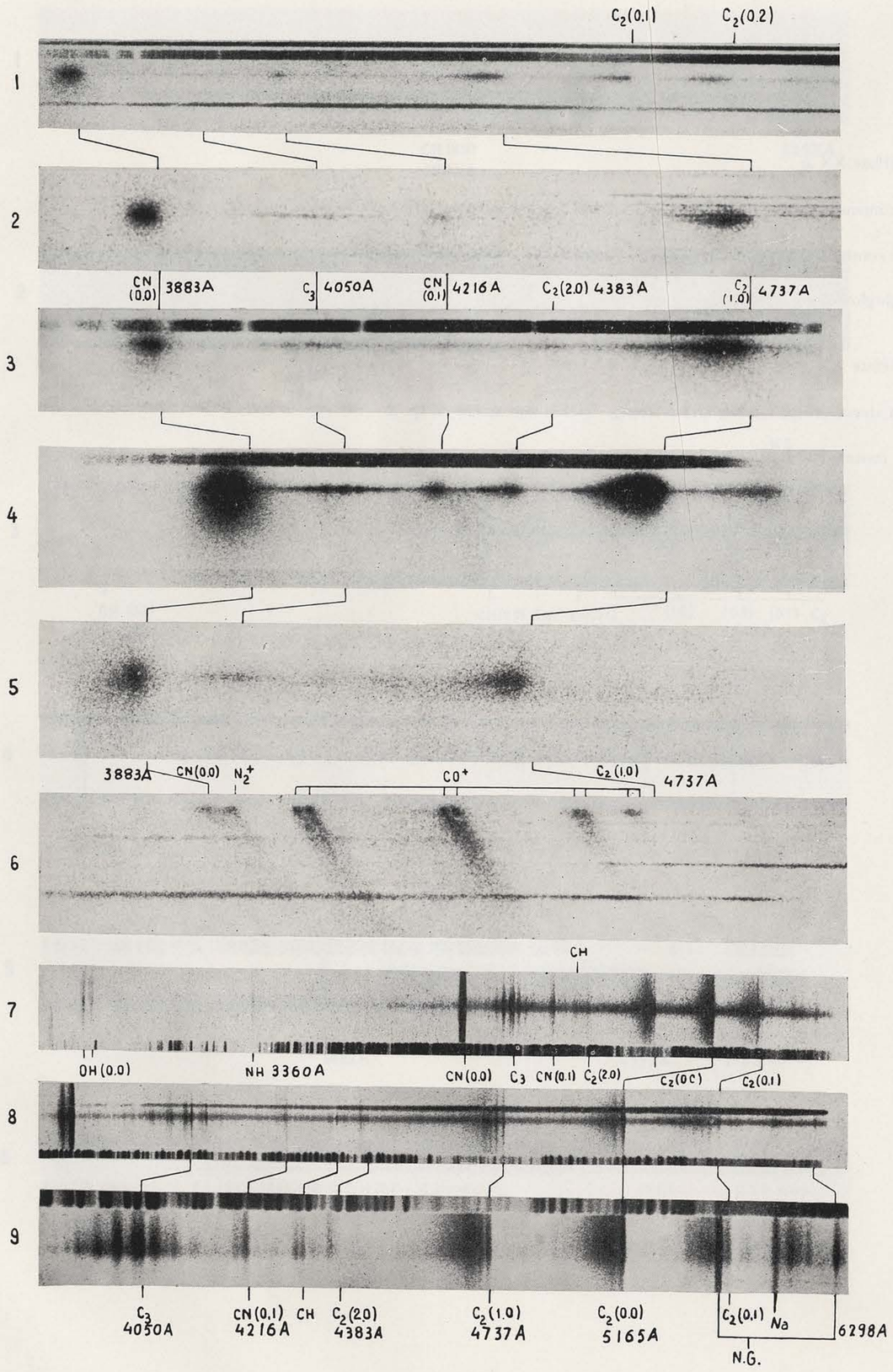

XIX*a* Spectrograms of comets at heliocentric distances 1.0 to 1.5 A.U., before perihelion passage.

PLATE XIX *b*

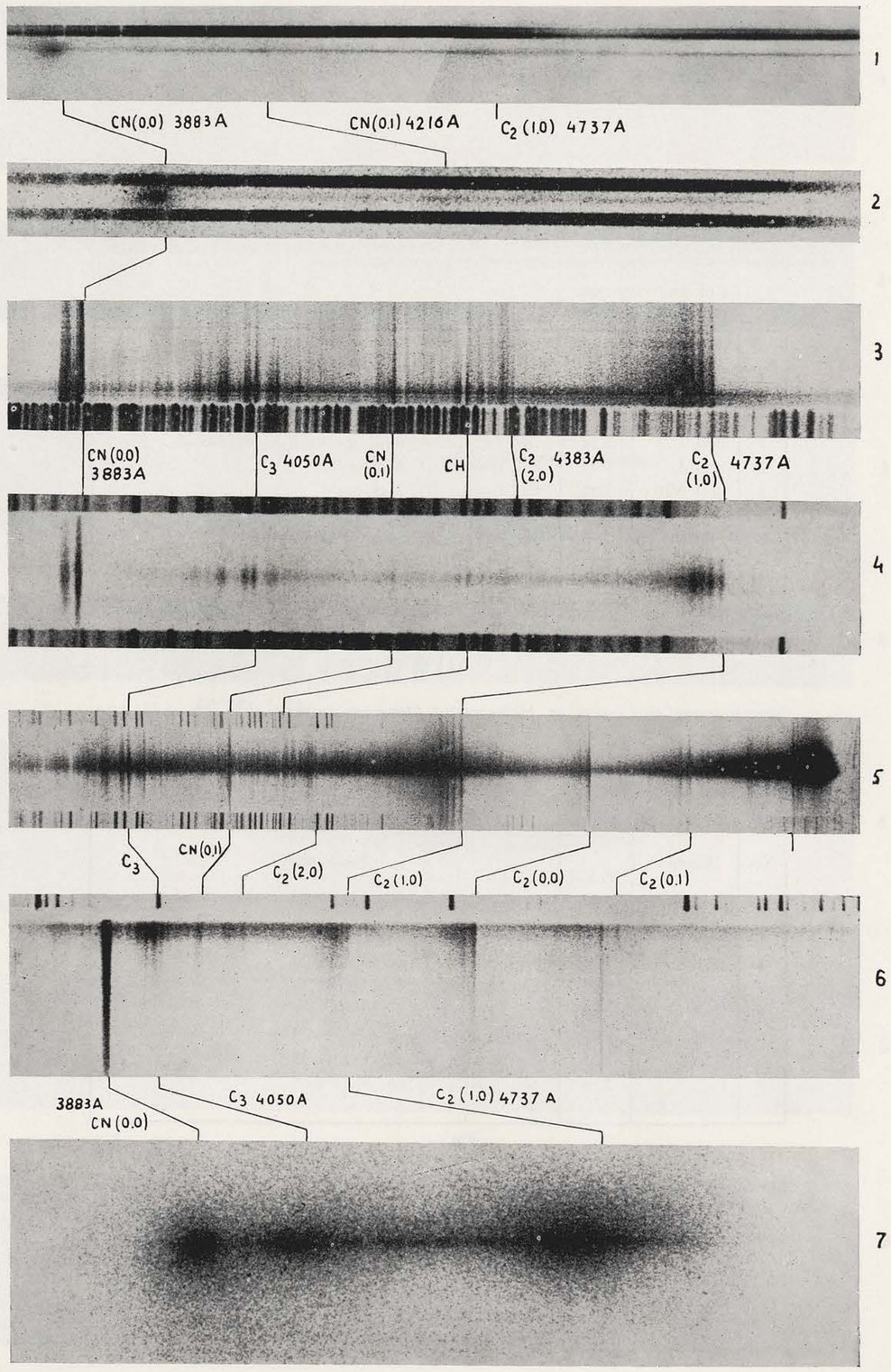

XIX*b* Spectrograms of comets at heliocentric distances 1.0 to 1.5 A.U., after perihelion passage.

PLATE XX *a*

Spectrograms of Comets at Heliocentric Distances greater than 1.5 *A.U. before Perihelion Passage*

List of spectrograms.

No.	Comet	*r* (A.U.)	Instrument
1	1941 I	2.24	Nebular spectrograph, quartz, *f*/1, McDonald.
2	1941 I	1.85	Slit, quartz, *f*/1, McDonald.
3	1941 VIII	1.52	Slit, quartz, *f*/1, McDonald.
4	1941 VIII	1.53	Slit, glass, *f*/1, McDonald.
5	1942 IV	1.76	Slit, quartz, *f*/2, McDonald.
6	1942 IV	1.73	Slit, glass, *f*/2, McDonald.

PLATE XX *b*

Spectrograms of Comets at Heliocentric Distances greater than 1.5 *A.U. after Perihelion Passage*

List of spectrograms.

No.	Comet	*r* (A.U.)	Instrument
1	1943 I	1.79	Slit, quartz, *f*/2, O.H.P. (Chalonge).
2	1948 I	1.55	Slit, quartz, *f*/1, McDonald.
3	1948 XI	2.22	Slit, quartz, *f*/1, McDonald.
4	1948 XI	1.63	Slit, quartz, *f*/1, McDonald.
5	1951 I	2.64	Slit, grating, *f*/0.65, McDonald.
6	1951 I	2.62	Slit, grating, *f*/0.65, McDonald.
7	1951 I	2.64	Slit, grating, *f*/0.65, McDonald.

Notes (Plate XX *a*) :

(1) The intensity ratio C_3/CN differs on sp. 2 and 5-6; the intensity ratio C_2/CN differs on sp. 2, 4 and 5-6.

(2) The continuum is present on all spectra (on sp. 5, the guiding was poor, or there was an effect of twilight).

(3) Nightglow lines present.

Notes (Plate XX *b*) :

(1) NH absent on sp. 1, while OH is strong. NH is also absent on sp. 2.

(2) No continuum on sp. 1 (strong molecular bands!), whereas the continuum is strong on sp. 2.

PLATE XX *a*

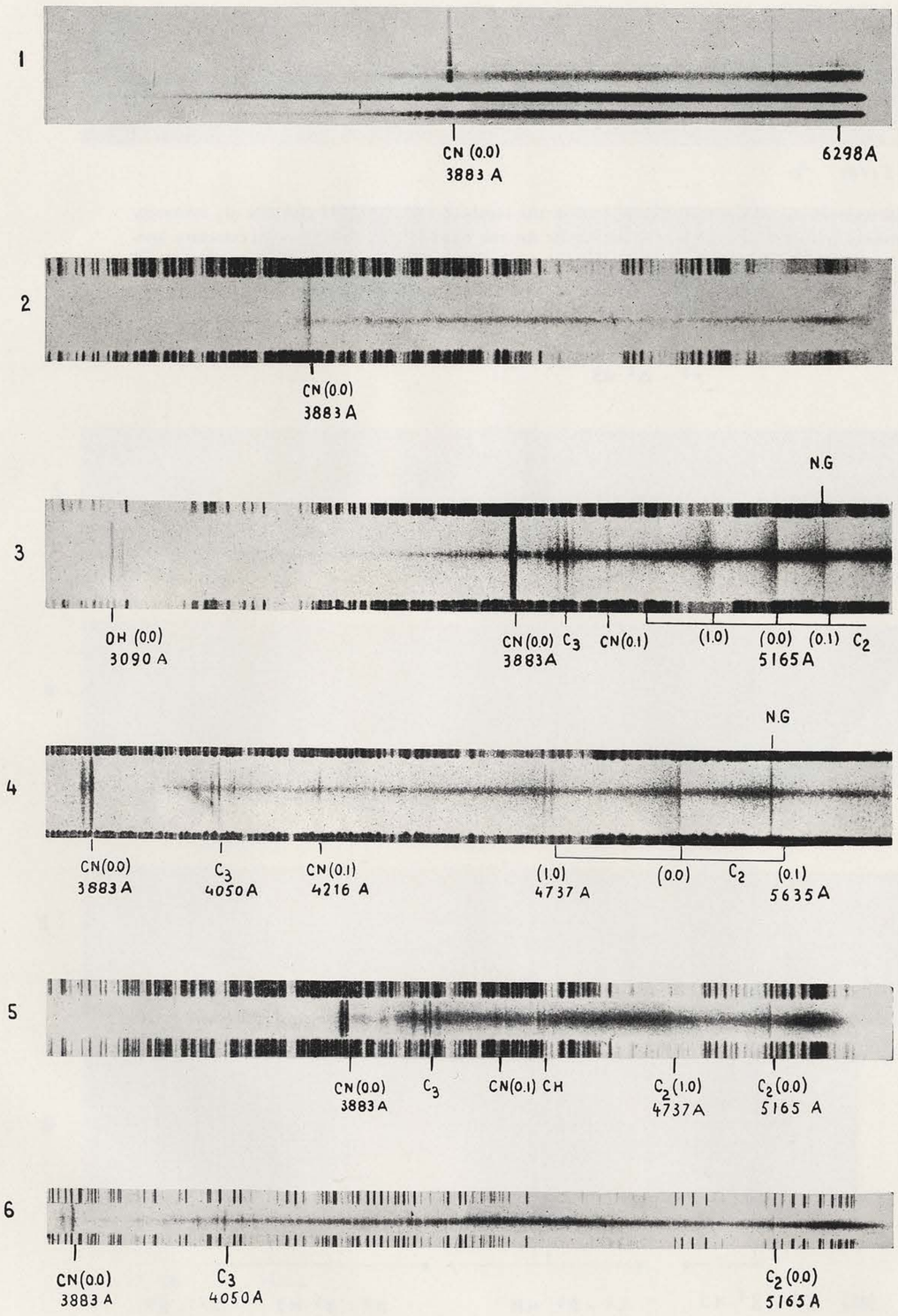

XX*a* Spectrograms of comets at heliocentric distances greater than 1.5 A.U., before perihelion passage.

PLATE XX *b*

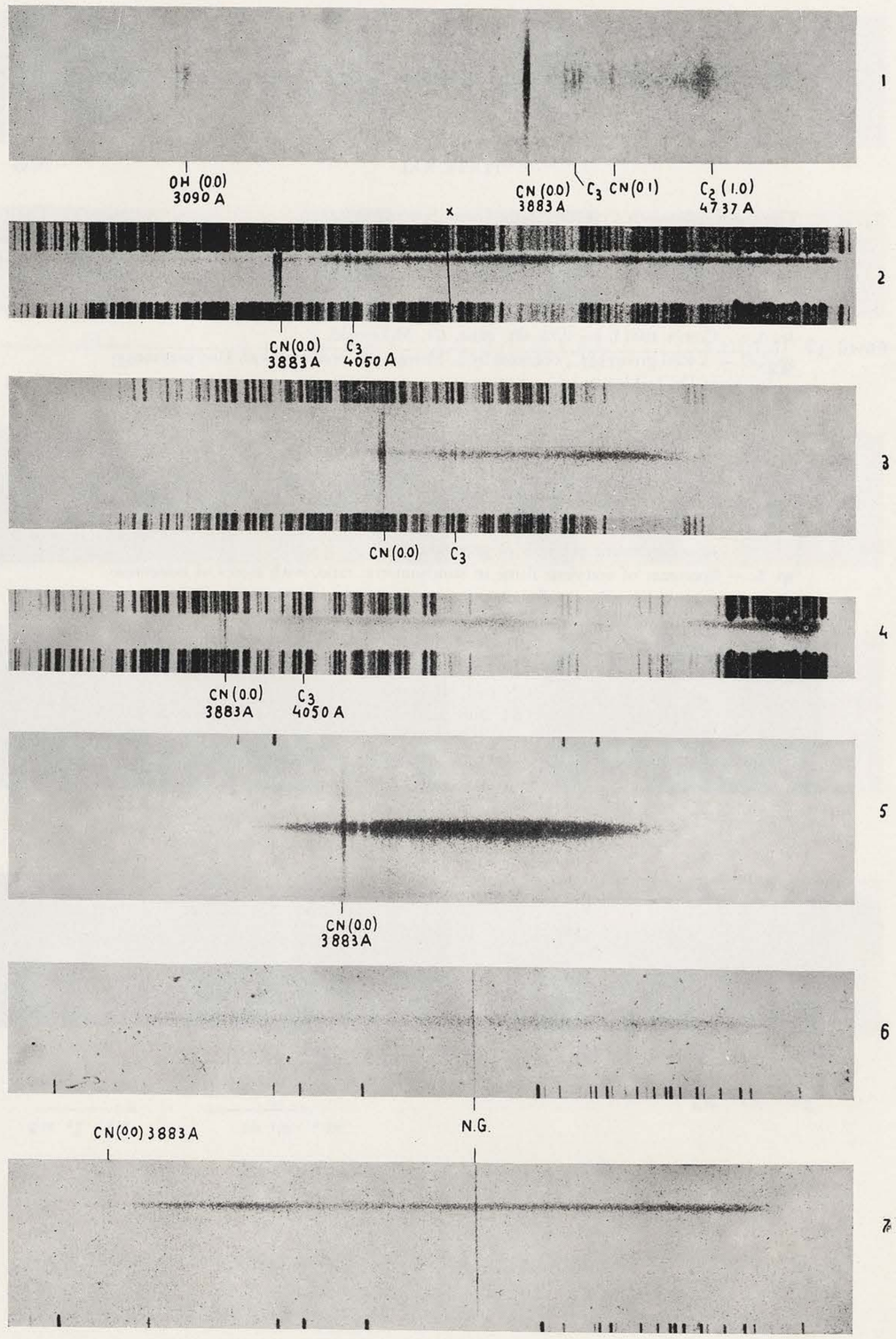

XX*b* Spectrograms of comets at heliocentric distances greater than 1.5 A.U., after perihelion passage.

PLATE XXI

Comparison between Cometary- and Flame Spectra

Description of the spectrograms.

sp. 1. — Comet 1941 I, $r = 0.73$, slit, glass, $f/1$, McDonald.

sp. 2*a*. — λ 4050 group of C_3 obtained by L. Herman (Reproduced with kind permission of Dr. L. Herman).

sp. 2*b*. — Three spectrographic exposures on a flame of acetylene, stoichometric mixture, inner cone. Main bands: C_2 and CH.

sp. 3. — Comet 1941 I, $r = 0.87$, slit, quartz, $f/1$, McDonald.

sp. 4. — Spectrum of rich acetylene flame with some addition of ammonia. Main features: bands of OH, NH (Q-branch), CN (violet system), C_3 (and associated continuum extending from λ 3200 to λ 4600), C_2 and CH; also red continuum of incandescent particles of graphite.

sp. 5. — Spectrum of acetylene flame in stoichometric ratio, with traces of ammonia; inner cone and part of outer cone,

Present in inner cone: CH ($^2\Sigma - {}^2\Pi$), NH, CN (blue, $\Delta v = +1,0,-1,-2$), CH ($^2\Sigma - {}^2\Pi$), CH ($^2\Delta - {}^2\Pi$), C_2 (Swan, $\Delta v = +2,+1,0,-1,-2$), CN (red, $^2\Pi - {}^2\Sigma$).

Present in outer cone: OH, NH, CN (blue and red), extremely weak CH, weak C_2.

sp. 6. — Spectrum of acetylene flame in stoichometric ratio, with ammonia. Strong exposure. Notice the rotational structures of OH, NH, CH, CN.

Note;

The rotational and vibrational intensity distributions in the bands of OH, NH, CH and CN are extremely different in comets and in flames, while they are similar for the bands of C_2. The observed cometary lines within each band of OH, NH, CH and CN correspond to the lowest rotational transitions (low rotational temperatures!).

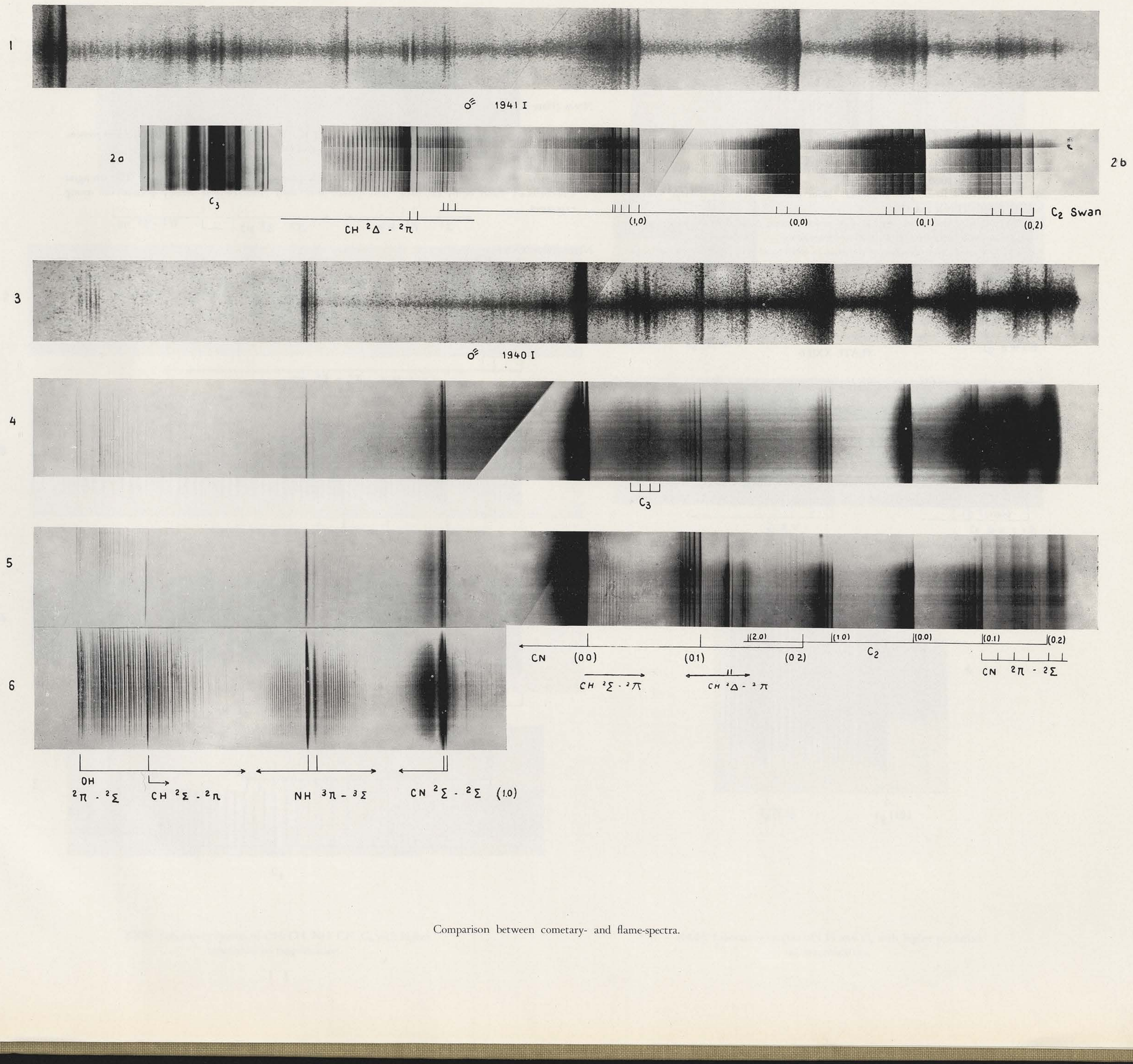

Comparison between cometary- and flame-spectra.

PLATE XXII *a*

Laboratory Spectra of OH, CH (Fortrat System), NH, CN, C_3, with Higher Resolution or Magnification

Description of the spectrograms.

Sp. 1. — Acetylene flame, plus ammonia. Main features: OH, CH (Fortrat System) and NH (0-0 and 1-1).

Sp. 2, 3 *and* 4. — Arc in air. Sp. 2: CN violet system, $\Delta v = +1$ sequence; sp. 3: $\Delta v = 0$ sequence; sp. 4: $\Delta v = -1$ sequence.

Sp. 5. — High resolution spectrum of the main (λ 4050) band of C_3, excited in a discharge through a mixture of xenon and hydrogen between carbon electrodes, see A. E. Douglas, Ap. J., *114*, 466, 1951 (reproduced with kind permission of the author and editor).

PLATE XXII *b*

Laboratory Spectra of CH and C_2 with Higher Resolution or Magnification

Description of the spectrograms;

Sp. 1, 2 and 3: acetylene flame (without ammonia).

Sp. 1: $^2\Delta - {}^2\Pi$ system of CH, weak $\Delta v = +2$ sequence of C_2.

Sp. 2: 3 exposures on the $\Delta v = +1$ and 0 sequences of C_2.

Sp. 3: 3 exposures on the $\Delta v = -1$ and -2 sequences of C_2.

Sp. 4: spectrum of the $\Delta v = +1$ sequence of a source enriched in C_{13}, showing the $C_{12}C_{12}$ and $C_{12}C_{13}$ bands (see A. S. King and R. T. Birge, Ap. J., *72*, 19, 1930, plate I) (*).

(*) Reproduced with kind permission of the Managing Editor of the Astrophysical journal.

Notes (Plate XXII *a*) :

(1) In comets, only the (0-0) band of NH appears, not (1-1). The Fortrat system of CH is absent in comets. Only the lines of very low rotational quantum number of OH and NH appear in comets.

(2) In comets, all the CN-bands show only lines of fairly low rotational quantum number. The strongest CN-cometary band is, by far, (0-0); next comes (0-1), then (1-0); (1-1) is weakly present on strong exposures.

Notes (Plate XXII *b*) :

Only the lines of low rotational quantum number of CH ($^2\Delta - {}^2\Pi$) appear in comets. The intensity distributions of the C_2-bands in comets do not differ greatly from those in the acetylene flame.

PLATE XXII *a*

XXIIa Laboratory spectra of OH, CH, NH, CN, C_3 with higher resolution or magnification.

PLATE XXII *b*

XXII*b* Laboratory spectra of CH and C_2 with higher resolution or magnification.

PLATE XXIII *a*

Comparison between the Bands of Cometary Tails and the Laboratory Spectrum of CO^+ *and* N_2^+

Description of the spectrograms;

Sp. 1: Comet 1948 I, $r = 0.97$; slit, grating, *f*/0.65, McDonald.

Sp. 2: Comet 1948 I, $r = 0.96$; idem.

Sp. 3: Laboratory spectra of CO^+ and N_2^+ obtained by F. Baldet by electron impact (see F. Baldet, Thesis, p. 96, plate III, sp. 1, 1926).

PLATE XXIII *b*

Influence of Instrumental Factors: (Poor Guiding, Chromatic Aberration) on the Appearance of Cometary Spectra

List of spectrograms.

No.	Object	*r* (A.U.)	Instrument
1	1948 XI	0.61	Objective prism, Cordoba (Sahade)
2	1937 V	0.87	Slit, Lick.
3	1937 V	0.87	Slit, Mt Wilson.
4	1937 V	0.88	Objective prism, Sonneberg (Richter)
5	1907 IV	0.59	Slit, Lick.
6	1907 IV	0.70	Objective prism, Meudon (Baldet).

Description;

(1) Slitless sp. 1 of Comet 1948 XI was poorly guided. Nevertheless the two main features are observable: presence of continuous emission in addition to CO^+, in tail; heavy continuous emission in central condensation of head.

(2) and (3) Slit sp. 2 of Comet 1937 V was poorly guided, while sp. 3 of same object at same *r* was carefully guided. Notice apparent difference in intensity ratio of CH and CN(0-1).

(4) Objective prism sp. illustrating the effect of the chromatic aberration of the objective (change in width of continuum from λ 3800 to λ 4500).

(5) Slit sp. showing the effect of the chromatic aberration of the objective (change in width of continuum).

(6) Objective prism sp. of same comet as on (5), showing a different *apparent* intensity ratio of C_3 and CN (0-1).

Notes (Plate XXIII *a*) :

(1) The CO^+ bands have a doublet structure; the main N_2^+ band is single.

(2) In the ultraviolet region of the spectra of comet tails, strong emissions belong to CO_2^+.

PLATE XXIII *a*

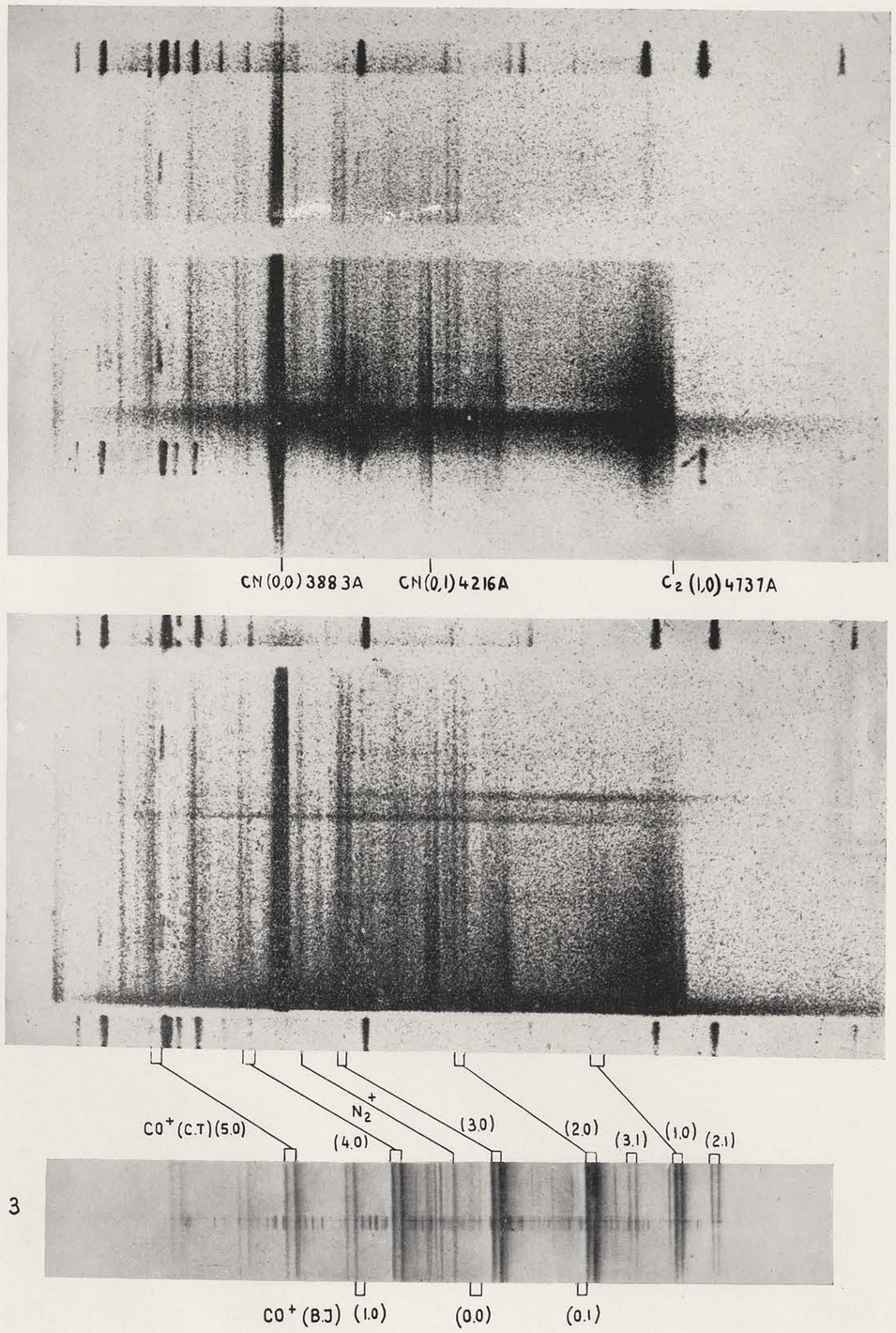

XXIII*a* Comparison between the bands of cometary tails and the laboratory spectra of CO^+ and N_2^+.

PLATE XXIII *b*

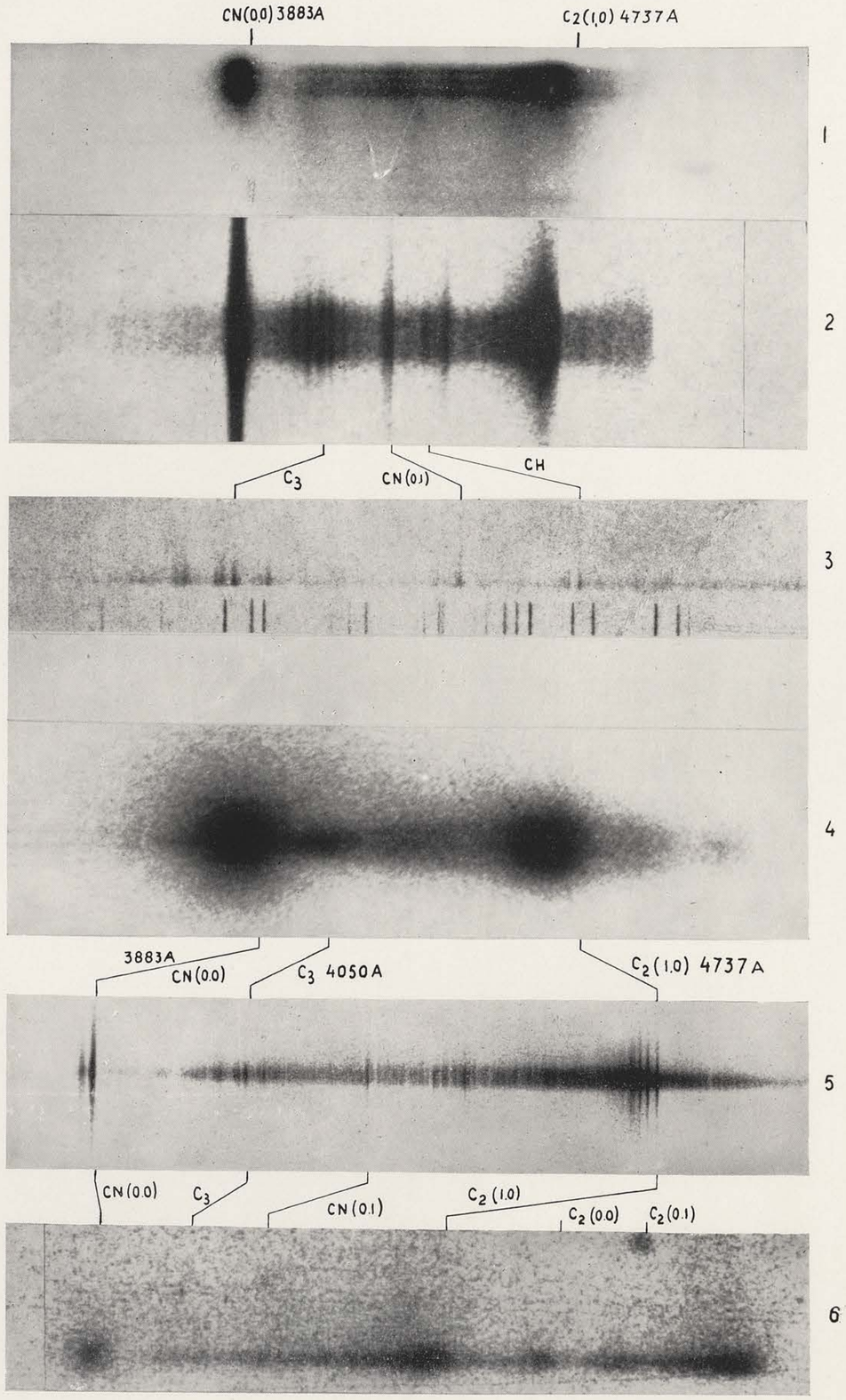

XXIII*b* Influence of instrumental factors (poor guiding, chromatic aberration) on the appearance of cometary spectra.

(24101) Imprimerie Ceuterick, s.c., 66, rue Vital Decoster, Louvain.
Resp. L. Pitsi, 25, rue Dagobert, Louvain (Belgique).